

OAK RIDGE NATIONAL LABORATORY

operated by
UNION CARBIDE CORPORATION
for the
U.S. ATOMIC ENERGY COMMISSION

ORNL-NSIC-74

CALCULATION OF DOSES DUE TO ACCIDENTALLY RELEASED PLUTONIUM FROM AN LMFBR

B. R. Fish, G. W. Keilholtz,
W. S. Snyder, S. D. Swisher

NUCLEAR SAFETY INFORMATION CENTER

NSIC

Contract No. W-7405-eng-26

Nuclear Safety Information Center

CALCULATION OF DOSES DUE TO ACCIDENTALLY
RELEASED PLUTONIUM FROM AN LMFBR

B. R. Fish, Health Physics Division
G. W. Keilholtz, Reactor Chemistry Division
W. S. Snyder, Health Physics Division
S. D. Swisher, Atmospheric Turbulence and
Diffusion Laboratory, NOAA

NOVEMBER 1972

OAK RIDGE NATIONAL LABORATORY
Oak Ridge, Tennessee 37830
operated by
UNION CARBIDE CORPORATION
for the
U.S. ATOMIC ENERGY COMMISSION

Printed in the United States of America. Available from
National Technical Information Service
U.S. Department of Commerce
5285 Port Royal Road, Springfield, Virginia 22151
Price: Printed Copy \$15.00; Microfiche \$15.00

This report was prepared as an account of work sponsored by the United States Government. Neither the United States nor the United States Atomic Energy Commission, nor any of their employees, nor any of their contractors, subcontractors, or their employees, makes any warranty, express or implied, or assumes any legal liability or responsibility for the accuracy, completeness or usefulness of any information, apparatus, product or process disclosed, or represents that its use would not infringe privately owned rights.

CONTENTS

	<u>Page</u>
PREFACE	v
ACKNOWLEDGMENT	vii
ABSTRACT	ix
1. INTRODUCTION	1
2. BEHAVIOR OF RELEASED SODIUM OXIDE AND PLUTONIUM- BEARING PARTICLES	4
2.1 Aerosol Behavior Considerations	5
2.1.1 Brownian motion	6
2.1.2 Gravity	6
2.1.3 Turbulence	7
2.2 Experimental Evidence for Decay of Mass Concentration and Changes in Particle Size of Airborne Aerosols with Time	10
2.3 Empirical Models and Equations for the Decay of Mass Con- centration and Changes in Particle Size with Time	12
2.3.1 Schikarski model	13
2.3.2 Davis model	14
2.3.3 Koontz model	15
2.4 Detailed Discussion of an Aerosol Model and Its Appli- cation	16
2.5 A Postulated Release of Radionuclides from an LMFBR- Type Reactor under Accident Conditions	24
References	27
3. TRANSPORT, SETTLING, AND REDISTRIBUTION OF AEROSOLS IN THE OUTSIDE AIR (TROPOSPHERE)	31
3.1 Meteorological Considerations	31
3.2 Properties of Na ₂ O Aerosols in the Atmosphere	32
References	35
4. CHEMISTRY OF PLUTONIUM	36
4.1 Compounds of Plutonium	36
4.1.1 Plutonium dioxide and mixed oxides	37
4.1.2 Plutonium carbides, nitrides, and silicides	44
4.1.3 Sodium-uranium-plutonium oxides	45
4.1.4 Other inorganic compounds	45
4.2 Solution Chemistry of Plutonium	46
4.2.1 Complex formation by plutonium in aqueous solutions	47
4.2.2 Solubility of plutonium compounds	49
4.2.3 Complex formation by plutonium in various oxida- tion states	50
4.3 Methods for Separation of Plutonium from Uranium and Fission Products	52
4.3.1 Solvent extraction	52
4.3.2 Ion exchange methods	53

4.4	Analytical Methods for Determining Plutonium	55
4.4.1	Conventional methods	55
4.4.2	Radiochemical methods	56
	References	57
5.	INTAKE AND METABOLISM OF PLUTONIUM DIOXIDE	60
5.1	Intake Pathways	61
5.1.1	Inhalation	61
5.1.2	Ingestion	77
5.1.3	Deposition on body surfaces	84
5.2	Systemic Distribution and Retention	86
5.2.1	Transport in the bloodstream	86
5.2.2	Deposition and retention in bone	87
5.2.3	Deposition and retention in liver	88
5.2.4	Deposition and retention in gonads	89
5.2.5	Elimination of plutonium from the body	90
	References	93
6.	COMPUTATION OF INTERNAL DOSE	104
6.1	Physical Dosimetry and Dose Equivalent	104
6.2	Dose Calculations for Inhaled Plutonium	106
6.3	Consideration of Other Plutonium Isotopes	110
6.4	Consideration of Other Transuranics	113
6.5	Gastrointestinal Tract Intake During Release	116
6.6	Ingestion of Plutonium in Food and Water	117
6.7	Summary Calculations	117
6.7.1	Source term evaluations	117
6.7.2	Leakage and dispersion	119
6.7.3	Calculation of dose	119
	References	121
7.	SUMMARY	122

PREFACE

The Nuclear Safety Information Center, established in March 1963 at the Oak Ridge National Laboratory under the sponsorship of the U.S. Atomic Energy Commission, is a focal point for the collection, storage, evaluation, and dissemination of nuclear safety information. A system of key words is used to index the information cataloged by the Center. The title, author, installation, abstract, and key words for each document reviewed are recorded at the central computer facility in Oak Ridge. The references are cataloged according to the following categories:

1. General Safety Criteria
2. Siting of Nuclear Facilities
3. Transportation and Handling of Radioactive Materials
4. Aerospace Safety
5. Heat Transfer and Thermal Transients
6. Reactor Transients, Kinetics, and Stability
7. Fission Product Release, Transport, and Removal
8. Sources of Energy Release under Accident Conditions
9. Nuclear Instrumentation, Control, and Safety Systems
10. Electrical Power Systems
11. Containment of Nuclear Facilities
12. Plant Safety Features -- Reactor
13. Plant Safety Features -- Nonreactor
14. Radionuclide Release and Movement in the Environment
15. Environmental Surveys, Monitoring, and Radiation Exposure of Man
16. Meteorological Considerations
17. Operational Safety and Experience
18. Safety Analysis and Design Reports
19. Radiation Dose to Man from Radioactivity Release to the Environment
20. Effects of Thermal Modifications on Ecological Systems
21. Effects of Radionuclides and Ionizing Radiation on Ecological Systems

Computer programs have been developed which enable NSIC to (1) operate a routine program of Selective Dissemination of Information (SDI) to individuals according to their particular profile of interest, (2) make retrospective searches of the stored references, and (3) distribute scope and progress information on R&D contracts from the Program and Project Information File (PPIF).

Services of the NSIC are available to government agencies, research and educational institutions, and the nuclear industry on a partial cost recovery basis designed to regain a portion of the expense associated with disseminating the information to the user. A minimal inquiry response is available free. NSIC reports (i.e., those with the ORNL-NSIC numbers) may be purchased from the National Technical Information Service (see inside front cover) while documents indexed by NSIC may be examined at the Center by qualified personnel. Inquiries concerning the capabilities and operation of the Center may be addressed to:

J. R. Buchanan, Assistant Director
(Phone 615-483-8611, Ext. 3-7253)
Nuclear Safety Information Center
Oak Ridge National Laboratory
Post Office Box Y
Oak Ridge, Tennessee 37830

ACKNOWLEDGMENT

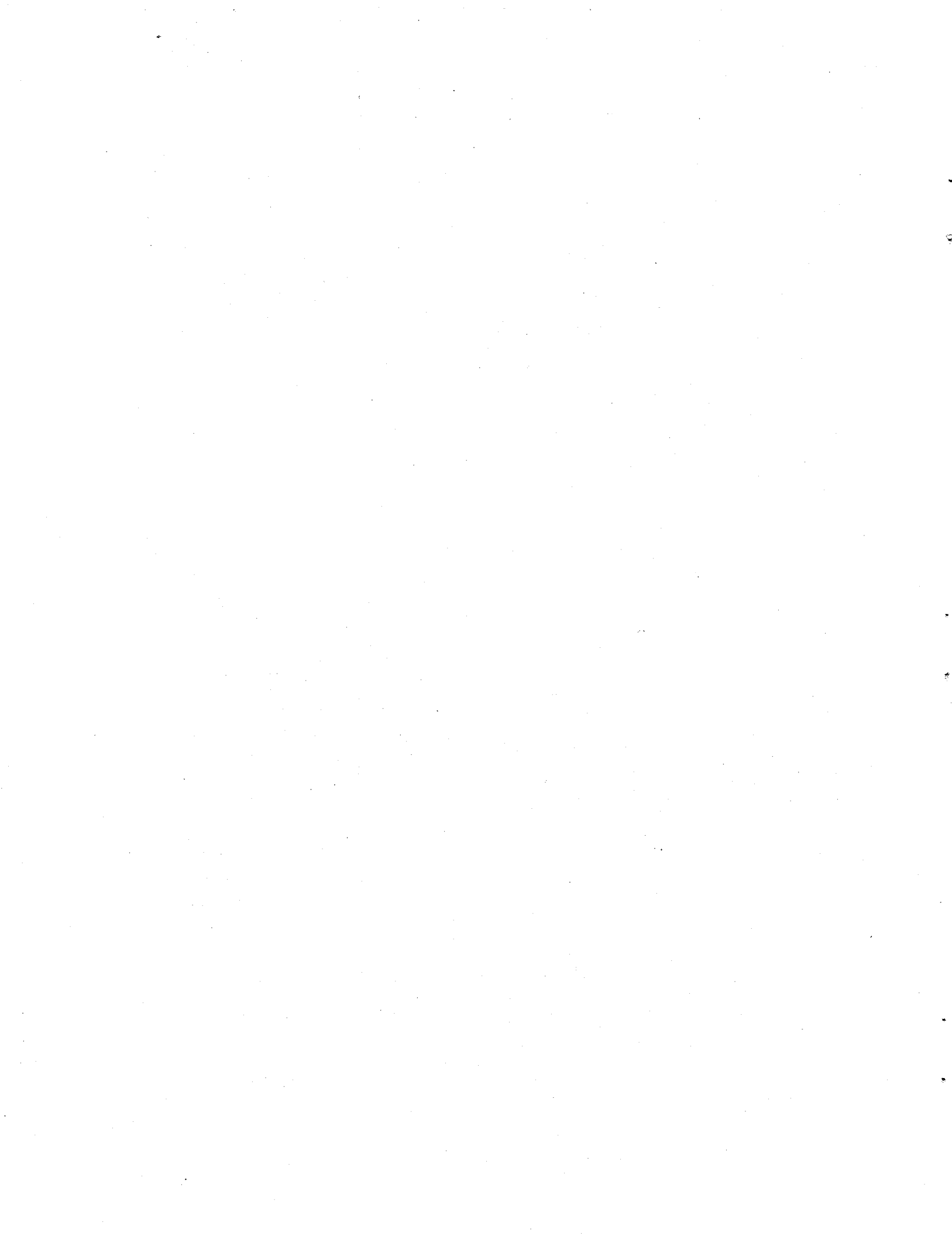
In the preparation of this report the authors benefitted from the review and comment of many people who are active in various aspects of the many fields of expertise involved in accident analysis and plutonium dose calculation. While this does not mean that all reviewers necessarily agree with the report in every detail, we do wish to acknowledge their contribution by listing the participants. Trusting that no one has been overlooked, they are as follows:

Internal Reviewers (ORNL)

C. J. Barton	Wm. B. Cottrell	F. L. Miller
S. R. Bernard	R. J. Davis	P. Nettesheim
R. H. Bryan	P. B. Dunaway	G. W. Parker
T. J. Burnett	M. H. Fontana	L. F. Parsly
J. R. Buchanan	A. P. Malinauskas	H. B. Piper

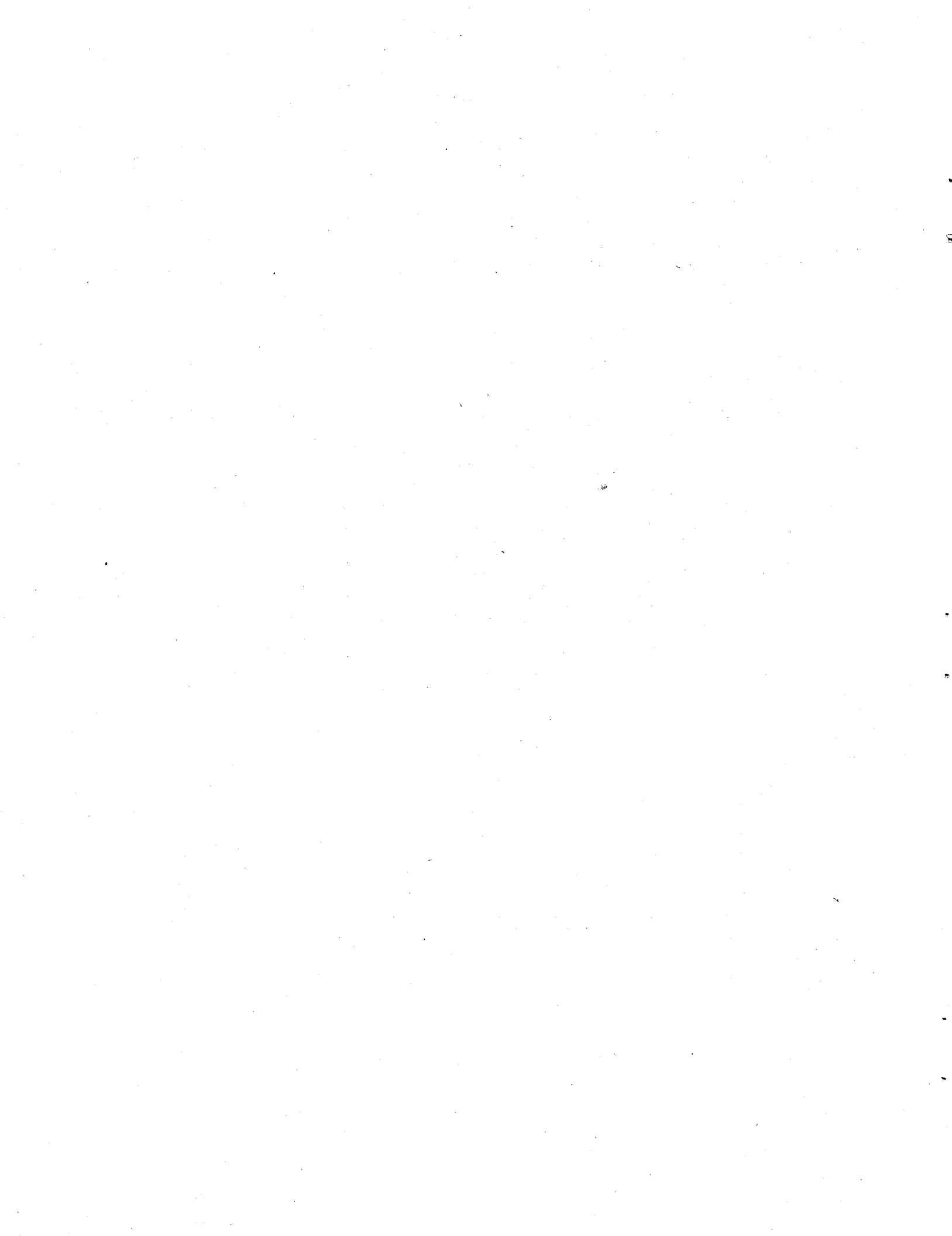
External Reviewers

A. W. Castleman, Brookhaven National Laboratory
 Patricia W. Durbin, Lawrence Berkeley Laboratory
 Headquarters Staff, U.S. Atomic Energy Commission
 M. M. Hendrickson, Battelle-Northwest Laboratories
 H. H. Hopkins, Atlantic Richfield Hanford Company
 R. L. Junkins, Battelle-Northwest Laboratories
 W. H. Langham (deceased), Los Alamos Scientific Laboratory
 J. N. P. Lawrence, Los Alamos Scientific Laboratory
 H. E. Meyer, Mound Laboratory
 H. A. Morewitz, Atomics International
 I. Nelson, Battelle-Northwest Laboratories
 W. D. Norwood, Hanford Environmental Health Foundation
 L. C. Schwendiman, Battelle-Northwest Laboratories
 R. C. Thompson, Battelle-Northwest Laboratories



ABSTRACT

Experimental data and analytical models that should be considered in assessing the transport properties of plutonium aerosols following a hypothetical reactor accident have been examined. Behaviors of released airborne materials within the reactor containment systems, as well as in the atmosphere near the reactor site boundaries, have been semiquantitatively predicted from experimental data and analytical models. The fundamental chemistry of plutonium as it may be applied in biological systems has been used to prepare models related to the intake and metabolism of plutonium dioxide, the fuel material of interest. Attempts have been made to calculate the possible doses from plutonium aerosols for a typical analyzed release in order to evaluate the magnitude of the internal exposure hazards that might exist in the vicinity of the reactor after a hypothetical LMFBR (Liquid-Metal Fast Breeder Reactor) accident. Intake of plutonium (using data for ^{239}Pu as an example) and its distribution in the body were treated parametrically without regard to the details of transport pathways in the environment. To the extent possible, dose-response data and models have been reviewed, and an assessment of their adequacy has been made so that recommended or preferred practices could be developed.



1. INTRODUCTION

There are many factors involved in adjudging the possibility for and consequences of accidents. In order to provide an extreme test of the capability of a nuclear reactor with all its attendant safety features to mitigate the consequences of releases of radioactive materials, accidents have often been analyzed which involve failures, or a multiplicity of failures, of vanishingly low probability. In the worst cases, these may lead to a release of fuel materials from the nuclear reactor core. Although such analyses may indicate that any released radioactive materials will be retained in the nuclear reactor primary system, releases into the containment atmosphere may be hypothesized and the resultant radiological consequences calculated. Data and calculational models for evaluation of potential releases from water-cooled reactors have been developed over the last two decades, and there is now substantial uniformity in their application. Because of the newly emerging LMFBR (Liquid-Metal Fast Breeder Reactor) technology, evaluation of sodium-cooled reactors using mixed oxides of uranium and plutonium as fuel has been treated on a case basis. On the basis of the results of the evaluations to date, it appears likely that any postulated releases of fuel materials will involve, as a necessary condition, a concomitant release of some sodium coolant. The released sodium and fuel will behave as particulates rather than as non-settling gases, and consequently their behavior requires use of different analytical techniques.

The purpose of this report is to assess the potential plutonium dose from a hypothetical release. Since the exact nature or even the possibility of any kind of release must be considered on a case basis, this report considers only those factors where commonality of calculation is possible. In order to do this, the transport of plutonium-bearing aerosols through the primary and secondary reactor containment systems to the reactor site boundaries was examined, and then an attempt was made to calculate the doses that might result.

The familiar analyses of postulated accidents in water- and gas-cooled reactors have determined the hazards of direct exposure from released noble gases, together with the usually controlling hazard from iodine isotopes

(which, however, as regards the food chain, is subject to countermeasures). With the LMFBR the affinity of the liquid alkali metal for halogens (decreasing the potential for a hazardous release of gaseous iodine), the radiotoxicity of the fuel, and the likelihood of a release of sodium coolant as a particulate aerosol, plus the buildup of fission products and the actinides, contribute to the potential hazards in an accident. However, quantitative considerations in this report have been limited to the potential plutonium dose. The models for transport of potentially released airborne plutonium aerosols have been examined. The complexities of such an examination are explored in order to provide information for use in evaluating the design, engineered safety features, and siting requirements of a proposed reactor and to suggest avenues of further study to eliminate some of the many uncertainties involved. This report also discusses realistically the impact of the specific circumstances of the postulated release, such as noting that the quantity of sodium assumed to be released strongly affects the subsequent behavior of any released PuO_2 . In this case the sodium vapor or oxide would significantly affect coagulation of the PuO_2 - UO_2 into an agglomerated aerosol and the subsequent fallout and removal of the aerosol. Models for aerosol behavior and transport and appropriate dosimetric models and parameters for the calibration of radiation doses from a given accidental release of plutonium-bearing aerosols from an LMFBR are considered.

The Fast Flux Test Facility (FFTF) and contractors conducting the LMFBR Demonstration Plant design studies for the USAEC have selected uranium-plutonium oxide as the fuel for their reference designs. In these designs the primary coolant is housed in inerted concrete structures that can also serve as an inner barrier in the event of a hypothesized release. The concrete structures in turn are enclosed in a building, which constitutes secondary containment.

In this report the behavior of plutonium-bearing aerosols in the primary barrier and the secondary reactor containment system is considered. Meteorological dispersion calculations are used to describe the possible dispersion of plutonium from the reactor containment system. Chapters 2 and 3 review the experimental data, analytical models, and calculations now being used to predict the quantities, mass concentrations, and particle

sizes of airborne plutonium-bearing particles released to the environment by the postulated accidents.

Chapter 4 reviews the chemical properties of plutonium.

Chapters 5 and 6 are presented from a health physics viewpoint. In Chapter 5, general models for the intake and metabolism of plutonium compounds are presented. It is of interest to note that some of the basic concepts of aerosol physics used to generate models for aerosol behavior in large containment vessels and ducts have similar applications in the nasopharyngeal, tracheobronchial, and pulmonary regions. In addition, a basic knowledge of the complex-ion and colloidal properties of plutonium in aqueous solutions is necessary for the interpretation of the transport mechanism in living systems. Chapter 6 is a critical review concerning the evaluation of internal dose and includes a summary calculation that begins with an assumed release from the reactor and carries through to computation of potential doses.

In attempting to cover the subject matter described here, the authors have drawn on all relevant published information in the many interrelated disciplines involved. These data and information are then interpreted to present a consistent and comprehensive picture beginning with the release and proceeding to the resulting dose. In so doing, it is evident that there will not be complete agreement on all facets. Some discrepancies could be resolved by the preponderance of the evidence; others could not and remain in this report as areas where additional work is necessary. Such expectations notwithstanding, this report achieves its desired end and adequately references the existing literature for those who wish to explore any of the facets to greater depth.

2. BEHAVIOR OF RELEASED SODIUM OXIDE AND PLUTONIUM-BEARING PARTICLES

To calculate the behavior of an aerosol within a reactor containment system as time elapses after its generation requires a knowledge of the initial condition of the aerosol and the effects of the conditions under which it would agglomerate, settle, and plate out. The estimates must be based on the scaleup of aerosol behavior from laboratory and intermediate-scale conditions to power reactor conditions. These estimates are related to reactor design features, experimental data, known effects of moderate scaleups, and application of established aerosol theory. Some of the major factors to be considered are initial aerosol concentrations, convection currents, containment sizes, and radiation levels.

There is considerable experimental data on the formation, agglomeration, transport, and deposition of the oxide aerosols of uranium, sodium, and cladding materials with which the plutonium oxide would be intimately mixed in a fast reactor containment vessel after a postulated release.¹ Experimental data on the agglomeration and settling of plutonium oxide aerosols, alone and in combination with aerosols of uranium oxide and sodium, have been obtained by Castleman.²⁻⁵

Several models describing the decay of mass concentration and changes in particle size with time are presented in this section. There have been significant developments in aerosol modeling that provide a basis for substantially improved predictions of aerosol behavior.

This report is primarily concerned with plutonium aerosols; however, the designer and analyst must also include the inventories of the fission products and other actinides in a survey of potential hazards from an LMFBR even though they are outside the scope of this report. As examples, curium, strontium, cesium, and ruthenium should be considered in safety evaluations. However, except for the data in Table 2.1, we have not attempted to cover these radionuclides in this report. Additional information is now available in a recent report.⁶

Table 2.1. Estimated steady-state inventory of actinides in 1000-MW(e) LMFBR power reactors^a

Nuclide	LMFBR inventory ^b (kg)
²³⁸ U	42,300
²³⁷ Np	2
²³⁸ Pu	29
²³⁹ Pu	2490
²⁴⁰ Pu	870
²⁴¹ Pu	141
²⁴² Pu	64
²⁴¹ Am	11
²⁴³ Am	6
²⁴² Cm	0.7
²⁴⁴ Cm	0.4
Total	46,000

^aStaff of the Chemical Technology Division, Aqueous Processing of LMFBR Fuels — Technical Assessment and Experimental Program Definition, ORNL-4436, pp. 321-91 (June 1970).

^bQuantities in core and blankets of Atomics International reference oxide LMFBR.

2.1 Aerosol Behavior Considerations*

The theoretical basis of contemporary aerosol models is that due to Brownian movement, turbulence, and the different rates of fall of various sized particles under the influence of gravity. Collisions between the particles take place, and upon collision agglomeration results. There will thus be a gradual increase in the average size of the particles and a reduction in smeared density of the agglomerates constituting the aerosol due to these collisions, and the problem is to determine what the resultant size and mass distribution of the aerosol will be as time increases.

*Largely reproduced from Ref. 1.

The basic coagulation equation for aerosols having a distribution of particle sizes has the form

$$\frac{\partial n(v, t)}{\partial t} = A_+(v, t) - A_-(v, t) , \quad (1)$$

where

$n(v, t)$ = concentration of particles of volume v ,

$A_+(v, t)$ = rate of formation of particles of volume v by agglomeration of smaller particles,

$A_-(v, t)$ = rate at which particles of volume v are lost by agglomeration to yield larger particles.

The terms A_+ and A_- are integrals over the various sizes (volumes) of particles that contribute to the processes they respectively represent. They contain the distribution function $n(v, t)$ and also a "coagulation coefficient,"

$$K(v, v') , \quad (2)$$

which represents the rate of collision between particles of volumes v and v' if such particles are at unit concentration. The three mechanisms given below are possible contributors to the collision of the aerosols. All assume an efficiency of 1 for particle collisions.

2.1.1 Brownian motion

Brownian motion of the aerosol particles arises from their collisions with air molecules that are in thermal motion.

2.1.2 Gravity

Particles falling under the influence of gravity will distribute themselves over a range of speeds because of the dependence of the resistance of air on particle size. As a result, coarse particles will tend to sweep past finer ones, thereby causing collisions. The coagulation constant is, of course, different than that defined in Eq. (2).

2.1.3 Turbulence

The two ways in which turbulence can cause collisions between adjacent particles are (1) spatial variations of the turbulent motion causing eddies to collide with one another and thereby producing collisions between the particles entrained in the eddies (shear) and (2) turbulent accelerations of an eddy and the size differences of entrained particles causing them to collide within an eddy. In both situations the magnitude of the effect depends on the values of the parameter ϵ , the rate of energy dissipation per unit mass of suspended material. A more thorough discussion of the relative importance of these three effects is presented in Ref. 1.

For application to reactor safety problems, it is necessary to modify Eq. (1) by adding terms that represent two effects not contemplated in the theory for colliding particles.

1. The aerosol production rate must be represented by a source term $S(v, t)$.
2. Aerosol particles are removed from the system by fallout, by leakage from the containing vessel or chamber, and by deposition on the walls of the container. This is represented by a removal term $R(v, t)$. With these modifications, the coagulation equation takes the form

$$\frac{\partial n(v, t)}{\partial t} = A_+(v, t) - A_-(v, t) - R(v, t) + S(v, t) . \quad (3)$$

The equation now develops in two stages.

1. The removal term $R(v, t)$ is described by a removal coefficient $R(v)$, while the agglomeration terms $A_+(v, t)$ are controlled by the coagulation coefficient $K(v, v')$. The physical processes that contribute to these effects have to be modeled and formulated as contributions to these coefficients, thus making specific the general Eq. (3).

2. The specific equation thus obtained must be solved to obtain the size distribution at all times, $n(v, t)$. The solutions are obtained from computers, and more rigorous treatment can be found in the next sections of this report.

The removal processes of primary practical concern are leakage, fallout, and plating. In the model used for the former, the mixture of air and aerosol particles is supposed to escape without change of composition at a rate determined by the nature of the leaks. This is conservative, since it makes no allowance for deposition of aerosol particles in the channels through which leakage occurs. The fallout model used is that of "stirred settling," in which the spatial variations in composition of the aerosol, due to concentration of larger particles in the lower part of the chamber by their more rapid fall, are assumed to be wiped out by the convection currents set up in the air by heat generated at the floor.

In small chambers, wall deposition is significant. A theory of this effect is therefore needed in the calculations for small chambers, even though it will not contribute appreciably in chambers used to house reactors. The theory used treats the deposition as occurring by Brownian diffusion to the wall through a laminar boundary layer whose thickness is adjusted to give the observed total amount of the deposition. This is in effect a semiempirical method of subtracting the wall deposition from the other phenomena involved, which are the real objects of the investigation. Its purpose is to derive from the total deposition the time dependence of the deposition. Since the deposition increases steadily with time, the latitude within which its time dependence can vary is limited, and since the total wall deposition is only about half the fallout, the error in treating the latter is still smaller. Hence, such a simplified interpolation theory for deposition should be adequate when extrapolations are made to large chambers.

In terms of the number density distribution $n(v,t)$ of the suspended material, the integrodifferential equation for the behavior of a heterogeneous aerosol is

$$\frac{\partial n(v,t)}{\partial t} = 1/2 \int_0^v n(v',t) n(v-v',t) F(v',v-v') dv' - n(v,t) \int_0^\infty n(v',t) F(v,v') dv' - R(v) n(v,t) + S(v,t), \quad (4)$$

where

$v = r^3$, that is, spherical particles are assumed,

r = particle radius,

$F(v, v')$ = normalized collision kernel which gives the probability of collision between two particles of radii r and r' due to Brownian motion and due to differences in settling velocities (gravity),

$R(v)$ = removal rate due to settling, wall plating, and leakage,

$S(v, t)$ = source rate for particles of radius r .

The first integral represents the rate of production of particles of size v due to all collisions between two particles of size v' and $v - v'$. The second integral gives the rate at which particles of size v grow to larger sizes due to collisions with particles of size v' .

The removal rate is given by

$$R(v) = G_R v^{2/3} [1 + C_1(v)] + P_R v^{-1/3} [1 + C_1(v)] + R_L, \quad (5)$$

where

$G_R = 2g\delta/9h\eta$, the settling constant,

h = height of chamber, V_c/A_F ,

η = viscosity,

δ = density of aerosol material,

g = acceleration due to gravity,

$P_R = kT A_w / (6\pi\eta \Delta V_c)$, the plating constant,

A_F = area of the floor,

A_w = area of surface for plating,

V_c = volume of chamber,

Δ = distance perpendicular to the wall over which a gradient of the particle density is assumed to exist (Δ is an adjustable parameter required to fit experimental wall plating data),

k = Boltzmann constant,

T = temperature.

The term containing G_R is the removal rate due to settling, and the term containing P_R is the removal rate due to plating. The R_L term is the removal rate due to leakage and is a constant, independent of particle size. Both G_R and P_R are geometry dependent.

2.2 Experimental Evidence for Decay of Mass Concentration and Changes in Particle Size of Airborne Aerosols with Time

The experimental results presented here constitute our primary source of information on plutonium dioxide aerosol behavior. Most of them were obtained by investigators at Brookhaven National Laboratory and at Atomic International.

The important properties of aerosols are physical rather than chemical. Aerosols are often referred to as solid-gas colloids, like smokes. The fact that they remain suspended in air for appreciable times is related to such physical properties as density, particle size, particle size distribution, and the electrostatic charge on the individual particles. The temperature and the rate at which the initial vaporization and ultimate condensation take place determine the stability of an aerosol. Particular attention must be directed to the formation of chainlike or fluffy agglomerates because their properties will be different from those of the small, dense particles of which they are made. Large, dense particles tend to settle rapidly. Either low-density agglomerates or small individual particles may remain suspended for an appreciable time (1 to 30 days).

Over the past three years investigators at Brookhaven have reported a series of studies of aerosols produced by vaporizing fast reactor fuel materials between about 2500 and 3000°C and of aerosols of these materials combined with sodium vaporized at 700°C. The aerosols were suspended in argon, nitrogen, and air, both dry and humid. The experimental work of Castleman and Horn, which has provided much of the basis for subsequent dose calculations, is summarized in the discussion below and is described in greater detail in Ref. 2.

The data from oxidation of plutonium metal and its compounds at and below 1200°C, which are essential to evaluations of hazards in the processing of plutonium fuel, may have very limited applicability to the prediction of aerosol behavior after a release in a sodium-cooled fast reactor.⁷⁻¹⁶ Airborne particles obtained in oxidation experiments have generally been at least 10 to 100 times as large as the agglomerated particles from vaporized PuO₂ or UO₂. The corresponding mean masses of the particles obtained from the oxidations at 1200°C and below would be 10³ to 10⁶ times

those from vaporized fuel. Data on accidental releases of plutonium from other events, such as fires and explosions, may also be of limited applicability.¹⁷⁻²¹

Recent experiments on the decay of the mass concentration of airborne particles indicate that in the case of aerosols generated by vaporization and condensation, high initial mass concentrations decay very rapidly during the first few minutes after aerosol generation is complete. This can be shown to hold for aerosols in reactor containment structures under post-release conditions, so that the peak airborne mass concentration in the outer containment structure following leakage from the inner containment barrier would be a factor of 10^{-3} or 10^{-4} lower than the high initial mass concentration generated in the inner containment vessel.

Most investigations of aerosols of interest have been conducted with oxides of uranium, stainless steel, or sodium. Studies of the decay of airborne mass concentration by Horn and Castleman,² Baumash, Nelson, and Koontz,²² Schikarski and Wild,²³ and Stoute and Van der Vate²⁴ cover a range from oxides of heavy- and medium-weight metals to the oxides of sodium, which is a very light metal, and include some results for metals in the metallic form.

Investigators at Atomics International have published experimental data on the behavior of oxides of sodium and uranium in small- and intermediate-scale vessels. They have recently published data on sodium aerosols in a large (30-ft-high) vessel with high initial concentrations. Koontz et al.²⁵ found that in the large vessel (about 60 m^3 in volume), an aerosol of sodium oxide settled out more slowly than a sodium oxide aerosol of about the same concentration in a smaller vessel (6 ft high) but much faster than would be expected from simple extrapolation based on the ratio of the heights of the two vessels. This enhancement of the ratio of settling rate to vessel height in the larger vessel was attributed primarily to an increase in the frequency of collisions as a result of gravitational agglomeration.

Horn and Castleman² showed that aerosols of PuO_2 , UO_2 , and $\text{UO}_2\text{-PuO}_2$ generated by high-temperature vaporization were similar in appearance, as seen by an electron microscope, and behaved similarly (in a 0.75-m^3 vessel). This may provide a basis for simulating the behavior of PuO_2 -bearing

aerosols in large containers by vaporizing UO_2 and observing and measuring its behavior. The UO_2 and $\text{UO}_2\text{-PuO}_2$ aerosols settled out more rapidly than the PuO_2 aerosol, but this may be accountable if we consider size, mass, and density factors that are required to model a hypothetical core disruptive accident (HCDA) in the simulation. Mixed oxide fuels for sodium-cooled fast breeders are expected to contain about 80% UO_2 and 20% PuO_2 , and in any aerosol resulting from a fuel release, the PuO_2 is expected to be intimately mixed with UO_2 .

Horn and Castleman's data² show that sodium in moderate proportions (Na/PuO_2 ratios of 1 and 12.5) increased the rate of removal of PuO_2 aerosols, but aerosols containing higher proportions of sodium settled more slowly. Baumash, Nelson, and Koontz²² found that in a larger vessel (1.1 m³, 6 ft high), an aerosol containing about 80% Na_2O , 15% UO_2 , and 5% iron and tungsten oxides settled slightly more slowly than a similar aerosol containing about 65% UO_2 and no sodium. They also found in a single test of mixed metallic oxides that the concentrations of airborne sodium oxide, uranium oxide, and iron oxide decreased at similar rates. This indicated that the aerosol particles behaved as a composite of the oxides rather than as separate materials.

It is concluded from these experiments and from an examination of pertinent phenomena that UO_2 may be an adequate simulant for mixed $\text{UO}_2\text{-PuO}_2$ fuel oxides in aerosol studies, that a mixture of UO_2 and sodium may be a good simulant for aerosols in the nitrogen-filled primary barrier, and that a mixture of UO_2 with sodium allowed to burn in air may be a good simulant for aerosols in the air atmosphere of the outer containment structure.

2.3 Empirical Models and Equations for the Decay of Mass Concentration and Changes in Particle Size with Time

Several groups of investigators have developed theoretically based models or empirical equations that describe the processes of agglomeration and settling and enable safety analysts to evaluate the reductions in the airborne amounts and concentrations of plutonium-bearing aerosols through these processes. These mathematical descriptions of the mechanisms involved

and of the effects of various parameters are all based, to various extents, on both established aerosol theory and consideration of experimental data. All have been compared with experimental results.

The primary objective of all the models and empirical equations is to calculate the decay of the mass concentration of plutonium-bearing aerosols in a contained volume with time. The usual approach is (not necessarily in this order) to calculate the number of airborne particles in each of many particle size increments during each of many time increments, convert particle size to particle mass, integrate or sum over the particle size (or mass) spectrum for each time increment to produce the total airborne particle mass during that time increment, and, finally, plot the results as a curve of airborne mass concentration vs time.

2.3.1 Schikarski model

Schikarski,^{26,27} at Kernforschungszentrum Karlsruhe, presented an aerosol model based on (1) an accident in a nuclear reactor releasing a very large amount of radioactive material that must stay airborne for a long time (hours) to leak through the containment barriers and present a hazard to the environment, (2) the released material existing essentially in the form of gases and aerosols, and (3) the release of gases from the reactor plant being fairly accurately predictable. The problems to be resolved lay in understanding the transport characteristics of nuclear aerosols generated in core-destructive accidents and suspended in the containment atmosphere. Schikarski concluded that his aerosol model provided several advantages that could lead to a realistic description of activity release. It does not require knowledge of how much active material is released from the fuel, but rather how much active material can stay airborne in the containment atmosphere during the accident.

Schikarski and Wild²³ found that high mass concentrations are unstable and decrease in a few hours. Dose calculations with the MUNDO code²⁸ to investigate the influence of a high initial mass concentration showed limited influence of initial concentration on the integrated dose due to PuO₂ aerosols.

2.3.2 Davis model

A computer code for estimating particle phase concentration vs time in a reactor containment structure was devised by Davis^{29,30} at Oak Ridge National Laboratory. Several approximations, but no empirical constants, were used. The objective was to provide a systematic hypothesis to guide experiments and to show that the change of the concentration with time could be simply estimated from theory. For the calculation the "self-preserving" particle size distribution was used, and it was presumed that two deposition mechanisms are important. The distribution function^{31,32} was assumed to be the one derived by Liu and Whitby³¹ from a steady-state postulate. It was assumed that the function applies approximately over the range of experimental values for the particle radius (r_{\min} to r_{\max}) to give

$$\frac{dn}{dr} = \frac{3}{4\pi} \phi r^{-4} \ln \frac{r_{\max}}{r_{\min}},$$

which is the distribution of number concentration n among particle radius values r ; ϕ is the volume of particle phase per unit volume of aerosol.

The first deposition mechanism applies to very dense smoke in which the particles run into many other particles before colliding with anything else. Some very large particles develop that fall quickly. The deposition rate is a simple function of the initial concentration, the minimum particle radius, and the time. The second deposition mechanism is the well-known "stirred settling" augmented by coagulation. In a well-mixed aerosol, particles drift into the boundary layer along the floor and settle. Coagulation maintains the size distribution. Deposition depends on maximum and minimum particle size, particle density, tank height, and the viscosity of air. This calculation is performed by computer iteration.

The general effect of particle size is clear. An aerosol composed of small particles (at high concentration) clears out fast at short times but has a persistent tail. An aerosol of large particles does not clear as fast at short times, settles faster at intermediate times, and does not leave a persistent tail.

2.3.3 Koontz model

The experimental results for Na_2O particulates described by Koontz, Nelson, and Baurmash³³ appear to fit the general behavior of an agglomerating aerosol in a stirred environment. Because of the empirical relations observed it has been possible to formulate models that effectively predict the results obtained with a laboratory test chamber. These models, in turn, can be used in extrapolations to make predictions for accidents in liquid-metal-cooled fast breeder reactors. When growth in particle size is allowed, for a given released mass concentration, a considerable reduction in the radiological source term occurs, since the fallout rate is increased and the concentration available for leakage is thus decreased.

Calculations of the rate of stirred settling of particles with size distributions characterized as log-normal are presented by Koontz, Hubner, and Greenfield³⁴ of Atomics International. The data are in a form that provides for estimating the fractional decrease of the concentration with time for a given initial distribution. A log-normal distribution is completely characterized by the median size and geometric standard deviation. Additional data are presented that permit determination of the fraction of the mass released into a vessel that leaks out as a function of time for a given distribution. Finally, an empirical relation is suggested for estimating the median particle size produced by agglomeration of the initial particles as a function of the mass introduced into the test chamber. The settling velocities are computed on the basis of Stokes law.

The computations show that the fraction of the radioactive materials released during an HCDA in an LMFBR that leaks out may be considerably reduced by agglomeration and settling of the aerosols. A procedure is given for computing the reduction factor for the radiological source term as a function of the particle size distribution of the aerosol. An empirical relation is derived from experiments performed at Atomics International by Koontz et al.¹ in a small test chamber that relates the mass concentration, in partially sealed containers, to the particle size distribution produced by agglomeration of the aerosol. When the particle size distribution, the leak rate, and the height of the enclosure are

specified, the fraction that has leaked at any time can be read from the figures presented in their report.

2.4 Detailed Discussion of an Aerosol Model and Its Applications

In comparing results obtained from the models with experimental results, both used initial radii (Atomics International used median radius by volume; Brookhaven National Laboratory used geometric mean radius) and initial geometric standard deviations based on averages of experimental observations during the first few minutes of each experiment. Both used heights of containing vessels and initial mass concentrations based on experimental data. Agreement with experimental results was quite good for both models.

Generally, there is agreement that the mass concentration of an aerosol with a very high initial number density (particles per unit volume) will decay rapidly during the first several hours, then less rapidly for a day or so to a very small (10^{-3} to 10^{-4} g/cm³) concentration, and finally still more slowly for an extended period. Accurate comparison of models for the prediction of aerosol behavior is exacting and requires careful, thorough, term-by-term examination of each model and its derivation from established theoretical or empirical equations. This need for detailed analysis results, in part, from the differences in approach, emphasis, and philosophy of the models. It is affected strongly by differences in the completeness and order in which derivations and sources of equations, constants, and correction factors are shown. Furthermore, each model is described in several reports and papers,^{3,4,35-37} each of which shows one, several, or a number of refinements in the model or its application.

To realistically assess aerosol behavior for application to a hypothetical accident, the more complex analyses are required. Treatments by Koontz and his colleagues³⁵⁻³⁷ at Atomics International and by Castleman and others^{3,4} at Brookhaven National Laboratory are very similar. Both installations include terms for addition of particles by (1) a source with a log-normal particle size distribution, (2) thermal (Brownian) motion,

and (3) gravitational agglomeration; both include terms for removal of particles by processes 2 and 3, (4) gravitational settling, and (5) wall plating; both originally included terms for turbulent agglomeration but found the effects of turbulence to be negligible and dropped the terms. At Brookhaven a calculated particle capture coefficient that varied according to particle size was used in the gravitational agglomeration term; a uniform capture coefficient of unity (not varied by size) has been employed at Atomics International, although recent code revisions have improved model flexibility in this area.

The amount of material that is available for leakage to the environment has been shown to be dependent on the amount of material released from the core during a hypothetical core disruptive accident (HCDA), the behavior of the resulting aerosol in both the primary and the secondary containment, and the leakage characteristics of both containment structures.³⁸ The mass of material released in an HCDA also depends on the estimated energy release for the HCDA, the interaction phenomena of molten and/or vaporized fuel and coolant that occur subsequent to the energy release but prior to an actual release from the primary system into the containment structures, the leakage rate expected for a given pressure, and the way in which the pressure varies with time. The following treatment of the problem, including tables and figures, has been extracted from Ref. 1.

The behavior of the aerosol and its decrease as an airborne phase involves several interacting mechanisms. The effect of these mechanisms on reducing the airborne concentration and the subsequent leakage to the atmosphere is a function of a number of input parameters used in the HAA-3A computer code to describe the behavior of an aerosol. Some of these parameters, such as height and volume of the containment vessel, leakage characteristics of the containment vessel, mass of material released, and gas temperature, are fixed by the description of the accident. Other parameters that are less well understood can be varied by the analyst to study the sensitivity of the computed results to their variations. The initial particle size distribution of the released material, the efficiency of gravitational and turbulent agglomeration, and the correction

to the Stokes settling velocities due to the presence of nonspherical loosely packed agglomerates are of this nature.

The input parameters for the LMFBR base case are shown in Table 2.2. A series of HAA-3A computations were performed to determine the sensitivity of the results to changes in the input parameters. The parameters that were varied were the mass median and the magnitude of the Stokes factor, the efficiency of gravitational agglomeration, and the gas temperature.

Table 2.3 gives the results of these calculations. They show that the mass of material that leaks from the outer containment building is

Table 2.2. Input parameters for the LMFBR base case

Parameter	Inner containment	Outer containment
Mass of sodium released, kg	420	
PuO ₂ released, kg	20	
Volume, m ³	5.2 × 10 ³	3.8 × 10 ⁴
Height, m	10.4	22.4
Ideal density, ^a g/cm ³	3.00	3.00
Leakage rate	Variable	Variable
Gas temperature, °K	800	400
Gas viscosity, poises	3.70 × 10 ⁻⁴	2.27 × 10 ⁻⁴
Initial mass median radius, μm	0.3	Variable
Initial sigma, geometric standard deviation (σ) based on the assumption of an initial log-normal distribution	2.0	Variable
Collision efficiency of gravitational agglomeration	1.0	1.0
Correction factor for Stokes settling velocity	0.33	1.0

^aWeight according to relative masses of fuel and sodium.

Table 2.3. Parameter sensitivity of LMFBR base case

Parameter	Mass leaked from primary (g)	Total mass leaked from outer (g)		Plutonium leaked from outer (g)	
		2 hr	30 days	2 hr	30 days
LMFBR base case, Stokes velocity correction in outer = 1.0	312.6	1.2×10^{-2}	2.1×10^{-1}	6.0×10^{-4}	1.0×10^{-2}
Initial mass median radius = 0.3 μ ; Stokes correction factor in inner and outer = 0.33; gravitational collision efficiency = 1.0	406.2	1.2×10^{-2}	6.6×10^{-1}	6.0×10^{-4}	3.3×10^{-2}
Initial mass median radius = 0.3 μ ; Stokes correction factor in inner and outer = 0.10; gravitational collision efficiency = 1.0	1.05×10^3	1.7×10^{-2}	1.83	8.5×10^{-4}	9.2×10^{-2}
Initial mass median radius = 0.3 μ ; Stokes correction factor in inner and outer = 0.33; gravitational collision efficiency = 0	5.23×10^3	5.6	6.2	2.8×10^{-1}	3.1×10^{-1}
Initial mass median radius = 0.1 μ ; Stokes factors = 0.33; efficiency = 1.0	430.9	1.3×10^{-2}	7.0×10^{-1}	6.5×10^{-4}	3.5×10^{-2}
Base case except viscosity = 1.86×10^{-4} ; temperature = 300°K	242.2	7.2×10^{-3}	3.9×10^{-1}	3.6×10^{-4}	2.0×10^{-2}

insensitive to a reduction of the initial mean particle radius from 0.3 to 0.1 μ . As the size is increased, the mass leaked decreases. The mass that leaks from the outer containment building in 2 hr is insensitive to a change in the Stokes correction factor from 1.0 to 0.1, but the 30-day value is inversely proportional to the Stokes factor; that is, small settling rates increase the leaked mass. A Stokes correction factor of 0.33 (which is in good agreement with experiment) increases the mass leaked in 30 days only by a factor of 3.0 over the base case. The effect of changing the gas temperature is as expected.

The parameter that has the greatest effect on the mass leakage is the efficiency of gravitational agglomeration. When it is assumed that there is no gravitational agglomeration (the coagulation efficiency is zero), the mass leaked by 2 hr is increased by a factor of almost 50, and the mass leaked in 30 days is increased by a factor of 10. Figures 2.1 and 2.2 show the behavior of the aerosol for the base case (efficiency of 1) and for the case with an efficiency of zero. An additional study of the effects of collision efficiency was made, and the results are shown in Table 2.4. Reduction of the efficiency from 1.0 to 0.5 increases the mass leaked by less than a factor of 2.0. It has been shown¹ that good agreement with experimental data was obtained for a collision efficiency of 1.0. Even if the efficiency were reduced slightly, the effect on the mass leaked from the outer containment building would be minimal.

Table 2.5 compares the total masses leaked for a monosize and a heterogeneous particle size distribution. For these calculations the containment volume was 4.25×10^9 cm³, the height was 914 cm, the leak rate was constant at 10 vol %/day, and the gravitational efficiency was 1.0. It can be seen that if the input material is monosized and the initial concentration is constant ($\sigma = 1.0$), changes in the initial size of the aerosol do not significantly alter the leaked mass. For heterogeneous aerosols ($\sigma = 2.0$), the mass leaked is inversely proportional to the initial median size. The total mass leaked at the lower initial concentration is higher because agglomeration is not as effective as it is at the higher concentration. The aerosol remains airborne longer and allows more material to leak.

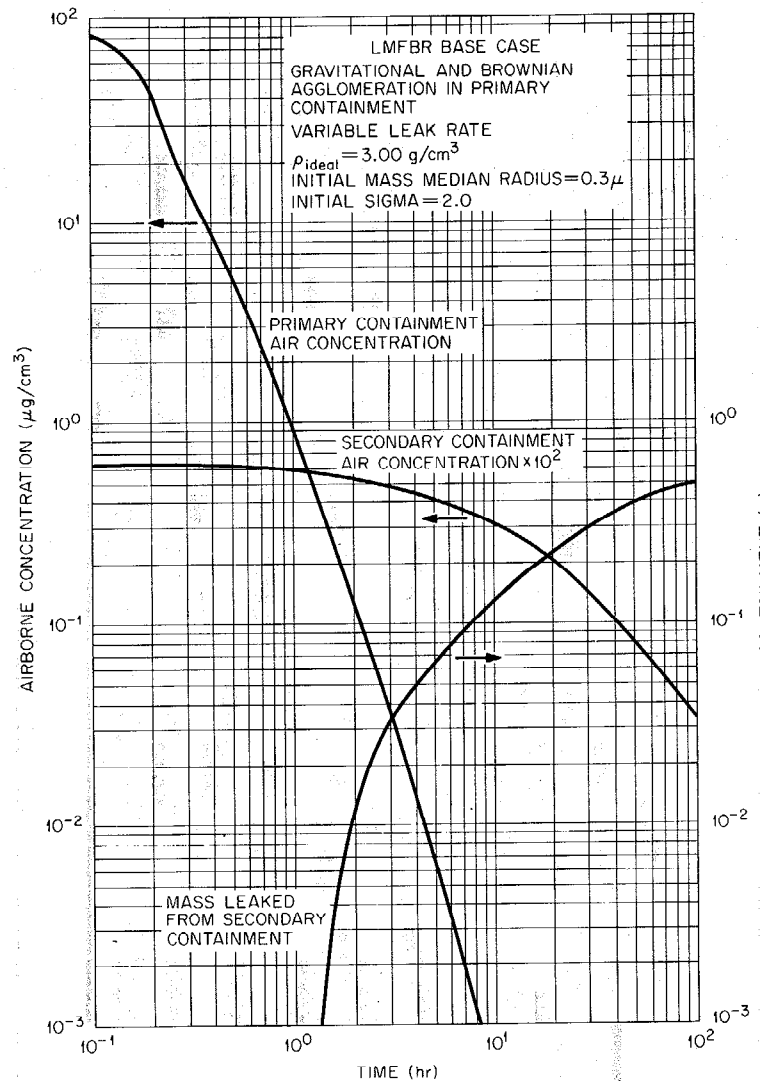


Fig. 2.1. LMFBR base case with Stokes correction factor = 0.33 and collision efficiency = 1.0.

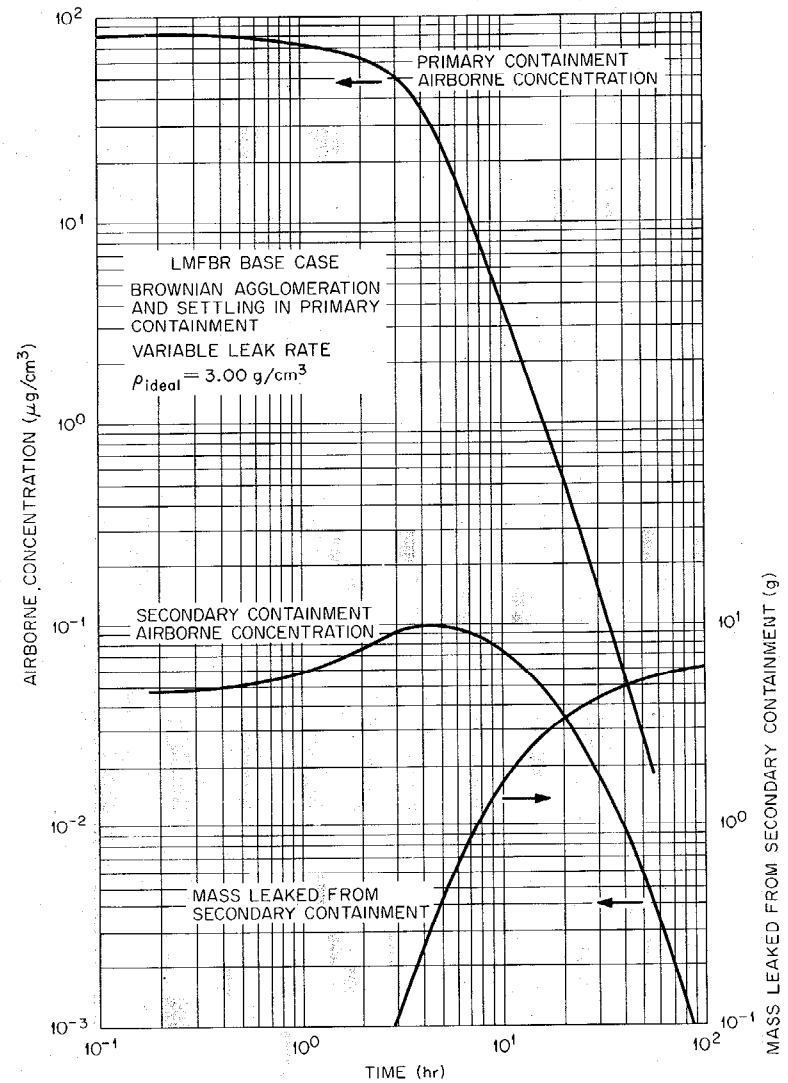


Fig. 2.2. LMFBR base case with Stokes correction factor = 0.33 and collision efficiency = 0.

Table 2.4. Effects of collision efficiency of gravitational agglomeration

	Collision efficiency of -		
	1.0	0.5	0
Initial airborne concentration, $\mu\text{g}/\text{cm}^3$	235	235	235
Initial air concentration half-time, sec	62.5	105	4.0×10^3
30-day mass leakage from inner containment, g	74.7	130	6.5×10^3
Initial airborne concentration, $\mu\text{g}/\text{cm}^3$	23.5	23.5	23.5
Initial air concentration half-time, sec	610	1040	1.0×10^4
30-day mass leakage from inner containment, g	86	156	1.6×10^3

Table 2.5. Effects of input particle size parameters

Airborne concentration ($\mu\text{g}/\text{cm}^3$)	$(\bar{r}_v)_0$	σ_0	ρ	Initial air concentration half-time (sec)	Total mass leaked from inner containment (g)
235	0.1	1.01	1.0	62.0	73.8
235	0.5	1.01	1.0	61.5	73.4
235	1.0	1.01	1.0	56.5	67.6
235	0.1	2.00	1.0	62.5	74.7
235	0.5	2.00	1.0	40.0	48.0
235	1.0	2.00	1.0	27.1	33.5
23.5	0.1	1.01	1.0	608	84.8
23.5	0.5	1.01	1.0	603	83.7
23.5	0.1	2.00	1.0	607	86.2
23.5	0.5	2.00	1.0	400	63.3
23.5	1.0	2.00	1.0	282	51.1

All previous safety analyses of hypothetical LMFBR accidents have been made with the assumption of an instantaneous source. Calculations were run to determine the effect of different source times on the leaked mass. Table 2.6 shows these comparisons. It can be seen that increasing the source time increases the mass leaking from the inner containment vessel to the outer and also increases the amount of material that could leak to the atmosphere. The table also shows that the leaked mass at 2 hr and at infinite time is the same when the source time is not too long. It is unlikely that the prolonged source will produce a concentration as high as the instantaneous source in the primary vessel.

The calculations presented here show the versatility of the model. High initial concentrations decay rapidly and reduce the amount of aerosol available to leak. If a constant released mass is assumed and the number of released particles at the time of the HCDA is calculated from the ideal density ($N_0 = \text{constant}$), then the use of a lower Stokes settling velocity will increase the amount of material that will leak from the containment. The increased leakage occurs because the lower settling velocity causes the aerosol material to remain airborne longer. However,

Table 2.6. Effects of continuous source release

	Source time (hr)		
	0	1	4
$C_R, \mu\text{g}/\text{cm}^3$	235	235	235
$(\bar{P}_V)_0$	0.5	0.5	0.5
σ_0	2.0	2.0	2.0
Mass leakage at 2 hr, g	48.0	480.0	446.8
Mass leakage at $t = \infty$ from inner containment, g	48.0	482.7	974.0
$C_R, \mu\text{g}/\text{cm}^3$	23.5	23.5	23.5
$(\bar{P}_V)_0$	0.5	0.5	0.5
σ_0	2.0	2.0	2.0
Mass leakage at 2 hr, g	61.7	167.0	126.2
Mass leakage at $t = \infty$ from inner containment, g	63.3	181.5	349.3

the increased residence time allows the aerosol to agglomerate to larger sizes, which in turn have greater settling velocities. The net result is that the amount leaked increases but not as much as one would predict from the ratio of the densities. At high initial concentrations of small particles, a decrease in the Stokes factor of 0.25 increases the mass leaked by less than a factor of 3. The computations agree with theories developed by Hidy et al. in 1965.³⁹

2.5 A Postulated Release of Radionuclides from an LMFBR-Type Reactor under Accident Conditions

LMFBRs are designed with multiple barriers so that the release of any fuel debris to the atmosphere is very unlikely. However, in this section we will postulate hypothetical conditions that could result in the release of plutonium, uranium, and sodium oxide aerosols from the primary reactor boundary.

The postulated HCDA will include gross cladding failure in many of the fuel elements, with partial meltdown and vaporization of the fuel. Such an accident would ultimately release sodium, sodium vapor, and gaseous fission products as well as solid fission products and fuel material from the primary reactor boundary into the inerted concrete vault structures. The aggregate behavior of the released material is a continued agglomeration and settling of suspended aerosols. The time-dependent aerosol concentration (with the associated particle size range) will then be used to calculate the release of plutonium-bearing aerosols into the atmosphere.

A schematic diagram is included here, as Fig. 2.3, showing the multiple barrier system employed in a conceptual design of a liquid-metal-cooled reactor.⁴⁰ The reactor vessel contains the reactor core in a pool of sodium covered by argon blanket gas. This vessel is enclosed in a steel-lined concrete vault, serving as the primary barrier, which contains nitrogen and will prevent combustion of sodium in case of leakage from the coolant system. It should be remembered that the vapor pressure of liquid sodium is low and that liquid-metal-cooled reactors operate at very low pressures in comparison with the PWR and BWR reactors. Figure 2.4

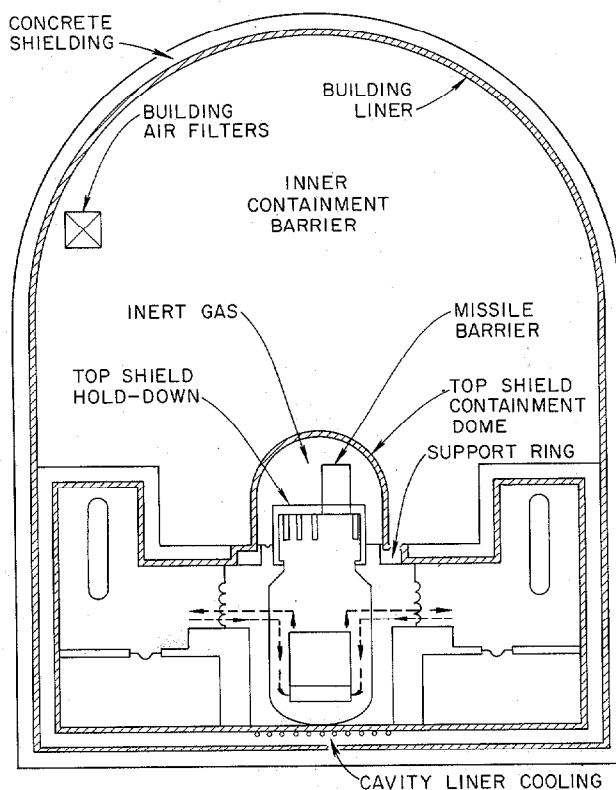


Fig. 2.3. Reactor containment features.

shows possible pathways by which aerosols might be released to the outer containment building.

In order to calculate the consequences of a plutonium-bearing aerosol release, we postulate an HCDA that will create a sodium vapor bubble in the core region, causing the sodium coolant to impact the vessel head and release some sodium into the reactor cavity (pathway 1, Fig. 2.4). After the initial surge the primary reactor vessel head will be essentially resealed by its weight and the reduced pressure. Thus, only the argon blanket gas and some of the sodium coolant will be released to the secondary containment; ultimate noncondensed gases (nobles) from the HCDA may break through the sodium pool above the core.

In order to further evaluate the consequences of a release of a plutonium aerosol, it is assumed that a quantity of fuel will be carried to the surface of the sodium coolant for release into the reactor cavity,

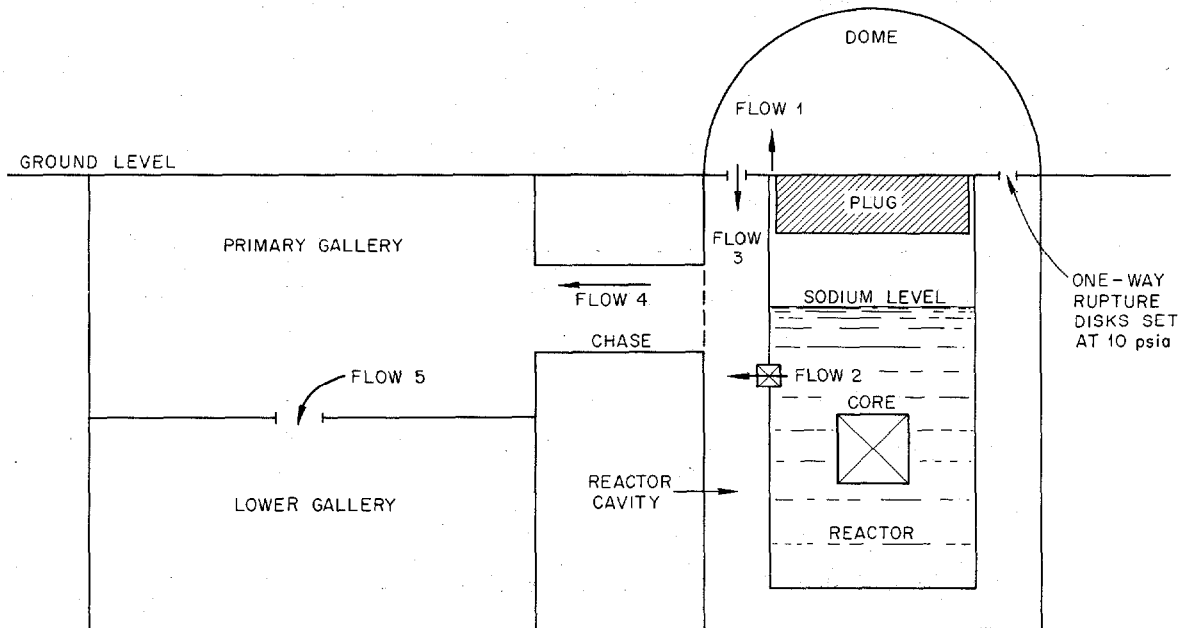


Fig. 2.4. Schematic flow diagram of vapor expansion model.⁴⁰

along with the sodium. The quantities that will ultimately be available for release to the environment will depend on the specific design concept employed, the resultant HCDA developed pressures and temperatures (leak rates), and the aerosol removal processes in containment.

In Figs. 2.1 and 2.2, it is shown that pressures, leak rates, and aerosol concentrations decrease with time.⁴⁰ It should be recognized that computers are needed to handle the continuously changing parameters. Computer codes based on models described previously are available for computing significant quantities.^{1,3,4,35,38,40,41} In Chapter 6, a systematic and integrated calculation of the consequences of a hypothesized release is made, using one such code.

References

1. R. L. Koontz et al., Aerosol Modeling of Hypothetical LMFBR Accidents, AI-AEC-12977 (1970).
2. F. L. Horn and A. W. Castleman, Jr., "PuO₂-UO₂-Na Aerosols Produced by Vaporization of Fast Reactor Core Materials," pp. 93-115 in Treatment of Airborne Radioactive Wastes, IAEA, Vienna, 1968 (also published as BNL-12757).
3. A. W. Castleman, Jr., F. L. Horn, and G. C. Lindauer, "On the Behavior of Aerosols under Fast Reactor Accident Conditions," Paper 32, presented at the International Congress on the Diffusion of Fission Products, Saclay, France, Nov. 4-6, 1969 (Proceedings to be published as CONF-691104); paper also published as BNL-14070.
4. G. C. Lindauer and A. W. Castleman, Jr., "On the Initial Size Distribution of High Number Density Aerosols," Trans. Amer. Nucl. Soc. 12(2), 897 (November 1969).
5. G. C. Lindauer and A. W. Castleman, Jr., Initial Size Distributions of Aerosols, BNL-14512 (February 1970).
6. Siting of Fuel Reprocessing Plants and Waste Management Facilities, ORNL-4451 (July 1971).
7. J. Mishima and L. C. Schwendiman, "The Airborne Release of Plutonium During Overheating Incidents," Trans. Amer. Nucl. Soc. 12(2), 445-46 (1969).
8. J. Mishima, A Review of Research on Plutonium Releases During Overheating and Fires, HW-83668 (August 1964).
9. J. Mishima, Plutonium Release Studies. I. Release from the Ignited Metal, BNWL-205 (December 1965).
10. J. Mishima, Plutonium Release Studies. II. Release from Ignited Bulk Metallic Pieces, BNWL-357 (November 1966).
11. J. Mishima, L. C. Schwendiman, and C. A. Radasch, Plutonium Release Studies. III. Release from Heated Plutonium Bearing Powders, BNWL-786 (July 1966).
12. J. Mishima, L. C. Schwendiman, and C. A. Radasch, Plutonium Release Studies. IV. Fractional Release from Heating Plutonium Nitrate Solutions in a Flowing Air Stream, BNWL-931 (November 1968).
13. R. E. Felt, Burning and Extinguishing Characteristics of Plutonium Metal Fires, ISO-756, Isochem, Inc. (August 1967).

14. S. H. Pitts, Jr., "Factors Influencing the Ignition of Metallic Plutonium," Nucl. Safety 9(2), 112-19 (1968).
15. L. C. Schwendiman, J. Mishima, and C. A. Radasch, "Airborne Release of Particles in Overheating Incidents Involving Plutonium Metals and Compounds," pp. 117-31 in Treatment of Airborne Radioactive Wastes, IAEA, Vienna, 1968 (also published as BNWL-SA-1735).
16. K. Stewart, "The Particulate Material Formed by the Oxidation of Plutonium," Progress in Nuclear Energy, Series IV, vol. 5, pp. 535-79, Pergamon, New York, 1963.
17. Fire - Rocky Flats Plant - May 11, 1969, Serious Accidents Issue No. 306, Dec. 1, 1969, Division of Operational Safety, USAEC.
18. D. C. Hunt, The Restricted Release of Plutonium, RFP-799, pp. 3-5, The Dow Chemical Company, Rocky Flats Division (October 1966).
19. G. Tuck and D. C. Hunt, Addendum to Report RFP-334, Safety Review of the Rocky Flats Proposed Nuclear Safety Facility, The Dow Chemical Company, Rocky Flats Plant (1965).
20. L. J. King and W. T. McCarley, Plutonium Release Incident of November 20, 1959, ORNL-2989 (1961).
21. H. M. Culver and W. B. Cottrell, Plutonium Release from the Thorex Pilot Plant, Nucl. Safety 1(3), 78-80 (1960).
22. L. Baumash, C. T. Nelson, and R. L. Koontz, "The Characterization of UO₂ Aerosols by Aerodynamic Parameters," pp. 63-76 (Paper SM-110/20) in Treatment of Airborne Radioactive Wastes, IAEA, Vienna, 1968.
23. W. Schikarski and H. Wild, "Experiments on the Behavior of Nuclear Aerosols in Fast Breeder Reactor Containment," Paper 29, presented at the International Congress on the Diffusion of Fission Products, Saclay, France, Nov. 4-6, 1969 (Proceedings to be published as CONF-691104).
24. J. R. D. Stoute and J. F. Van der Vate, "The Behavior of Fission Product Aerosols in Relation to the Safety of Sodium-Cooled Fast Breeder Reactors," Paper 39, presented at the International Congress on the Diffusion of Fission Products, Saclay, France, Nov. 4-6, 1969 (Proceedings to be published as CONF-691104).
25. R. L. Koontz et al., "Large-Scale Sodium Aerosol Experiments," Trans. Amer. Nucl. Soc. 12(1), 331 (1969).

26. W. Hafele, F. Heller, and W. Schikarski, "The Principle of Double Containment and the Behavior of Aerosols in Relation to the Safety of Reactors with a High Plutonium Inventory," pp. Vb-4-1-Vb-4-7 in Proceedings of the International Conference on the Safety of Fast Reactors, Aix-en-Provence, France, Sept. 19-22, 1967, Documentation Francaise, Paris, 1968.
27. W. Schikarski, "The Karlsruhe Research Program on Nuclear Aerosols and Its Relation to the Plutonium Hazard of Fast Sodium Reactors," pp. 77-91 in Treatment of Airborne Radioactive Wastes, IAEA, Vienna, 1968 (also published as Kernforschungszentrum Karlsruhe Report KFK-798).
28. F. Heller, W. Schikarski, and A. Wickenhauser, MUNDO - Digital Program zur Berechnung von Unfalldosen in der Umgebung einer Reaktoranlage, Kernforschungszentrum Karlsruhe Report KFK-653 (September 1967).
29. R. J. Davis, "Estimation of Aerosol Concentration in a Nuclear Reactor Containment after an Accident," Paper 34, presented at the International Congress on the Diffusion of Fission Products, Saclay, France, Nov. 4-6, 1969 (Proceedings to be published as CONF-691104).
30. R. J. Davis, A Nuclear Safety Particle Primer, ORNL-4337 (January 1969).
31. B. V. H. Liu and K. T. Whitby, *J. Coll. Int. Sci.* 26, 161-65 (1968).
32. W. E. Clark and K. T. Whitby, *J. Atm. Sci.* 24, 677-87 (1967).
33. R. L. Koontz, C. T. Nelson, and L. Baumash, "Modeling Characteristics of Aerosols Generated During LMFBR Accidents," pp. 51-61 in Treatment of Airborne Radioactive Wastes, IAEA, Vienna, 1968.
34. R. L. Koontz, R. S. Hubner, and M. A. Greenfield, The Effect of Aerosol Agglomeration on the Reduction of the Radiological Source Term for the LMFBR Design Basis Accident, AI-AEC-12837 (Sept. 15, 1969).
35. M. A. Greenfield, R. L. Koontz, and D. H. Hausknecht, Characteristics of Aerosols Produced by Sodium Fires. II. Comparison of Experiment with a General Equation for the Coagulation of Heterogeneous Aerosols, AI-AEC-12878 (Oct. 31, 1969).
36. P. Spiegler et al., Characterization of Aerosols Produced by Sodium Fires. I. Solutions of a General Equation for the Coagulation of Heterogeneous Aerosols, NAA-SR-11997 (May 1967).
37. D. F. Hausknecht and M. A. Greenfield, "A Model Describing the Behavior of the Aerosols Produced by a Sodium Fire," *Trans. Amer. Nucl. Soc.* 10(2), 690 (1967).

38. R. L. Koontz and L. Baumash, Analysis of Aerosol Behavior for FFTF Hypothetical Accidents, AI-69-memo-95 (Oct. 28, 1969).
39. G. M. Hidy, J. Colloid Sci. 20, 123 (1965); G. M. Hidy and J. R. Brock, J. Colloid Sci. 20, 477 (1965); G. M. Hidy and D. K. Lilly, J. Colloid Sci. 20, 867 (1965).
40. 1000 MWe Liquid Metal Fast Breeder Reactor Follow-On Study Conceptual Design Report. III. Plant Safety Analysis, AI-AEC-12792.
41. C. A. Willis et al., "COMRADEX - A New Technique for Reactor Siting Dose Calculations," presented at 13th Annual Health Physics Society Meeting, Denver, Colo., June 16-20, 1968.

3. TRANSPORT, SETTLING, AND REDISTRIBUTION OF AEROSOLS IN THE OUTSIDE AIR (TROPOSPHERE)

Many meteorological variables influence the concentration of aerosols at a particular site. Some of these are (1) fluctuations of the wind direction and speed with time, (2) changes in the atmospheric stability, and (3) precipitation, possibly including rain or snow and the rate and size of each respectively. These variables at one site and the topographical variations between sites dictate that no one model can be used to cover them all. Nonmeteorological variables include variations in release rates, particle size, and the chemical behavior of the aerosol.

3.1 Meteorological Considerations

The basis for the meteorological calculations is discussed below. The Gaussian plume formula is the commonly used method of determining the diffusion of an effluent:

$$\chi(x,y,0) = \frac{Q}{\pi \sigma_y \sigma_z \bar{u}} \exp \left[-1/2 \left(\frac{y^2}{\sigma_y^2} + \frac{h^2}{\sigma_z^2} \right) \right], \quad (1)$$

where χ is concentration, grams or curies per cubic meter; Q is the source strength, grams or curies per second; \bar{u} is the mean wind speed along the x axis, meters per second; x , y , and z are coordinate distances from the source, meters; σ_y and σ_z are dispersion coefficients in the horizontal and vertical direction, meters; and h is the effective source height, meters. Equation (1) was used in determining plutonium concentrations for various release rates and distances.

Since in this study the concern was with the concentration at some distance from the source, the atmosphere was considered, on the average, to be stable, and therefore minimum dispersion of the effluent was assumed. The aerodynamic effects of the containment building were ignored, and the source was considered to be at ground level. Both assumptions are valid for calculating concentrations several hundred meters from the source and for releases of a few hours in duration. As long as the material released is considered to be of small enough size that the terminal velocity of

airborne particles can be ignored, the models for meteorological dispersion and deposition which are generally employed in light-water reactor safety evaluations^{1,2} can be used in evaluations for hypothesized releases from LMFBRs.

3.2 Properties of Na₂O Aerosols in the Atmosphere

A comparison of the aerosol properties of vaporized sodium, uranium, and plutonium dioxides has pointed out the similarities of their behavior under accidental release conditions. References 2 and 23 to 25 in Chapter 2 indicate that it is reasonable to consider sodium as the carrier, with plutonium as a contaminant.

As shown in Chapter 2, the release of plutonium in a hypothetical core disruptive accident (HCDA) in an LMFBR is accompanied by the release of large quantities of sodium, which is rapidly converted to Na₂O particles. Although the fate of dispersed materials may be conservatively estimated by assuming that no substantial growth (modification) will occur of aerosols released to the environment, the properties of Na₂O may be of interest in this regard, since the overall aerosol properties will then be determined by the Na₂O.

Clough and Garland³ studied the properties of Na₂O aerosols in the atmosphere. Sodium, which forms the greater total mass of the aerosol (greater than 100 to 1) is very reactive with the major constituents of the atmosphere (i.e., oxygen, water, and carbon dioxide). Hygroscopic products result in consequent changes in particle size and atmospheric deposition characteristics.

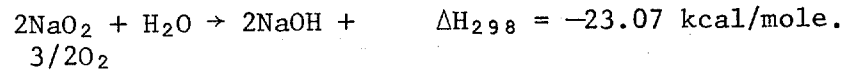
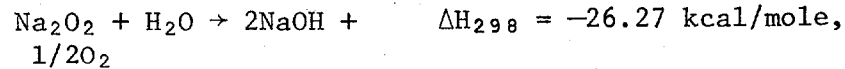
In an environment containing an excess of sodium (e.g., in a reactor containment), oxygen reacts with sodium according to the reaction



However, in the presence of excess oxygen for the case when metallic sodium is released to the atmosphere, peroxides and superoxides are formed:



Sodium peroxide and the superoxide are not stable in the presence of water vapor, and each of them reacts to form sodium hydroxide:



The sodium hydroxide formed is hygroscopic and will condense more water, forming a droplet.

The atmosphere normally contains carbon dioxide at a partial pressure of 0.00033 atm. The reaction of carbon dioxide and sodium hydroxide is energetically favorable:



Continued absorption of carbon dioxide into a droplet of sodium hydroxide will lead to the formation of a solution which, at equilibrium, will be a mixture of carbonate and bicarbonate.

The equilibrium size of droplets containing deliquescent materials may be calculated.⁴ Hydroxide particles are present as solution drops when the relative humidity is above 35%, but the carbonate does not dissolve until the humidity reaches 95%. Under conditions of $35\% < \text{R.H.} < 92\%$, the droplets of sodium hydroxide will dry out rapidly as carbon dioxide is incorporated, the final product being a particle of hydrated carbonate. At higher humidities a relatively large droplet of carbonate solution will be produced.

Table 3.1 presents information on the size and deposition velocity attained by particles under a number of relative humidities.⁵ The larger particles ($>10 \mu$) will deposit much more rapidly than the submicron particles.

At high relative humidities the final state will be a droplet of solution. At humidities below 95% the final state will be a particle of sodium carbonate, although droplets of hydroxide solution may be present for about 1 or 2 min. The appreciable change in size due to changes in relative humidity may lead to important changes in residence time and deposition of the particles in the atmosphere.

Table 3.1. Examples of particle size and deposition velocity attained by sodium particles under various atmospheric conditions

Deposition velocities are based on experimental results of Chamberlain⁵ and apply to a wind speed of 7 m/sec over grass 10 cm high. The experiments were carried out with dry particles, and there was some evidence that droplets, which would adhere to the grass, would have deposition velocities a few times greater.

Mass of sodium particle (g)	Particle as sodium hydroxide								Particle as sodium carbonate decahydrate					
	Dry		70% R.H.		90% R.H.		99% R.H.		Dry ^a		90% R.H.		99% R. H.	
	Radius (μm)	Deposition velocity (cm/sec)	Radius (μm)	Deposition velocity (cm/sec)	Radius (μm)	Deposition velocity (cm/sec)	Radius (μm)	Deposition velocity (cm/sec)	Radius (μm)	Deposition velocity (cm/sec)	Radius (μm)	Deposition velocity (cm/sec)	Radius (μm)	Deposition velocity (cm/sec)
5×10^{-14}	0.3	3×10^{-2}	0.41	3×10^{-2}	0.55	3×10^{-2}	1.1	4×10^{-2}	0.37	3×10^{-2}	0.60	3×10^{-2}	1.0	4×10^{-2}
2×10^{-12}	1.0	4×10^{-2}	1.4	5×10^{-2}	1.8	7×10^{-2}	3.8	0.3	1.2	4×10^{-2}	2.0	7×10^{-2}	3.3	0.2
5×10^{-11}	3.0	0.15	4.1	0.4	5.5	0.7	11	2	3.7	0.3	6.0	0.8	10	0.1
2×10^{-9}	10	1.5	14	2	18	3	40	6	12	2	20	3	33	4
5×10^{-8}	30	4	42	6	55	9	120	35	37	5	65	12	110	30

^aLower states of hydration than the decahydrate are stable at relative humidities smaller than about 80%. The particle size will then be slightly smaller.

References

1. D. H. Slade (ed.), Meteorology and Atomic Energy 1968, TID-24190 (July 1968).
2. Safety Guide 4, "Assumptions Used for Evaluating the Potential Radiological Consequences of a Loss of Coolant Accident for Pressurized Water Reactors," Division of Reactor Standards, Atomic Energy Commission, Nov. 2, 1970.
3. W. S. Clough and J. A. Garland, The Behavior in the Atmosphere of the Aerosol from a Sodium Fire, British Report AERE-R-6460 (1970).
4. J. A. Garland, Atmos. Environ. 3, 347 (1969).
5. A. C. Chamberlain, Symposia of the Society for General Microbiology, No. XVII, Airborne Microbes, p. 138 (1967).

4. CHEMISTRY OF PLUTONIUM

This chapter will assist the reader in understanding the biological chemistry of plutonium, which follows in Chapter 5. Plutonium chemistry is both interesting and complex under conditions which relate to variations in hydrogen ion concentration, ionic states, and low concentrations in solutions (see Sect. 4.2). The properties of plutonium dioxide and mixed oxides have received particular attention in Sect. 4.1.1, since these oxides will be components of the fuel elements for the LMFBRs.

In the absence of surface oxidation, plutonium is a silvery white metal resembling iron or nickel. Its oxidation rate in air depends on the relative humidity. At approximately 0% relative humidity the rate is lower by a factor of 100 to 1000 than at 50%. Oxidation occurs much more rapidly in moist argon than in moist air, suggesting that oxidation is caused by moisture (rather than air) and is anodically controlled. Apparently the absence of air prevents the formation of a tight protective coating on the metal that would inhibit reaction with moisture. Reaction with a limited amount of water vapor produces a mixture of plutonium oxide and plutonium hydride.

Plutonium metal is also attacked by all the common gases at elevated temperature. Thus ammonia and nitrogen form nitrides, hydrogen forms hydrides, the halogens and gaseous halogen acids produce halides, CO forms carbides, and CO₂ produces carbides and oxides.

Because of its highly electropositive nature, plutonium metal is soluble in a number of mineral acids. Since a number of dilute acids will attack a metal, frequently a residue is left that is probably polymeric plutonium hydroxide.

Source material on the chemistry of plutonium is voluminous, and comprehensive reviews may be found in Refs. 1 to 3.

4.1 Compounds of Plutonium

Plutonium forms compounds with all the nonmetallic elements except the noble gases and the halogen astatine and, in addition, forms many complex compounds containing more than one other element. Plutonium(III)

and (IV) form a number of stable compounds; fewer compounds of Pu(V) and (VI) are known, and they are less stable than the corresponding uranium compounds. Plutonium compounds tend to vary slightly in stoichiometry and hydration, depending on the method of preparation. Some compounds of plutonium are listed in Tables 4.1 and 4.2.

Plutonium forms many compounds with oxygen, including the simple binary oxides, the peroxide, the hydroxides (or hydrated oxides), and a series of ternary and quaternary oxides in which plutonium is present along with other metallic elements. The dioxide is the most stable and is the compound formed under most conditions. It is formed when plutonium or its compounds (except the phosphates) are ignited in air and often results when oxygen-containing compounds are heated in vacuum or in an inert atmosphere to 1000°C.

Plutonium dioxide may be prepared in a pure crystalline form by heating Pu(III) or (IV) oxalate to 1000°C in air. It is normally green, but since the color is a function of purity and particle size, the color varies with the method of preparation. X-ray crystallographic data show that the lattice constant of PuO₂ increases with time due to expansion resulting from alpha-radiation damage. It is a very refractory material, particularly that prepared at high temperature, and is difficult to dissolve by normal techniques. The decreased reactivity of PuO₂ prepared by ignition at higher temperatures appears to be due to imperfections of the crystal lattices.¹

Several different values have been obtained for the melting point of PuO₂ in various atmospheres: oxygen, about 2400°C; argon, 2330 ± 10°C; helium, 2280 ± 30°C. The solid dioxide phase becomes oxygen deficient during volatilization.

Ternary oxides have been prepared that contain plutonium in all oxidation states. The reaction of Li₂O or Na₂O with PuO₂ in an oxidizing atmosphere for 8 hr at 700 to 900°C produces Li₃PuO₄ or Na₃PuO₄ [Pu(V)].

4.1.1 Plutonium dioxide and mixed oxides

The physical, thermal, electrical, thermodynamic, and mechanical properties of the mixed oxides have been extensively studied.

A summary of (U,Pu)O₂ properties compiled by Rubin⁴ includes physical properties such as the UO₂-PuO₂ phase diagram, lattice parameters of

Table 4.1. Summary of material properties

Properties	UO ₂	PuO ₂	(U, 20 wt % Pu)O ₂
Theoretical density, g/cm ³	10.96	11.45	11.04
Melting point, °C	2840 ± 40	2400 ± 30	2810 ± 25
Crystal system and parameters	Fcc (fluorite) $a_0 = 5.4705 \pm 0.0003$	Fcc (fluorite) $a_0 = 5.3960 \pm 0.0003$	Fcc (fluorite) $a_0 = 5.4559 \pm 0.0005$
Coefficient of linear thermal expansion, °C ⁻¹ (range 25 to 1000°C)	10.1×10^{-6}	10.9×10^{-6}	10.3×10^{-6}
Thermal conductivity, at 95% TD, W cm ⁻¹ (°C) ⁻¹	0.022 > 1600°C	0.023 at 1000°C	0.021 > 1600°C
Electrical resistivity, Ω-cm	1×10^3	1.3×10^8	2×10^4
Resistance to thermal shock	Good	Fairly good	Good
Compatibility with cladding material	Excellent	Compatible with SS, Inconel, Cr, Mo, Nb, V, below 1400°F; not compatible with Ti, W, Zircaloy-2	Same as PuO ₂ ; hyperstoichiometric compound reacts with SS and Inconel at temperatures to 1400°F
Young's modulus, kilobars	1930		1400 ± 100 (O/M = 1.98)
Shear modulus, kilobars	770		550 ± 50 (O/M = 1.98)
Poisson's ratio	0.302		0.28-0.29

Table 4.2. Compounds of plutonium

Compound	Formula	Color	Density (g/cm ³)	Melting point (°C)	Boiling point (°C)
Refractory-type compounds					
Nitride	PuN	Black	14.25	2770	
Carbide	PuC	Black	13.6	1650	
Silicide	PuSi		10.15	>1500	
Dioxide	PuO ₂	Greenish brown	11.46	2400	
Lower-melting compounds					
Tribromide	PuBr ₃	Green	6.69	681	
Trichloride	PuCl ₃	Emerald green	5.70	760	
Hexafluoride	PuF ₆	Volatile, reddish brown		50.75	62.3
Dioxalate	Pu(C ₂ O ₄) ₂ ·6H ₂ O	Yellow-green			Decomposes above 350°C
Triiodide	PuI ₃	Bright green	6.92	777	Decomposes at 1000°C

the $\text{PuO}_2\text{-UO}_2$ systems, and theoretical density (see Fig. 4.1). The thermal properties are listed for thermal expansion, thermal conductivity of mixed oxides, and specific heat as well as the electrical and mechanical properties of $(\text{U,Pu})\text{O}_2$. In addition, there are sections on solid-state reactions of $(\text{U,Pu})\text{O}_2$ and mixed-oxide fuel fabrication processes.

Mixed-oxide fuel pins intended for testing fast breeder reactor concepts are smaller in diameter (about 0.25 in. with 0.015-in. tubing) than UO_2 pins in thermal reactors (0.57 in. with 0.035-in. tubing). The mixed-oxide pins operate with fuel surface temperatures of 900 to 1000°C, about 500 to 600°C hotter than UO_2 fuels. When operating with high heat fluxes and center temperatures to $\sim 2500^\circ\text{C}$, the fuel is irradiated in a steep thermal gradient, accentuating thermal processes such as diffusion, fission gas release, and microstructural changes that are driven by a thermal gradient. Irradiation performance of the mixed oxide resembles the behavior of UO_2 fuels in regard to microstructural features, fission gas release, or fission product segregation, varying only in degree.

The oxygen concentration in UO_2 is usually equivalent to an oxygen/uranium ratio of 2.00, although it may be prepared in the hyperstoichiometric form of UO_{2+x} . The mixed oxide is generally prepared in the hypostoichiometric state with an oxygen/metal ratio of about 1.97 to 1.98.

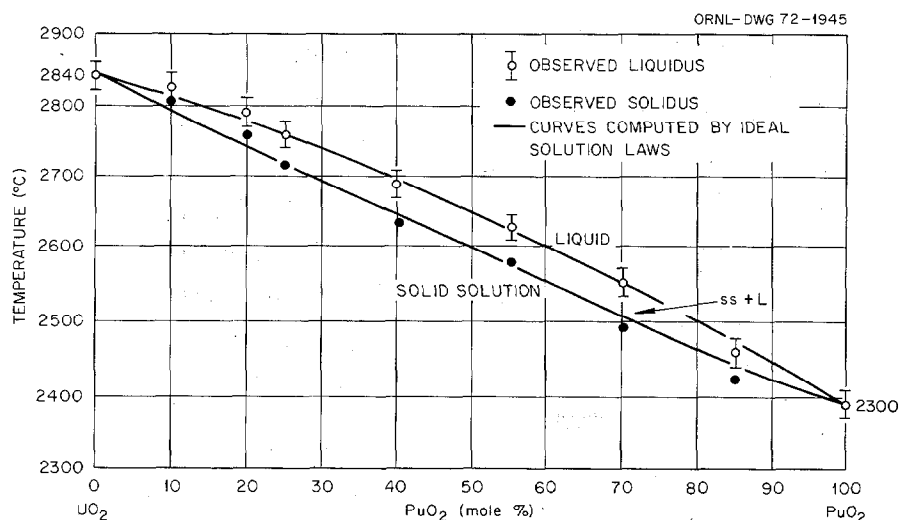


Fig. 4.1. $\text{UO}_2\text{-PuO}_2$ phase diagram.

On a molecular basis, such a mixed oxide would consist of UO_2 and PuO_{2-x} . The oxygen/metal ratio of the mixed oxide is controllable over the range 1.93 to 2.04, with most interest concentrated in the 1.97 to 1.98 range. As will be shown, the ratio has a significant effect on fuel element properties and behavior: melting point, thermal conductivity up to about 1400°C , creep characteristics, and reactions with cladding or sodium. Under the influence of the steep thermal gradient referred to above, oxygen in hypostoichiometric fuel migrates from the high-temperature regions at the fuel center to the cooler region at the pellet radius, altering the regional behavior of the fuel from that anticipated by the preirradiation stoichiometry. More investigations of this effect and its consequences must be made to improve understanding of actual in-pile behavior.

This compilation of properties and fabrication techniques is intended to serve as a reference for those interested in ceramic oxide fuels for fast breeder reactor applications. The PuO_2 content of such fuels is ≥ 15 wt %, and these compounds are thereby distinguished from the mixed-oxide fuels with lower PuO_2 concentrations that are recycled in thermal reactors. The bulk of the data and results were developed by investigators at General Electric, NUMEC, Westinghouse, Argonne National Laboratory, and Battelle Northwest Laboratory. The work of British and French researchers is also included in the references.

Uranium and plutonium both form stoichiometric oxides of the modified face-centered cubic (CaF_2) type, with lattice parameters of 5.4705 and 5.396 \AA respectively.

Although UO_2 may accept oxygen interstitially to form hyperstoichiometric compounds U_4O_9 , $\alpha\text{-U}_3\text{O}_8$, and UO_3 , plutonium is more stable as a sesquioxide, $\beta\text{-Pu}_2\text{O}_3$ (body-centered cubic with an O/Pu ratio from 1.58 to 1.62), and $\alpha\text{-Pu}_2\text{O}_3$ (close-packed hexagonal with O/Pu ratio from 1.498 to 1.510). PuO_2 is the plutonium compound with the highest mole fraction of oxygen. Therefore, in nonstoichiometric mixed oxides, hyperstoichiometric compounds contain PuO_2 and hyperstoichiometric UO_2 , and hypostoichiometric compounds contain UO_2 and substoichiometric PuO_2 . Many characteristics and properties of UO_2 have been compiled in Bell's comprehensive book,⁵ and a tabulation of PuO_2 features is included in the *Plutonium Handbook*.⁶

The Pu-O system has been investigated by Gardner, Markin, and Street,⁷ Chikalla, McNeilly, and Skavdahl,⁸ and Holley et al.⁹

Structural uniformity and nearly equivalent ionic radii, 1.10 Å for the uranium and 1.07 Å for the plutonium, result in complete substitutional solid solubility between UO₂ and PuO₂. The UO₂-PuO₂ phase boundaries have been studied by Markin and Street,¹⁰ Chikalla,¹¹ and Lyon and Baily.¹² The phase boundaries, as determined by Lyon and Baily, are shown in Fig. 4.1. This diagram was also predicted by Epstein,¹³ using ideal solution relationships and values of the heats of fusion for the end components obtained from melting point data.

Comparison of melting point data. The melting point measurements for UO₂ and PuO₂ correspond to accepted values for the compounds. The 2840°C melting point of UO₂ approximates the 2805°C value reported by Hausner¹⁴ and the 2870°C value reported by Latta and Fryxell.¹⁵ The 2390°C value for PuO₂ agrees well with the 2400°C melting point obtained by Hough and Marples.¹⁶

The melting point of arc-fused Pu₂O₃ has also been determined. Measurements were taken in an argon atmosphere, and melting temperatures of 1940 and 1985°C were observed. These specimens were reported to melt congruently. It is believed that the melting points of the stoichiometric mixed-oxide system have now been fully established and that the effect of stoichiometry in the composition range of 1.94 to 2.00 in 20% PuO₂ specimens has been determined.

Effect of burnup. Melting points of mixed-oxide fuels of 20 and 25 wt % PuO₂ compositions irradiated in a thermal flux have been measured over the burnup range 55,000 to 255,000 MWd/ton.¹⁷ The melting point of (U, 25 wt % Pu)O_{2.00} decreased 50°C at 85,000 MWd/ton, and that of (U, 20 wt % Pu)O_{2.00} decreased 100°C at 55,000 MWd. One sample of (U, 25 wt % Pu)O_{2.00} with a burnup of 255,000 MWd/ton was found to have a melting point decrease of 60°C. A decrease in the melting point of (U, 25 wt % Pu)O_{2.00} from 2790 to 2740°C could result in a decrease in integral thermal conductivity ($\int k d\theta$) to melting of about 0.5 W/cm based on low-burnup in-pile data.

The decrease observed in the melting point of the mixed oxides in the burnup range from 50,000 to 100,000 MWd/ton was approximately equivalent to that predicted by assuming that the melting point of the irradiated fuel decreased in direct proportion to the amount of the fission products present and their melting points. The decrease at 250,000 MWd/ton, however, was less than predicted.

An extensive series of out-of-pile tests was conducted using (U, 25 wt % Pu) O_{2+x} fuel pellets immersed in sodium and sodium-potassium within sealed stainless steel capsules.¹⁸ These were intended to simulate the exposure of fuel to a liquid-metal coolant. The effects of stoichiometry, density, uranium-plutonium composition, synthesized fission product concentration, and sodium purity were investigated. The test consisted of a 150-hr exposure to 750°C liquid and vapor sodium or sodium-potassium. The results, compiled by Rubin,⁴ are listed below.

1. Hyperstoichiometric fuel (O/M = 2.04) was chemically reduced by sodium liquid or vapor; physical damage was severe, resulting in complete disintegration of the pellets.
2. Stoichiometric fuel underwent little or no chemical reduction by sodium, but swelling, cracking, and marked loss of strength occurred.
3. Hypostoichiometric fuel (O/M = 1.97) did not undergo chemical reduction by sodium at 750°C, but the fuel pellets were physically weakened, with some swelling and cracking. Sodium penetration into the pellet interior was observed.
4. The compatibility of low O/M ratio (1.94) pellets with sodium was found to be excellent, as indicated by surface appearance and by the absence of any significant swelling.
5. Fuel pellets that were subjected to thermal cycling in an argon atmosphere without sodium showed only slight dimensional change, indicating that the changes noted above were due to reaction with sodium or sodium-potassium.
6. Behavior of mixed-oxide fuel pellets in sodium-potassium liquid or vapor was similar to behavior in sodium. Stoichiometric pellets underwent slight swelling and cracking in comparison with hypostoichiometric specimens, which were essentially unscathed.

7. Low-density, 86% of theoretical, fuel of 3 and 25 wt % PuO_2 compositions showed a larger degree of dimensional instability than the high-density, 95%, fuel due to sodium penetration.

8. The presence of synthetic fission product elements, homogeneously dispersed in the fuel at concentrations approximating those predicted for 100,000 MWd/ton exposure, did not appear to affect the otherwise satisfactory compatibility of (U, 25 wt % Pu) $\text{O}_{2.00}$ even at low density. Additives included Zr, Mo, Ru, Pd, Sr, Ba, and Ce.

9. Very impure sodium (~ 1800 ppm Na_2O) resulted in excessive crumbling of a stoichiometric pellet, but there was no evidence of compound formation.

In-pile testing. A series of in-pile tests with mixed-oxide fuel in contact with sodium has been conducted by O'Neill et al.¹⁹ Operating 72 min at 25 kW/ft and with a peak power of 30 kW/ft, the capsule underwent four complete power cycles from 0 to 125% of full power in less than 3 sec, a rate several hundred times greater than normal power changes. No dimensional changes were recorded, indicating that for the sample geometry tested, sodium logging is not a major problem.

4.1.2 Plutonium carbides, nitrides, and silicides

Plutonium carbides are currently under development for use as reactor fuels, since their higher thermal conductivity and increased plutonium density give them potential advantages over PuO_2 for this purpose. The plutonium carbides are prepared by the reaction of graphite with plutonium metal, PuO_2 , or plutonium hydride.

Only one nitride, PuN , is known. It is most efficiently prepared by reacting plutonium hydride with NH_3 vapor at 600 to 650°C or with nitrogen at temperatures above 230°C. The PuN lattice expands with time because of alpha self-damage. Plutonium silicides have received some consideration for possible use as reactor fuels. Plutonium silicides are difficult to prepare, but they can be formed by the reaction of silicon with plutonium metal or PuF_3 .

Several plutonium-containing refractory compounds are attractive as reactor fuel materials because they have high melting points, high metal atom densities, and relatively good thermal conductivities (see Table 4.2).

To date, PuC and (U,Pu)C have been investigated most extensively. Mixtures of UC and PuC are of particular interest as a high-temperature fuel for fast breeder reactors, while PuC holds potential as a fuel for fast reactors in which a minimum core size must be combined with a high power density.

4.1.3 Sodium-uranium-plutonium oxides

A number of mixed compounds of sodium and uranium oxide have been prepared and their properties have been studied in detail.^{20,21} Aitken²² and his associates have investigated the thermodynamic properties and possible chemical interactions in the system UO_2 - PuO_2 fuel and sodium. Their analysis indicates that the oxygen activity is a crucial parameter for predicting compatibility.

The mechanism and theory of transport processes in fuel systems under a temperature gradient were also studied by Aitken et al.²² Preliminary results indicated that the reaction compound formed near but not at the coldest end of the capsule when heated in the temperature range of 555 to 1150°C. A second series of experiments showed similar results between 900 and 1450°C.

4.1.4 Other inorganic compounds

The fluorides of plutonium have been used in the preparation and purification of the metal (see Table 4.2). Plutonium(III), (IV), and (VI) form binary fluorides. Volatile plutonium hexafluoride, PuF_6 , may be prepared by reaction of PuF_4 with a stream of fluorine at elevated temperatures, 550 to 750°C. It can also be prepared by the fluorination of the dioxide, but it cannot conveniently be prepared by the reaction of PuF_4 and oxygen. Because of its volatility, PuF_6 is the most hazardous of all plutonium compounds, and all work with it must be done with great care in leak-tight equipment. It is a solid with a melting point of 51.59°C and a boiling point of 62.16°C and is normally yellowish brown, although the freshly condensed material is frequently bright red. The vapor is brown and resembles N_2O_4 .

The chemical properties of PuF_6 differ greatly from those of its uranium analog, UF_6 . Plutonium hexafluoride is thermodynamically unstable

and decomposes more easily than the uranium compound, which has a negative free energy of formation. Reaction of the hexafluoride with moist air or water at room temperature is reported to be violent and accompanied by flashes of light. The rate of decomposition of solid PuF_6 caused by its own alpha radiation is about 1.5%/day for the isotope of mass 239.

Compounds of trivalent plutonium with chlorine, bromine, and iodine have been prepared and characterized, but they have no important process applications. The carbonates and oxalates of plutonium differ greatly in their chemical and physical properties. Carbonates are rather ill-defined unstable compounds, while the oxalates are well-characterized stable compounds that are widely used as intermediates in the conversion of plutonium nitrate to metal. Stable oxalates of Pu(III), (IV), and (VI) are known, and a number of complex compounds of Pu(IV) and (VI) have been prepared.

Sulfates of Pu(III) and (IV) have been prepared and characterized. There is interest in the use of a hydrate of $\text{Pu}(\text{SO}_4)_2$ as a primary standard for plutonium due to its stability and its precise, reproducible composition.

Although most of the research and essentially all the chemical processing of plutonium have been conducted in nitrate solutions, plutonium nitrates have rarely been prepared as solid compounds. Solid Pu(IV) and PuO_2^{2+} nitrates have been prepared. Tributyl phosphate is important in solvent extraction processes, but the study of solid phosphate compounds has been limited.

4.2 Solution Chemistry of Plutonium

The chemistry of plutonium in aqueous solutions is complex. The multiplicity of oxidation states in solution and the involved equilibrium and kinetic relationships between them, combined with the strong complexing tendencies of Pu(IV) ions, result in very complicated systems.

Plutonium ions in solution can exist in the (III), (IV), (V), and (VI) oxidation states as Pu^{3+} , Pu^{4+} , PuO_2^+ , and PuO_2^{2+} respectively. Because of the relationships between the equilibria and the kinetics of converting from one state to another, it is possible for all four oxidation

states to coexist in appreciable concentrations in the same solution. Solutions of Pu(III) are blue by reflected light and blue with a green tinge when seen by transmitted light. Tetravalent plutonium forms brown solutions in dilute acids. The oxidation state produced by dissolution of plutonium metal depends on the acid employed; HCl, HBr, H_3PO_4 , and $HClO_4$ yield blue trivalent ions, and HNO_3 -HF yields green tetravalent ions.

The oxidation state of plutonium ions in solution is affected by radiation, either its own alpha radiation or external gamma rays. The most common effect is a decrease in the average oxidation number. The alpha reduction of plutonium ions in dilute acid solution appears to be due primarily to H_2O_2 formed by radiolysis of water, and the induction periods observed are due to the slowness of reduction by H_2O_2 .

Some physicochemical characteristics of interest for simple plutonium compounds in aqueous solutions are acid properties, dissociation constants, solubility products, etc. In studying complex formation by Pu(III), (IV), and (VI) in acetate, oxalate, and phosphate solutions by the solubility method, the corresponding simple compounds are Pu(III), (IV), and (VI) oxalates, sodium plutonyl triacetate, and Pu(IV) phosphate. For calculating the instability constants of complex plutonium ions, data are required on the solubility products of these compounds. Data on the solubility of simple compounds not only make possible the calculation of the solubility products of these compounds but may be used to explain the mechanism of processes that occur during the solution of the compounds in an acid medium. The constants of the equilibria established when these compounds are dissolved bear definite relationships to the instability constants of complex plutonium ions formed in the intermediate stages during solution of the given compound in inorganic acids. They characterize the stability of the complex ions, determine the composition of the simple or complex forms of plutonium formed, and in addition show how the ratio between the individual forms depends on the hydrogen ion concentration.

4.2.1 Complex formation by plutonium in aqueous solutions

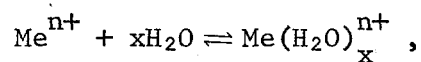
The properties of solutions of some complex compounds are such that the compositions of the solid compounds sometimes do not correspond to

the compositions of the complex groups in solution. This occurs because in aqueous solutions there usually exists a mixture of the complex ions, MeA_1 , MeA_2 , MeA_3 , ..., MeA_n (Me is the central atom and A is the ligand), generated by the stepwise nature of complex formation.

The most important characteristic of a complex in solution is its stability, which is determined by the energy of the chemical bond between the central ion and the coordinated ligands. The instability constants characterizing the stability of complex groups in solution may be found by studying the equilibrium of the complex with the starting components, which are also the dissociation products of the complex.

The main processes in aqueous solutions are the formation of aquo, hydroxo, and acido complexes and, in addition, various forms intermediate between them. The effects of hydration, hydrolysis, and acido-complex formation are determined by the concentrations of hydrogen ions and complex-forming anions of the particular acid. For example, in solutions of perchloric acid, whose anion complexes weakly or not at all, varied forms of complex groups may exist, depending on the hydrogen ion concentration. In the absence of hydrolysis of the complex-former ions, the latter exist in solution as hydrated complexes.

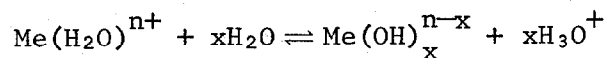
For investigations of the hydration of ions in solution, attempts are made to characterize the hydration of an ion quantitatively by the number of molecules of water bound by the ion; that is, the so-called hydration number. The overall process of ion hydration in aqueous solutions may be represented by



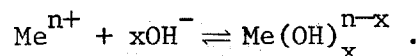
where x is the coordination number of the central atom or hydration number.

When complex-forming acids are added gradually to such solutions, there will be stepwise formation of mixed acido-aquo complexes and then acido complexes. With dilution of the solutions (i.e., with a decrease in the hydrogen ion concentration), hydrolysis processes take an increasing part in leading to the formation of hydroxo complexes.

With a decrease in the hydrogen ion concentration in aqueous solutions, hydrolysis of the metal ion may lead to its complete dehydration, according to the equations



or



With the same type of bond in the aquo complexes, the relative tendency for replacement of a hydrogen ion in the coordinated water molecules must increase in the order $\text{U}^{3+} < \text{Np}^{3+} < \text{Pu}^{3+} < \text{Am}^{3+}$ for trivalent positive ions and $\text{Th}^{4+} < \text{U}^{4+} < \text{Np}^{4+} < \text{Pu}^{4+} < \text{Ce}^{4+} < \text{Hf}^{4+} < \text{Zr}^{4+}$ for tetravalent positive ions; that is, in the order in which the ionic radii decrease.

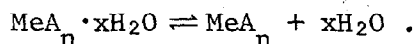
Thus the mechanism of complex formation evidently consists in the successive replacement or displacement of water molecules from the solvation envelopes surrounding the central metal atom by coordinating acid ions or OH^- groups.

The types of complex compounds formed in aqueous solutions will be large; there are complexes of complicated compositions containing anions of two and more different acids. The different forms of complexes may be classified as: (1) hydrates, (2) hydroxo compounds, (3) hydroxo-aquo compounds, (4) acido complexes, (5) mixed acido-aquo complexes, (6) mixed acido-hydroxo complexes, and (7) mixed acido-hydroxo-aquo complexes.

4.2.2 Solubility of plutonium compounds

The physicochemical properties of oxalates, phosphates, phenylarsonates, and other sparingly soluble compounds of tetra- and hexavalent transuranium elements reveal interesting regularities in their solubilities in water under certain conditions. The solubility of the molecular undissociated forms of these compounds in water at pH values where hydrolysis is absent and where, at the same time, there are still no solution processes under the action of hydrogen ions acts according to the

equation



4.2.3 Complex formation by plutonium in various oxidation states

There is both qualitative and quantitative information on complex formation by plutonium with anions of inorganic acids. Most of the data were obtained by spectrophotometry, measurement of transport numbers, potentiometry, ion exchange, extraction, etc.

In addition to the differences in absorption spectra of plutonium in different valence states, the absorption spectra change in the presence of different complex forms. Therefore changes in the absorption spectra of plutonium in solutions of different acids make it possible to estimate the degree of complex formation with anions of these acids.

The tendency of a cation to form complexes depends on the ionic potential, that is, on the formal charge of the ion divided by its radius. Relatively small, highly charged ions such as Pu(IV) form complexes readily. The solution chemistry in the tetravalent state is largely the chemistry of its complexes. The order of decreasing complex-forming ability is $\text{Pu}^{4+} > \text{Pu}^{3+} > \text{PuO}_2^{2+} > \text{PuO}_2^+$. Plutonium in any given valence is more strongly complexed than the corresponding uranium and neptunium ions. The complexing tendencies of the more common anions with Pu(IV) are found to decrease in the order $\text{F}^- > \text{NO}_3^- > \text{Cl}^- > \text{ClO}_4^-$. Other groups that complex with plutonium are phosphate and peroxide anions, as well as a number of organic anion-containing nitrogen, phosphorus, or carbonyl groups, which form stable chelate complexes.

The experimental methods for determining the association quotients of complexes are (1) ion exchange, (2) solvent extraction, (3) potentiometry, (4) polarography, (5) spectrophotometry, and (6) solubility measurements.

Trivalent plutonium has only a limited tendency toward complex formation. The complexes of chlorides, bromides, nitrates, oxalates, citrates, tartrates, acetates, ethylenediaminetetraacetic acid (EDTA), and thiocyanate have been studied.

Tetravalent plutonium forms complexes of great stability with many different anions, and many of these complexes are encountered in the chemical processing of plutonium. Complexes of Pu(IV) can be formed with the following ligands: fluoride, chloride, bromide, nitrate, sulfate, sulfite, phosphate, peroxide, carbonate, citrate, tartrate, acetate, and EDTA.

Plutonium(V), as PuO_2^+ , has the least tendency of all plutonium species to form complexes, and very few such complexes are known. Plutonium(VI) is known to form a number of complexes, although most have been studied only qualitatively (i.e., chloride, nitrate, sulfate, carbonate, oxalate, acetate, and EDTA).

Information on the potentials of the different oxidation-reduction systems of plutonium is helpful in studying its chemistry. The oxidation-reduction potentials make it possible to determine the limits of stability of plutonium ions of various degrees of oxidation, to calculate their equilibrium concentrations in solutions where disproportionation occurs, and to estimate their behavior toward various oxidizing and reducing agents. In addition, a knowledge of the oxidation-reduction potentials of various plutonium couples makes it possible to estimate the degree of complex formation by plutonium ions in different media.

Because of the lack of information on the activity coefficients of plutonium ions of various degrees of oxidation, in all investigations the standard potentials, E_s , are given; that is, the potentials when the ratio of the concentrations of the oxidized and reduced forms equals one. The potentials thus correspond to a definite solution at some given ionic strength.

Only the potentials of the couples Pu(III)-Pu(IV) and Pu(V)-Pu(VI) can be measured directly. The potentials of all other oxidation-reduction systems cannot be measured in this way because of their irreversibility. However, from the oxidation-reduction potentials of the couples Pu(III)-Pu(IV) and Pu(V)-Pu(VI) and the concentrations of Pu(III), (IV), (V), and (VI) under equilibrium conditions, it is possible to calculate the standard potentials of all the oxidation-reduction systems.

4.3 Methods for Separation of Plutonium from Uranium and Fission Products

The methods of isolating plutonium from irradiated uranium are based largely on coprecipitation, extraction, and ion exchange, where an important part is played by complex formation. Some methods of isolating and separating transuranium elements in which complex compounds of these elements are used have been tested only under laboratory conditions, while others have been applied in separation processes on an industrial scale.

The best extraction methods for isolating and purifying uranium and plutonium employ such solvents as methylisobutyl ketone, tributyl phosphate (TBP), β, β' -dibutoxydiethyl ether, and diethyl ether. Because of high ionic potential, plutonium may be readily adsorbed onto cation exchange resins. Its ability to form anionic complexes also makes plutonium readily adsorbable on anion exchangers.

4.3.1 Solvent extraction

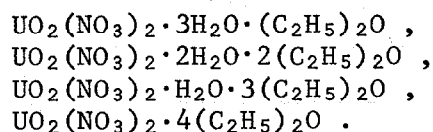
Plutonium is separated from uranium and fission products by solvent extraction. A compilation of solvent extraction data for plutonium is available that contains over 100 tables and 200 graphs.²³

The most important classes of extractants for plutonium are the organophosphorus compounds, ketones, ethers, and the organonitrogen compounds. A number of the organic compounds form water-insoluble but organic-soluble complexes with plutonium and thus may function as extractants (i.e., salicylate, cupferron, neocupferron, and trifluoroacetic acid).

Three processes dominate solvent extraction processing of plutonium: (1) the purex process, which uses the TBP-hydrocarbon extractant; (2) the redox process, which is based on extraction with methylisobutyl ketone (hexone); and (3) the butex process, in which dibutyl carbitol is the extractant. All three processes are based on the high organic extractability of plutonium and uranium of the higher valences, the inextractability of the trivalent ions, and the ease of reducing plutonium selectively to the trivalent state in the presence of hexavalent uranium.

Ether extraction. In the presence of a salting-out agent, ethyl ether has a high extraction capacity with respect to uranyl and plutonyl nitrates,

while fission products are extracted by it to a very slight extent. The high solubility of uranyl and plutonyl nitrates is caused by the formation of complexes with molecules of ethyl ether, $(C_2H_5)_2O$. Depending on various experimental conditions, complexes are formed in the system uranyl nitrate-water-ethyl ether of the following compositions:



Molecules of ethyl ether displace water molecules from the hydration envelope surrounding the uranyl nitrate during complex formation. Complex formation processes of a similar type evidently occur in the system plutonyl nitrate-water-ethyl ether.

Extraction with amines. There is a possibility of using amines for the extraction of plutonium.^{24,25} The plutonium is extracted selectively as the complex anion $Pu(NO_3)_6^{2-}$. It is possible to extract Np(IV) and Pu(IV) successfully from nitric acid solutions with dilute solutions of tri-*n*-octylamine and trilaurylamine. The degree of extraction of plutonium in this case is so great that it is unnecessary to introduce a salting-out agent into the system; and moreover the extraction may be carried out with highly active waste solutions, since the amines are quite resistant to the effect of radioactive radiation.

Application of inner complex compounds. Uranium, plutonium, and fission products are also separated by benzene or chloroform extraction of transuranium elements as their compounds with 1,3-diketones, in particular, acetylacetone, dibenzoylmethane, and cupferron.²⁶

4.3.2 Ion exchange methods

Ion exchange resins are used for the separation of transuranium elements by means of various complex formers under laboratory conditions. The possibility of separating ions by means of cationites and anionites is associated with the difference in their ion exchange capacities and with the difference in the stabilities of compounds formed by the ions adsorbed by the resin with the eluting agent. Both these factors depend on the charges and dimensions of the ions.

Plutonium in all valence states and concentrations is readily adsorbed on cation exchange resins from acidic solution, the order of decreasing adsorption being $\text{Pu(IV)} > \text{Pu(III)} > \text{Pu(VI)}$. Dowex 50-X10, zirconium phosphate, zirconium pyrophosphate, hydrated titanium oxide, and basic zinc carbonate have cation exchange properties. Anion exchange resins include Dowex 1-X10 and Permutit-SK.

Both cation and anion exchange are used for concentrating and further decontaminating plutonium product streams from solvent extraction processes, and both have specific advantages. Cation exchange is most useful for concentrating large volumes of dilute solutions when low waste losses and only moderate decontamination are required.²⁷ Anion exchange, on the other hand, achieves higher decontamination and is preferable for the processing of concentrated acid and salt solutions.

If concentration is to be effected by cation exchange, final solvent stripping of the plutonium is done with an aqueous reducing agent, such as ferrous sulfamate, or, more commonly, hydroxylamine, since the cation exchange cycle is best operated with trivalent, rather than tetravalent, plutonium.

The superior decontamination obtained by anion exchange relative to cation exchange is due to the greater anion complex-forming ability of Pu(IV) compared with U(VI) and fission products. Thus at moderate HNO_3 concentrations it is possible to adsorb plutonium as an anionic complex, while other metal ions remain in the cationic form and pass through the resin unadsorbed. A disadvantage of anion exchange (the slow rate of adsorption) has been largely overcome by the operation of the columns at elevated temperature.²⁸

The concentration of the product solution depends on the method of eluting plutonium from the resin. Two techniques have been used for this purpose: elution with a reagent that will change the plutonium to the unadsorbed hexavalent or trivalent oxidation states and elution with dilute HNO_3 , which causes a shift in equilibrium away from plutonium anionic complexes.²⁸

4.4 Analytical Methods for Determining Plutonium

Analytical work connected with the quantitative and qualitative determination of plutonium entails a number of difficulties. In aqueous solution of weak acids, plutonium compounds undergo hydrolysis rather easily. The products of the hydrolysis are often insoluble and precipitate out of the solutions. When small quantities of plutonium are used at low concentrations (of the order of 1 $\mu\text{g/ml}$) and in a low concentration of acids, a major portion of the hydrolysis products settles on the walls of the vessel.

In highly acidic solutions, however, the plutonium forms anion complexes. Further difficulties in the analysis of plutonium compounds are caused by the low stability of compounds of plutonium in intermediate oxidation states [e.g., Pu(V)] and the fact that compounds of plutonium in the intermediate oxidation states [Pu(IV) and (V)] undergo self-reduction and self-oxidation (disproportionation).

The methods employed in the chemical analysis of plutonium can be roughly divided into two groups: conventional and radiochemical. Several aspects of both groups of analytical methods are discussed below.

4.4.1 Conventional methods

The conventional methods employed for the determination of plutonium are gravimetric, volumetric, colorimetric, spectral, and polarographic.

An example of a method of chemical analysis of plutonium in aqueous solution is the cerometric titration method.²⁹

The coulometric method for plutonium determination is convenient and relatively easy to perform.³⁰ This analysis may be realized by means of characteristic absorption bands for an oxidation state of plutonium.

Volumetric analysis of plutonium with a complexone (EDTA) is also known. Plutonium cation forms a complex with the EDTA in a 1:1 proportion. The error of the measurement is less than 1%.³¹

There are a number of chemical methods for the determination of plutonium in microquantities. Potentiometric analysis of plutonium with controlled potential is useful within a range of concentrations of 0.05 to 50 g of Pu per liter.³² Electrolysis has been used for separation of a

small quantity of plutonium in aqueous solutions. The emission spectrographic method is not used extensively because the plutonium specimen must be in a gaseous state, and the quantity of plutonium used for spectral analysis usually exceeds the permissible level of radioactive contamination.³³

4.4.2 Radiochemical methods

The most common methods for quantitative and qualitative analysis of plutonium are based on utilization of its alpha activity. Measurement of beta or gamma activity may also be employed for some plutonium isotopes.

Alpha-radiometric detectors used for plutonium determination may be gas-filled counters, with an electrical field for collecting ions created in the gas by alpha particles passing through. These counters include impulse-integrating ionization chambers, proportional counters, and G-M counters.

The preparation of the specimen for alpha-radiometric measurement is a difficult and important operation, as far as the accuracy of the measurement is concerned, because the alpha particles have a high specific ionizing power and are quickly stopped upon traveling through matter. Alpha particles ejected by ^{239}Pu , for instance, with an energy of 5.1 MeV undergo total absorption in air after traveling 4.5 mg/cm² of aluminum (which is the equivalent of a 3.61-cm layer of air). For plutonium compounds in the solid state, the layer that absorbs the alpha particles amounts to approximately 20 mg/cm², which corresponds to about a 10- μ layer. The problem of accurate measurement of plutonium is basically solved when a very thin layer of plutonium is obtained so that all alpha particles travel through it and get to the detector.

A number of methods are available for obtaining thin layers of plutonium compounds for measurement: evaporation of a pure solution of a plutonium salt on a tray in the presence of wetting agents, coprecipitation, and vacuum condensation of a salt on a tray.

In spite of the difficulties involved, radiometric methods have many advantages. The most important advantage is the ability to detect very small amounts of plutonium.

Measurements of alpha particles may be carried out even in the presence of relatively large quantities of beta particles and gamma quanta. This facilitates the analysis of plutonium in the presence of other radioelements emitting beta and gamma rays.

References

1. J. M. Cleveland, "Chemistry," pp. 327-520 in Plutonium Handbook, a Guide to the Technology, ed. by O. J. Wick, vol. 1, sect. III, Gordon and Breach, New York, 1967.
2. Mieczyzslaw Taube, Plutonium, Pergamon and Macmillan, New York, 1964.
3. G. T. Seaborg, J. J. Katz, and W. M. Manning (eds.), The Transuranium Elements, McGraw-Hill, New York, 1949.
4. B. F. Rubin, Summary of (U,Pu)O₂ Properties and Fabrication Methods, GEAP-13582 (November 1970).
5. J. Bell (ed.), Uranium Dioxide Properties and Nuclear Applications, U.S. Government Printing Office, Washington, D.C. 1961.
6. O. J. Wick (ed.), Plutonium Handbook, a Guide to the Technology, Gordon and Breach, New York, 1967.
7. E. R. Gardner, T. C. Markin, and R. S. Street, "The Plutonium-Oxygen Phase Diagram," J. Inorg. Nucl. Chem. 27, 541-51 (1965).
8. T. D. Chikalla, C. E. McNeilly, and R. E. Skavdahl, The Plutonium-Oxygen System, HW-74802 (September 1962).
9. C. E. Holley et al., "Thermodynamics and Phase Relationships for Plutonium Oxides," International Conf. on Peaceful Uses of Atomic Energy, P/107, 1958.
10. T. L. Markin and R. S. Street, "The Uranium-Plutonium-Oxygen Ternary Phase Diagram," J. Nucl. Chem. 29, 2265-80 (1967).
11. T. Chikalla, The Liquidus for the System UO₂-PuO₂, HW-68732 (1961).
12. W. L. Lyon and W. E. Baily, "The Solid-Liquid Phase Diagram for the UO₂-PuO₂ System," J. Nucl. Mat. 22, 332-39 (1967).
13. L. F. Epstein, "Ideal Solution Behavior and Heats of Fusion from the UO₂-PuO₂ Phase Diagram," J. Nucl. Mat. 22, 340-49 (1967).
14. H. Hausner, "Determination of the Melting Point of Uranium Dioxide," J. Nucl. Mat. 15, 179 (1965).

15. R. E. Latta and R. E. Fryxell, "Determination of the Melting Point of UO_{2+x} ," *Trans. Amer. Nucl. Soc.* 8(2), 375 (1965).
16. A. Hough and J. C. Marples, "The Pseudo Binary Phase Diagrams of PuO_2 with Alumina, Beryllia and Magnesia and the Pseudo Ternary, PuO_2-ThO_2-BeO ," *J. Nucl. Mat.* 15, 298 (1965).
17. J. L. Krankota and C. N. Craig, "Melting Point of High Burnup PuO_2-UO_2 ," *Trans. Amer. Nucl. Soc.* 11(1), 132 (1968).
18. Sodium Cooled Reactors, Fast Ceramic Reactor Development Program, 16th Quarterly Report, GEAP-4982 (January 1966).
19. G. L. O'Neill et al., Experimental Studies of Sodium Logging in Fast Ceramic Reactor Fuels, GEAP-4283 (September 1963).
20. Investigations in the Field of Uranium Chemistry, Russian Symposium Papers, V. I. Spitsyn (ed.), translated by Lydia Vinters, ANL-TRANS-33 (1961).
21. R. T. Pepper, J. R. Stubbles, and C. R. Tuttle, "Constitution of the Sodium-Uranium-Oxygen System," Applied Material Research, p. 203, October 1964.
22. E. A. Aitken, Thermodynamic Analysis of Possible Chemical Interactions in the System: UO_2-PuO_2 Fuel-Sodium-Stainless Steel, GEAP-5683 (July 1968); E. A. Aitken and S. K. Evans, A Thermodynamic Data Program Involving Plutonia and Urania at High Temperatures, GEAP-12153 (December 1970); E. A. Aitken et al., A Thermodynamic Data Program Involving Plutonia and Urania at High Temperatures, Quarterly Report No. 14, GEAP-12182 (January 1971).
23. L. L. Smith, Solvent Extraction for Plutonium, DP-700 (December 1962).
24. R. D. Baker and J. Leary, "Recent Developments in Plutonium Processing in the United States," *Proc. Int. Conf. Peaceful Uses At. Energ.*, Geneva, 1958, 17, 356-60 (1958).
25. A. S. Wilson, "Tertiary Amine Extraction of Plutonium from Nitric Acid Solutions," *ibid.*, pp. 348-51.
26. A. Martell and M. Calvin, Chemistry of the Metal Chelate Compounds, Prentice-Hall, New York, 1952.
27. D. A. Orth, "Objectives of Savannah River Plant Ion Exchange," p. 44 in Plutonium Ion Exchange Processes, (Proc. of the US-UK Technical Exchange Meeting, ORNL, Apr. 25-27, 1960), TID-7607 (February 1961).
28. J. L. Ryan and E. J. Wheelwright, "The Recovery, Purification and Concentration of Plutonium by Anion Exchange in Nitric Acid," *Ind. Eng. Chem.* 51, 60 (1959).

29. C. W. Koch, "The Quantitative Micro Determination of Plutonium," pp. 1337-38 in The Transuranium Elements, ed. by G. T. Seaborg, J. J. Katz, and W. M. Manning, part II, McGraw-Hill, New York, 1949.
30. I. W. Handshuh, Ion-Exchange Separation and Coulometric Titration of Plutonium, HW-66441 (1960).
31. G. W. C. Milner and J. L. Woodhead, "The Volumetric Determination of Pu with Ethylenediaminetetraacetic Acid," Analyst 81, 427 (1956).
32. F. A. Scott and R. M. Peekema, "Analysis for Plutonium by Controlled Potential Coulometry," Proc. Int. Conf. Peaceful Uses At. Energ., Geneva, 1958, 28, 573-78 (1958).
33. E. M. Cramer and F. W. Schonfeld, "Techniques for the Metallography of Plutonium," ibid., 17, 668-75.

5. INTAKE AND METABOLISM OF PLUTONIUM DIOXIDE

The magnitude of internal radiation exposure to man resulting from the release of plutonium into the environment depends, in a complex way, on the physical, chemical, and biological characteristics of the released material, of the local environment, and of man, as well as on the nature of the release. The complexity of the environmental pathways through which man may be exposed to plutonium is illustrated in Fig. 5.1. Intake routes that would be significant only for soluble compounds are shown as dashed lines.

A large amount of the information on this subject has been summarized in the *Plutonium Handbook, a Guide to the Technology*.¹⁻³ The material in Refs. 4 and 5 provides a comprehensible introduction to the properties of plutonium and its compounds. A more modern quantitative treatment of plutonium transfer mechanisms will be treated in more detail in later chapters. However, some relatively new information on plutonium dioxide behavior in biological systems has been included here.

The earliest biological studies with plutonium were conducted in the Health Division of the Manhattan District plutonium project. The history of this early period has been reviewed by Stone,⁶ who was Director of the Health Division. Most of the problem areas were recognized and effectively investigated during World War II and the early postwar period.⁷ A key to this early literature is provided in the bibliography published by Committee II of the International Commission on Radiological Protection (ICRP).⁸ Papers were presented on the biology of the transuranic elements at a symposium held at Richland, Washington, in May 1962.⁹ Langham¹⁰ and Williams⁷ have reviewed certain aspects of transuranic elements in relation to the environment. There is also a published collection of Russian papers on biological studies with plutonium.¹¹

In this chapter, intake of plutonium dioxide by inhalation and ingestion and through deposition on body surfaces is treated parametrically without regard to the details of transport pathways in the environment.

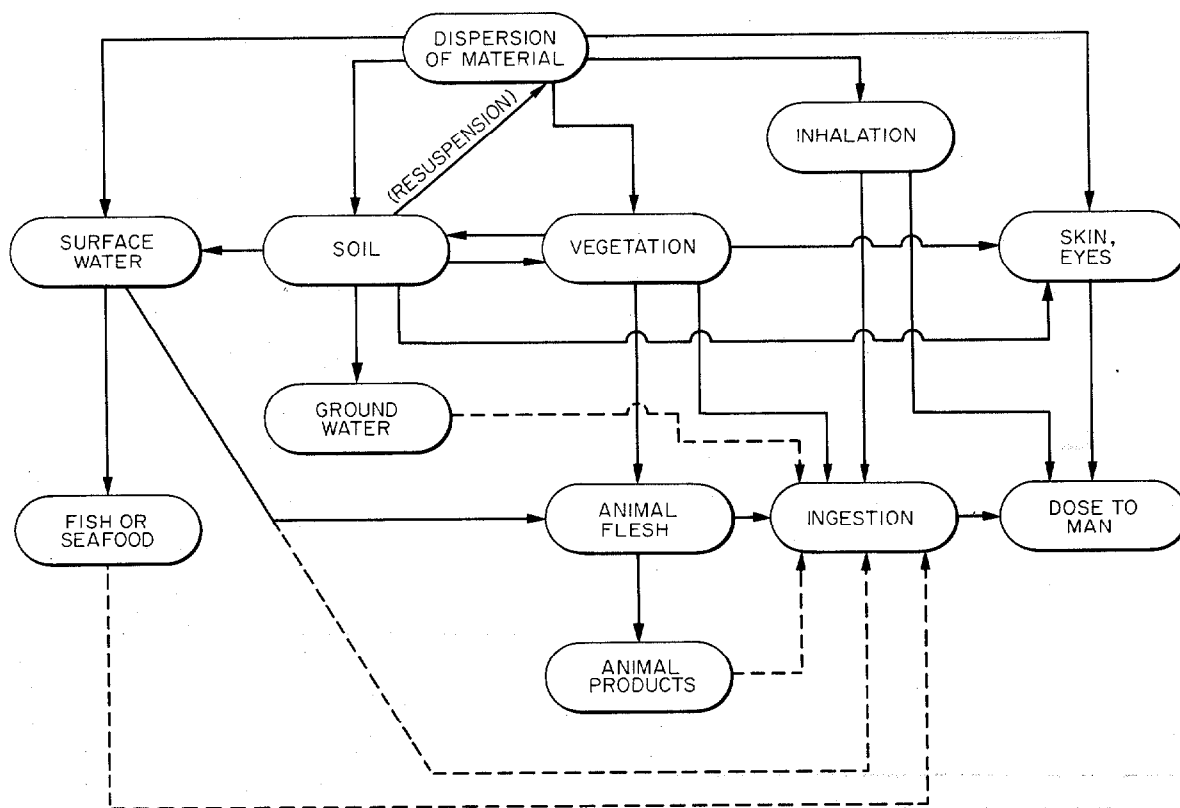


Fig. 5.1. Environmental pathways for exposure of man to released plutonium.

5.1 Intake Pathways

5.1.1 Inhalation

General model. The inhalation model used is basically an adaptation of the lung model developed by the ICRP Task Group on Lung Dynamics.¹² As described in Chapter 2, realistic assessments of the transport and deposition of plutonium either in containment or in the body must utilize basic principles of aerosol physics. A schematic diagram illustrating the deposition sites and clearance pathways is shown in Fig. 5.2. Quantities labeled D_1 through D_5 represent amounts of plutonium entering or leaving various segments of the respiratory tree. These amounts, expressed as fractions of the total amount of plutonium contained in the volume of air inhaled, are discussed below.

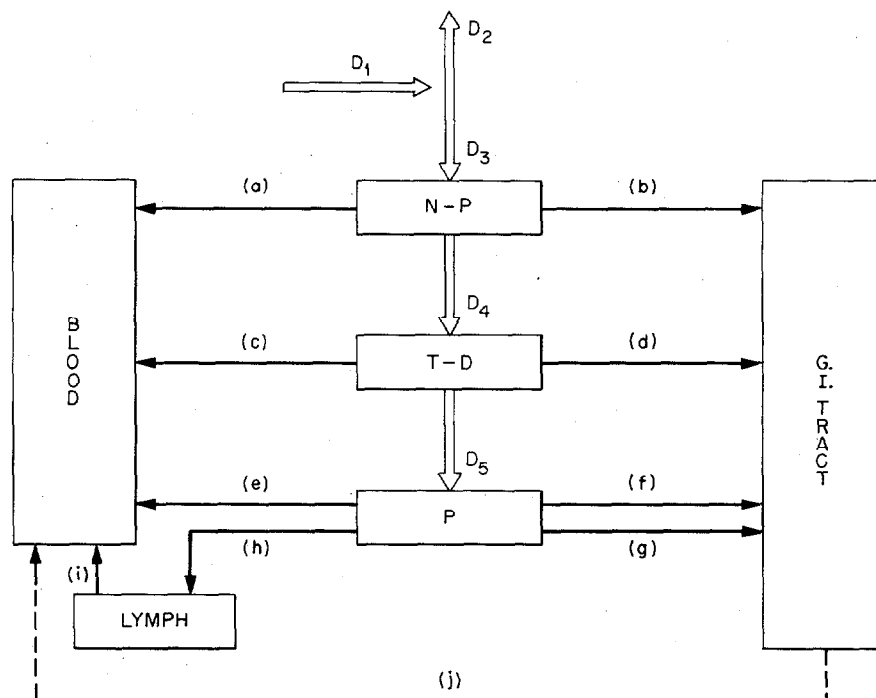


Fig. 5.2. Inhalation intake (based on work of ICRP Task Group on Lung Dynamics). [Reproduced from Health Phys. 12, 190 (1966) by permission of the Health Physics Society.]

(a) Aerosol physics. Although various effects such as electrical charge, hygroscopicity, etc., can be important in the deposition of some particulates, they are expected to play a relatively minor role in the deposition of plutonium particles in the respiratory system. The two mechanisms that control the deposition of uncharged particles in the lungs are inertia and diffusion.

Inertial deposition includes sedimentation during transit of particulates through the various segments of the respiratory system, as well as impaction of particles at the junctions of the branching airways. It is easily shown that the terminal velocity of a spherical particle under the action of gravity is given by

$$V_g = \frac{d^2 \rho C}{18\eta} g = \tau g ,$$

where

- d = diameter of sphere (cm),
- ρ = particle density,
- C = Cunningham slip correction, $\approx 1 + 0.16 \times 10^{-4}/d$,
- η = gas velocity,
- g = acceleration due to gravity,
- τ = relaxation time.

This relationship is based on the Stokes approximation to the aerodynamic drag on the particle and is valid to within 10% for spheres from 0.1 to 70 μm in diameter.¹³

The parameter τ is a measure of the time required for the movement of a particle to become adapted to a relative change in the motion of the fluid medium. Thus, the so-called Stokes number (Stk. No.) may be taken as an index of the impaction efficiency of particles at a branch point in a conduit,¹⁴ that is,

$$\text{Stk. No.} = \frac{V_0 \tau}{L},$$

where V_0 is velocity of particle entering junction and L is distance from entrance to deposition site. It is clear that for a given system of air passages and for given air velocities, the controlling factor for deposition by either sedimentation or impaction is $d^2\rho$, which is sometimes called the inertial, or impaction, parameter. This parameter decreases in significance as the particle size becomes small, and usually it may be disregarded for particles less than about 0.3 μm in diameter.

At the lower extremes of particle diameter, Brownian diffusion accounts for the major part of the deposition in the respiratory air passages. Diffusional deposition from laminar flow in a cylindrical conduit may be estimated from an expression due to Gormley and Kennedy:¹⁵

$$P = 0.819 \exp(-3.657K) + 0.097 \exp(-22.3K) + 0.032 \exp(-57K) + \dots,$$

where

P = fraction of particles that escape deposition,

$$K = \frac{Dx}{Q} \pi,$$

and

Q = volume flow rate in conduit,

x = length of conduit,

D = diffusion constant of particle.

The diffusion constant for a particle having a radius comparable with the mean free path of the gas molecules may be computed from an expression derived by Einstein;¹⁶ thus

$$D = \frac{kTC}{3\pi\eta d},$$

where

k = Boltzmann's constant,

T = absolute temperature,

η = gas viscosity,

C = Cunningham's correction factor, $\frac{C}{d} \approx \frac{1}{d} + \frac{0.16 \times 10^{-4}}{d^2}$.

Although the Gormley-Kennedy (G-K) equations have been used to predict deposition by diffusion of particles and gases in the respiratory airways,^{12,17} there are good reasons to believe that these predictions are somewhat in error. Because there is turbulent flow in some portions of the proximal airways, the deposition rate can be expected to be greater than would be calculated from the G-K equations, which are based on laminar flow. In either case, however, deposition efficiency should be correlated with a parameter similar to K in the G-K equation above. Clearly the diffusion constant becomes smaller with increasing particle size; hence, diffusional deposition becomes less significant as the particle size increases.

In principle, it may be expected that at some intermediate size — too large for efficient deposition by diffusion and too small for inertial deposition — a minimum should occur in the particle retention curves. Theoretically, the minimum should be in the neighborhood of 0.3 μm for retention in the total respiratory tract.¹⁸

Particle deposition estimates are affected also by the structure and dimensions of the air passages assumed in the calculations. The ICRP Task

Group on Lung Dynamics¹² assumed the Findeisen¹⁹ model for the anatomical structure of the lungs. This model is open to criticism regarding the details of anatomical structure; nevertheless, it has the advantage of relative simplicity and results in predictions of particle retention that are in reasonable agreement with inhalation experiments.

(b) Mechanical clearance. Once deposited, dust experiences two biological processes that produce clearance by mechanical transport: endocytosis and the ciliary movement of mucus. Since the lining of the respiratory tract is ciliated only in the region from the posterior end of the nasal vestibule to the level of the terminal bronchioles, it is clear that the aerodynamic parameters of an aerosol that determine the amounts and sites of deposition will also indirectly affect its clearance. Although in some respects it may be an oversimplification, it is suggested that mechanical clearance is predominantly mucociliary, except in the pulmonary region of the lung, where the rate of movement to the ciliary-mucus "escalator" is dominated by the mechanism of endocytosis. The cilia of the respiratory tract (nasopharynx and tracheobronchial tree) continuously move a layer of mucus toward the esophagus. Experimental data are available for the velocity of movement of mucus in these areas; it ranges from millimeters to centimeters per minute.²⁰⁻²⁴ Unfortunately there is no reliable information on the ciliary movement of mucus in the finer bronchiolar structures, where clearance appears to be far less rapid. Thus it is probably correct to consider reported values of mucociliary clearance as maximal rates.

(c) Solubility. In competition with the mechanical clearance mechanisms, plutonium can be removed from the lungs by dissolution in the fluids lining the respiratory tract. Compounds that are highly soluble in body fluids may, indeed, be absorbed through the lumen of the nasopharyngeal passages or the tracheobronchial tree, but in the case of PuO_2 , the rate of dissolution is so small that solubility is not a significant factor except for deposits retained for long periods of time. Consequently, solubility will be treated in detail only for parenchymal and lymphatic deposits.

Nasopharyngeal region. The nasopharyngeal region (N-P) begins with the anterior nares and extends through the anterior pharynx, back and down through the posterior pharynx (oral) to the level of the larynx or epiglottis. This compartment corresponds to the established medical description of the upper respiratory tract.¹²

(a) Probability of particle entry into the nose. The air entering the nasal passages is deficient in particles having settling velocities of the same order of magnitude as the linear velocity of air entering the nose. This effect has been estimated for PuO₂ particles under the assumptions that the particles are spherical, uniformly mixed in the air under the external nares, and falling at terminal velocity having no horizontal component and that the cross-sectional area of the intake port is fixed at 2.5 cm² (total for both nostrils).²⁵ The effect of assuming uniform mixing is to produce an overestimate in that any "shadowing" effect of the nose is ignored.

The computations were based on

$$U_t = \frac{Q}{A},$$

where Q is air flow rate at a time t (cm³/sec), A is cross-sectional area of external nares (cm²), and U_t is flow velocity at time t (cm/sec). If the particles are uniformly mixed and suspended in the exposure volume, the rate of entry to the nares will be nUA (particles/sec) for weightless particles, where n is the concentration (particles/cm³). However, since the particles have a downward velocity $-V_s$, only $n(U_t - V_s)A$ particles/sec can enter the nose. An efficiency factor e_s can be calculated for the case $V_s \leq U_t$:

$$e_s = \frac{n(U_t - V_s)A}{nU_t A} = 1 - \frac{V_s}{U_t}.$$

For $V_s > U_t$, $e_s = 0$. This gives the fraction of particles entering the nose as compared with the number originally contained in the volume of air inhaled. The factor e_s must be adjusted for the fraction of time during inspiration that the flow velocity is U_t .

It is easy to show that the intake probability for a given particle size is given by the fraction of the total inspired volume that is obtained when the curve of inspired velocity vs time is integrated above the line $U = V_g$. Graphs of intake velocity as a function of time were constructed based on pneumotachograms reported by Silverman and Billings²⁶ for four conditions of work rate. The appropriate areas under the curves were determined numerically, and the particle intake probabilities were computed. The results for PuO_2 particles (assumed $\rho = 10 \text{ g/cm}^3$) are shown in Fig. 5.3. Curves 1, 3, and 4 correspond roughly to the three conditions considered by the ICRP Task Group on Lung Dynamics;¹² namely, tidal volumes of 0.75, 1.45, and 2.15 liters. Although the effect is not very significant for PuO_2 particles in the size range of most concern, the curves shown in Fig. 5.3 do represent an upper limit to the likelihood of any large particle entering the nose.

(b) Deposition in the N-P region. Deposition of density 1 and 10 (g/cm^3) particles in the N-P region is shown in Fig. 5.4 as a function of

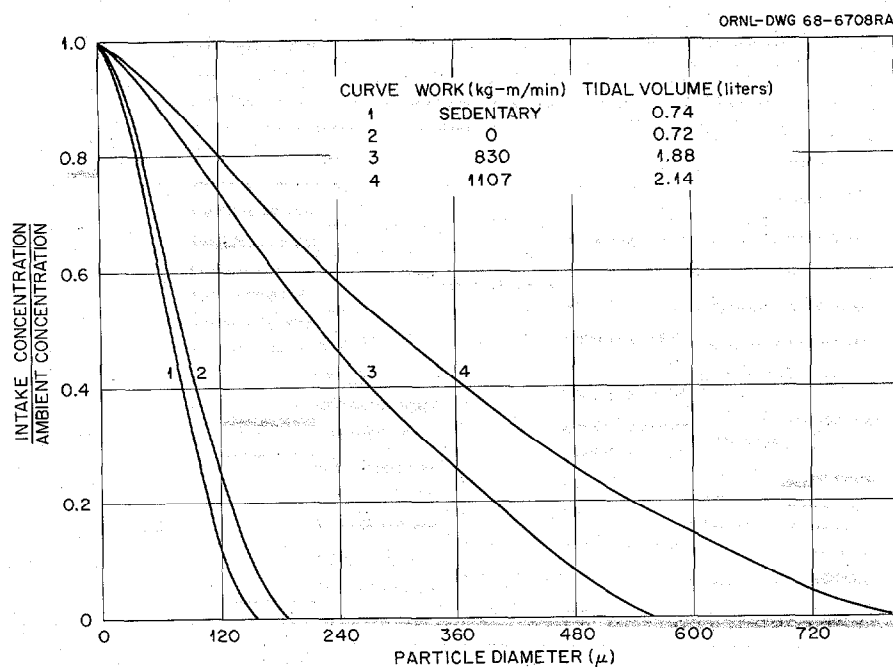


Fig. 5.3. Intake probability to the nose as a function of particle diameter and for different breathing rates.

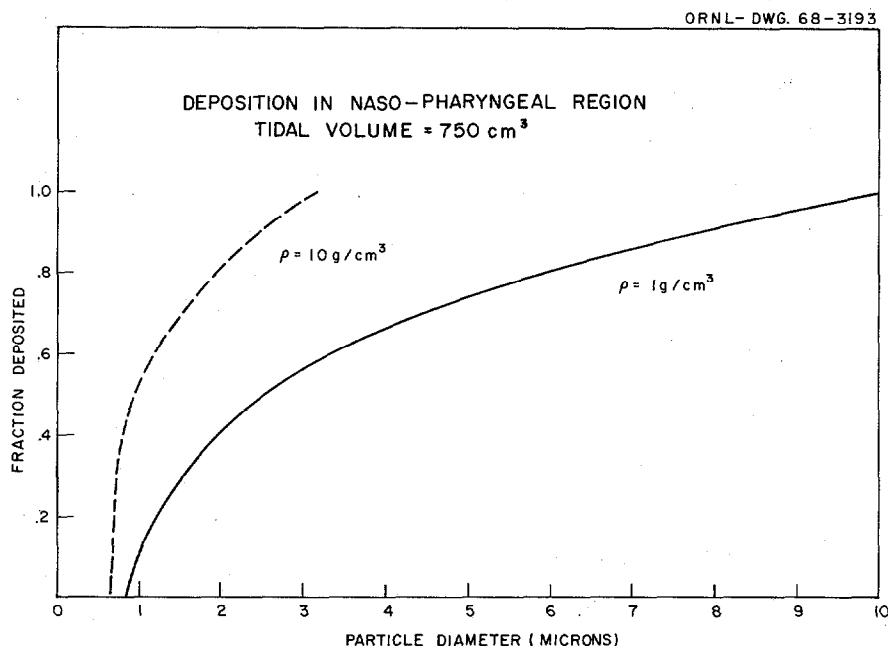


Fig. 5.4. Fraction deposited of spherical particles entering naso-pharyngeal region.

particle diameter.²⁷ The curves in Fig. 5.4 are not corrected for intake loss; however, the effect is not very significant in the size range predicted. It amounts to only about 2% for 10- μ -diam particles of density 10. Two significant points may be seen from these curves: first, particles larger than about 3 μ ($\rho = 10$) to 10 μ ($\rho = 1$) are not likely to penetrate to the tracheobronchial or the pulmonary regions of the lung; also, if large particles are involved, the nose and subsequently the gastrointestinal tract will be exposed to significant quantities of radioactivity. The curves in Fig. 5.5 show the deposition fractions corrected for intake loss.²⁷

(c) Mechanical clearance and retention. The general statement given above concerning the effect of deposition site on clearance rate applies equally to the mechanical translocation of particles deposited in the nasal passages. Not all nasal passages are lined with ciliated epithelium. The vestibule, representing the first centimeter or so beyond the external openings, is not ciliated but is lined with skin that bears numerous relatively coarse hairs (vibrissae) and sebaceous glands.²⁸ At the posterior end of the vestibular portion of the nasal passages, there is a constriction in

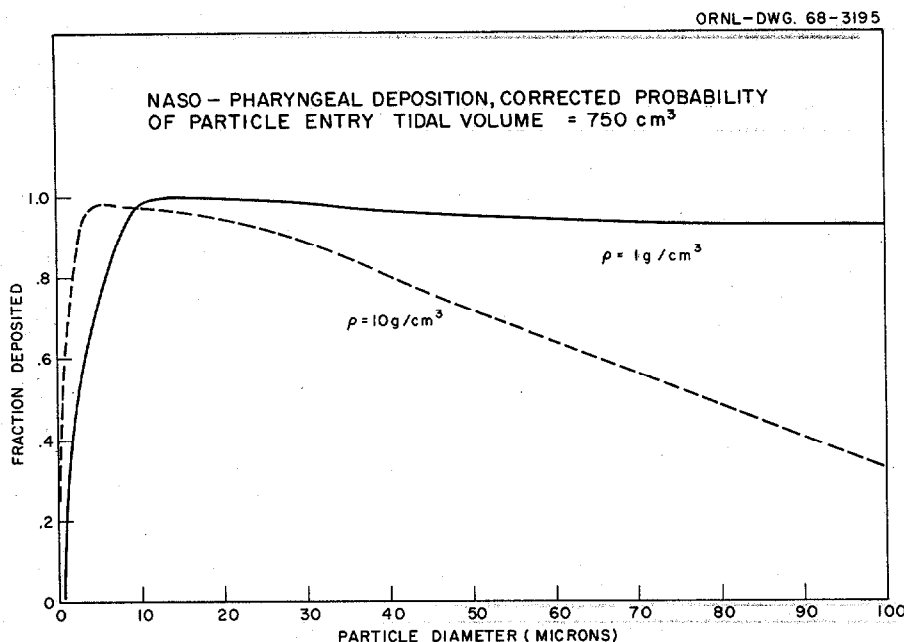


Fig. 5.5. Nasopharyngeal deposition, corrected for probability of particle entry (tidal volume = 750 cm³).

the airway where the lining changes to a mucus membrane having a surface epithelium composed primarily of ciliated cells with a few mucin-secreting goblet cells interspersed among the columnar epithelial cells.^{29,30} Ciliary streaming is directed generally in a posterior direction, so material deposited on the mucus blanket is transported rapidly, in a matter of perhaps 10 min, to the pharynx. However, there are no clear mechanisms to account for clearance of particles deposited on the nasal hairs. As a rough first approximation, it might be assumed that the half-life for attrition of particles on nasal hair is on the order of two months as a result of hair loss, nose blowing, etc. It has been found that sizable fractions (30 to 100%) of the total nasal deposition occurs on the nasal hairs;³¹⁻³³ the overall average is 50% for particles in the size range 2 to 40 μ ($\rho = 1$). Thus, without deliberate efforts to cleanse the nasal vestibule, there is reason to expect significant retention in the entry portion of the N-P region. Although dust particles have been recovered from the mucosa of the nasal sinus, Proetz³⁴ suggests that the normal sinus clears itself quickly of such foreign materials. However, Proctor³⁵

pointed out that the mucus stream of a child passes near or over the adenoid tissue and possibly leads to the long-term entrapment of particles in the adenoid crypts.

(d) Solubility. The chemical composition of nasal mucus can be expected to vary, depending on the state of health and other factors; however, Proetz³⁶ indicated that mucus can be assumed to contain about 95 to 97% water, 1 to 2% salts, and 2.5 to 3% mucin. Mucin is a complex polysaccharide combined with proteins. From the work of Hilding³⁷ and Tweedie,³⁸ it may be assumed that the pH of nasal mucus ranges from neutral to perhaps 8.4 and normally will be somewhat on the alkaline side at about pH 7.5. In any case, removal of plutonium from the nose is a competitive process between mechanical clearance and dissolution. If the possibility of dissolving any portion of the plutonium collected on the vestibular hairs is ignored, the remaining portion, with a half-life of perhaps 4 min, is cleared by mechanical means;¹² thus, the fraction removed per unit time is $\lambda_m = 0.693 \div 4 = 0.17 \text{ min}^{-1}$, or approximately 250 day^{-1} . The rate of removal of particle mass depends on the solubility factor k ($\text{g cm}^{-2} \text{ day}^{-1}$) and the specific surface of the particle (cm^2/g).³⁹ The fractional removal rate by dissolution would be $6k/d\rho$ for a spherical particle of diameter d and density ρ . For the solubility mechanism to represent as much as 1% of the total removed, the solubility factor k would have to exceed $0.42d\rho$, which for 1- μm -diam unit-density particles would be $42 \mu\text{g cm}^{-2} \text{ day}^{-1}$. Since the solubility factor for PuO_2 is at least a factor of 1000 smaller than this (see discussion on solubility in the pulmonary region, below), it may be assumed that dissolution during transit along the nasal mucosa is negligible. There is some evidence of the direct passage of dye⁴⁰ and virus⁴¹ particles into the cervical lymph duct, and according to Tonndorf and his associates,⁴² absorption of some materials through the nasal mucosa occurs rapidly, resembling absorption from subcutaneous injection. To summarize, it may be assumed that soluble particles can be transferred directly from the nose to the bloodstream, but PuO_2 is cleared mechanically; and, except for some possibility of an unknown fraction appearing in the lymphatic system, clearance proceeds toward the pharynx and then to the gastrointestinal tract.

Tracheobronchial region. The tracheobronchial region (T-B) includes the respiratory airways from the glottis through the trachea and the bronchial tree down to and including the terminal bronchioles. Taken together, the N-P and T-B regions constitute the anatomical dead space of the respiratory tract and represent the entire epithelial area of the respiratory system that is ciliated and covered with mucus arising from goblet cells and secretory glands.¹²

(a) Deposition in the T-B region. Although many significant studies have been made of total retention in the lower respiratory tract,⁴³⁻⁴⁵ in general it has not been possible to determine the fraction of inhaled particles deposited in the T-B region directly as a function of particle size. Indirect determinations are in reasonable agreement with theoretical calculations.⁴⁶ The results of calculations by the ICRP Task Group on Lung Dynamics are given in Table 5.1 for deposition in the T-B region in terms of unit-density and density-10 particles.¹²

Table 5.1. Calculated deposition probability for PuO₂ particles in the tracheobronchial airways

Particle diameter (μm) ^a		Deposition in T-B region (% of intake)
$\rho = 1 \text{ g/cm}^3$	$\rho = 10 \text{ g/cm}^3$	
0.6	0.2	1.9
1.0	0.3	2.7
2.0	0.6	5
3.0	1.0	6.4
4.0	1.3	6.9
6.0	1.9	4.3
10	3.2	0

^aRefers to particles of a single size.

(b) Mechanical clearance and T-B retention. Particles deposited on the mucus blanket of the T-B region are transported proximally toward the throat, where they eventually are swallowed, expectorated, or, in some cases, introduced into the nose and nasal sinuses by sneezing. The rate of clearance is quite unclear; estimates of total transit time from the

terminal bronchioles to the glottis vary from 15 to 20 min, based on work of Barclay and Franklin⁴⁷ with dogs and cats, to approximately 20 hr or more cited by Davies.⁴⁸ It seems likely that the smaller values of transit time may have been unduly influenced by the rapid clearance of large particles from the trachea and the major bronchi, while excessively long transit times probably reflect the relatively slower clearance of particles deposited in the proximal portions of the pulmonary region. Fish¹⁷ has calculated the total transit time of particles through the T-B region to be approximately 3 hr, based on Davies' anatomical model of the human lung⁴⁹ and on velocity measurements made by Hilding.⁵⁰ An approximate value of 30 min for the clearance half-life can be assumed if the time for "total" clearance is taken to be six half-lives.

(c) Solubility. Based on the relative significance of dissolution in lung fluids as compared with the competing process of mechanical clearance, it can be shown, as was done for solubility in the N-P region, that for 1% to be dissolved in transit, the solubility factor k must exceed about $0.06 d\rho$. For $1\text{-}\mu$ -diam unit-density particles, k would have to be greater than $6 \mu\text{g cm}^{-2} \text{ day}^{-1}$, but for PuO_2 the solubility factor is more than a factor of 100 smaller than this. Thus it is reasonable to neglect dissolution during mechanical transport of PuO_2 particles through the T-B region.

Pulmonary region. The pulmonary region (P region) consists of several structures, including the respiratory bronchioles, alveolar ducts, atria, alveoli, and alveolar sacs.¹² The region can be regarded functionally as the gas exchange space of the lungs. Its surface is covered with a moist, unciliated epithelium, and it is lacking in the secretory elements found in the T-B region.

(a) Deposition. Calculated values for the fraction of unit-density and density-10 particles expected to be deposited in the P region are shown in Fig. 5.6. The solid curve for unit-density particles was obtained by plotting the values given in Table 1 of the report of the ICRP Task Group on Lung Dynamics.¹² For the density-10 particles it was assumed that, for $d \geq 0.5 \mu$, deposition probability is the same as for unit-density particles of a size such that $d^2\rho$ is the same. For particles below about 0.5μ , diffusional deposition, which is independent of particle density, becomes

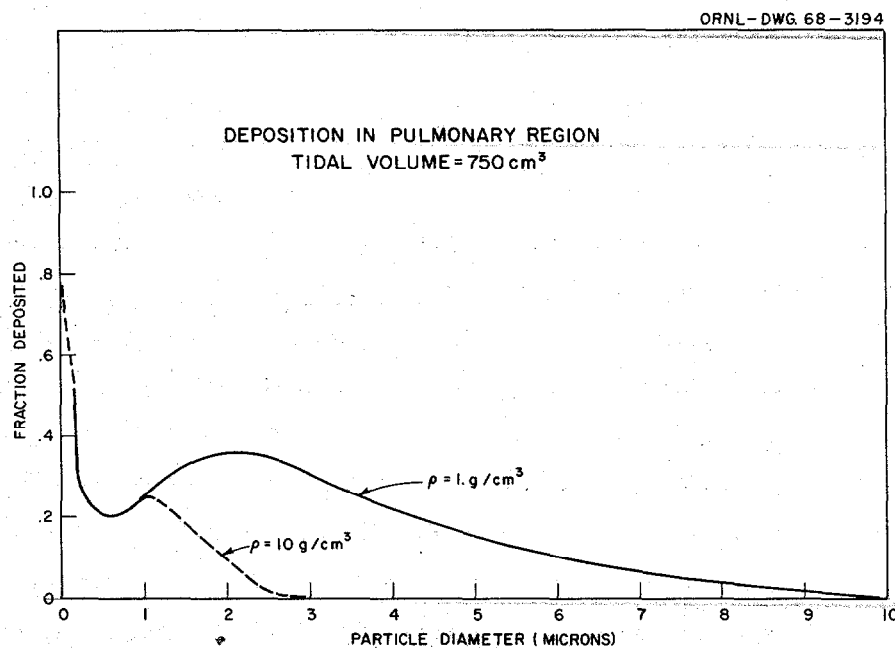


Fig. 5.6. Deposition in pulmonary region (tidal volume = 750 cm³).

dominant. The curves in Fig. 5.6 are for a tidal volume of 750 cm³ and a respiration rate of 15 per minute; this corresponds to a total intake of 10.8 m³ in 16 hr, which is approximately the amount assumed by the ICRP⁵¹ for the time away from work (10 m³). A tidal volume of 1450 cm³ at 15 respirations per minute corresponds to 10.4 m³ in 8 hr; ICRP⁵¹ assumes 10 m³ breathed during 8 hr of work. Comparison of the deposition probabilities for 750-cm³ vs 1450-cm³ tidal volumes shows a slightly reduced fraction deposited at the higher tidal volume; however, the curve given in Fig. 5.6 is the proper one for the general public and can be used with little error (slightly conservative) for occupationally exposed persons as well.

While Fig. 5.6 may be taken to be a fair representation of the deposition of monosized particles, it is difficult to apply in the practical case where invariably a distribution of sizes exists. The Lung Dynamics Task Group computed the total deposition of particles having sizes that are distributed log normally and found that, within perhaps 10 or 15% error, deposition can be related to the mass median aerodynamic diameter characterizing the size distribution without regard to the geometric standard deviation. The calculated percent deposition in the pulmonary region, shown in Fig. 5.7, is taken from the Lung Dynamics Task Group

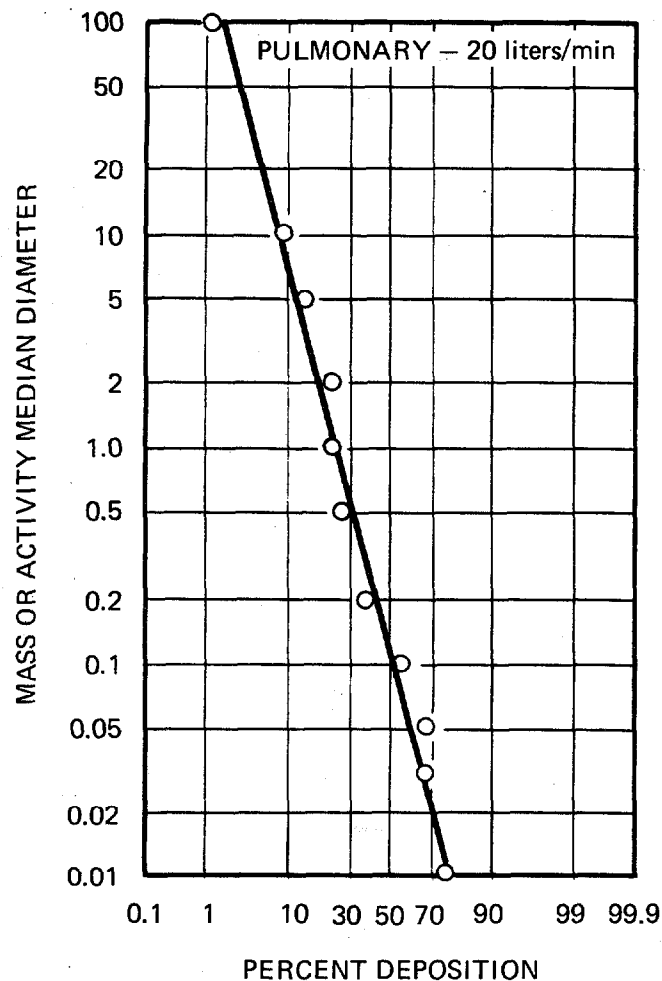


Fig. 5.7. The deposition estimate for the pulmonary compartment while breathing at a moderate work rate. Different aerosol distributions are represented by the mass or activity median aerodynamic diameters (0.01 to \sim 100). [Reproduced from Health Phys. 12, 173-207 (1966) by permission of the Health Physics Society.]

report and will be used for estimating the pulmonary deposition of accident released LMFBR fuel particles.

(b) Mechanical clearance. There are essentially two pathways for mechanical transport of particles out of the pulmonary region: (1) transport to the mucus blanket of the T-B tree and (2) translocation to the lymphatic system. Whether, and exactly how, particles may be actively transported by phagocytic cells moving selectively toward the ciliated areas of the T-B region is poorly understood.^{12, 52} It is clear that with barely soluble particulates, such as PuO_2 , some of the particles deposited

in the P region are removed from the lungs via the ciliary-mucus "escalator" of the tracheobronchial airways.⁵³ It is suggested that most, if not all, particles cleared in this way are within macrophages.⁵⁴ In the case of single exposures at low mass concentrations, a relatively rapid early phase clearance is usually observed.¹² Phase I clearance from the P region commonly is ascribed to "rapidly recruitable" phagocytes and ciliary-mucus transport. This phase may be characterized by a half-life of about 24 hr and may account for perhaps 40% of the PuO₂ deposited in the P region.¹² A portion of the PuO₂ particles deposited on the pulmonary epithelium is introduced into some of the lining cells by phagocytosis. The local entrainment of ²³⁹PuO₂ particles produces intense radiation fields in the engulfing cell. Thus, for example, a 1- μ -diam ²³⁹Pu particle will produce an average dose rate of 225 rads/hr to a 12- μ -diam cell;⁵⁵ consequently, phagocytosis that does not lead to the T-B region or to the lymphatic system within a few days is likely to result in the death of the macrophage and further delay in clearance.

Some of the deposited PuO₂ particles may be retained in association with local structural elements for long periods of time. Mechanical clearance of such material probably is related in a complex way to its cytotoxicity; thus, because of lack of irritant action, inert dust may be retained for long periods of time, while moderately toxic dusts may stimulate local reactions leading to enhanced clearance, and highly toxic particles may produce reactions so severe that the clearance mechanisms are damaged or inhibited. The latter may well describe the case for parenchymal deposits of ²³⁹PuO₂. Following endocytosis, some of the cells apparently become migratory phagocytes,¹² which can transport their contained PuO₂ either to the ciliated epithelium of the T-B region or interstitially into the lymphatic system. There are no direct measures of the apportionment between the various clearance pathways for the PuO₂ that is retained for long periods of time. The various estimates of clearance rates and fractions cleared by way of the different routes are indirect and rely to some extent on intuition.

The ICRP Task Group on Lung Dynamics suggests that relatively insoluble materials are cleared about 80% via the T-B region — half of this rapidly (24-hr half-life) and the remainder with the appropriate long-term

half-life — 15% to the lymphatic system, and 5% to the bloodstream by solubilization.¹² Clearance to the lymph nodes and to the bloodstream is assumed to follow the same rate constant as the fraction cleared slowly via the T-B region. In support of the assumed fraction transferred to the lymphatic system, reference can be made to the work of Bair,⁵⁶ who observed that an average of 14.5% of the initial lung deposit had been translocated to the lymph nodes of two dogs 40 weeks after a single inhalation of PuO₂ particles. Biological half-life for the slow clearance pathways is not well known — estimates range from 150 to 1400 days¹² — and probably depends upon solubility and particle size,³⁹ but it may be assumed to be approximately 500 days for a single acute exposure.

(c) Solubility. In connection with studies on the radiological safety of aerospace nuclear electric systems, a study was made by Clark and his associates²⁷ on the solubility of PuO₂ microspheres in water and in a simulant of lung fluids. The work was crude and incomplete but does provide an estimate of solubility that is in rough agreement with observed rates of plutonium clearance from the lung. Thus the observed solubility factor k was approximately $5 \times 10^{-8} \text{ g cm}^{-2} \text{ day}^{-1}$, corresponding to a solubility half-life of $2300d$ days, where d is the diameter in microns. These data suggest that for particle sizes between 0.1 and 1 μm the solubility half-life may range from 230 to 2300 days, more or less in agreement with the range 150 to 1400 days observed in experiments with animals.^{12,56,57}

Pulmonary lymph nodes. In terms of tissue mass, as well as fraction of the lung deposit reaching a retention site, probably the pulmonary lymph nodes (PLN) are among the most variable tissues in the body.^{58,59} However, when several individuals are involved, average values seem to follow reasonably predictable trends.⁵⁹

(a) Translocation to the PLN. Based on work of Bair⁵⁶ and the recommendations of the ICRP Task Group on Lung Dynamics,¹² it may be assumed that 15% of the PuO₂ deposited in the pulmonary region of the lungs is translocated to the PLN with a 500-day half-life. More recent results of Bair's study with dogs suggest that perhaps as much as 25% of the PuO₂ deposited in the alveoli is transferred to the PLN with a half-time as long as 1000 days.^{150,151}

(b) Clearance from the PLN. There are no data adequate to describe the clearance of PuO_2 from the PLN. The nearest approximation may be the study of uranium dioxide inhalation reported by Leach and his associates,⁶⁰ who exposed rats, dogs, and monkeys to chronic inhalation of UO_2 for periods of time up to approximately five years and observed some of the exposed animals for nearly two years after exposure ceased. The primary retention sites were observed to be lungs, PLN, spleen, liver, bones, and kidneys. The data indicate slow but definite clearance from the PLN; however, the relatively large deposits in spleen and liver and the time relationship of equilibrium organ burdens suggest that much, perhaps nearly all, clearance to the bloodstream was in the form of debris of damaged tissue or in some other nondiffusible phase. If this interpretation is correct and applicable to PuO_2 , the relative rate of tissue damage from a plutonium deposit compared with a uranium deposit would not be known. For a first approximation, it might be assumed that PuO_2 is cleared at the same rate as UO_2 or perhaps somewhat faster. Morrow⁶¹ has suggested a clearance half-time of 1000 days for the pulmonary lymph nodes, which appears reasonable in comparison with the results of the uranium studies and in view of the fact that the released fuel is a mixed Pu/U oxide comprised mostly of UO_2 .

Transfer from lung to bloodstream. Because of the low solubility of PuO_2 in the body fluids lining the respiratory system, the relatively large particles deposited, and their rapid clearance from the N-P and T-B regions, it is reasonable to conclude that only minor amounts of plutonium are absorbed into the bloodstream from those portions of the respiratory tract. On the other hand, the longer retention of particles in the P region leads to the absorption of about 5% into the bloodstream with a half-life of 500 days. Presumably, the 15% of the P-region deposit that is transferred to the pulmonary lymph nodes will eventually reach the circulatory system; thus, approximately 20% of the particles deposited in the P region will, in time, be transported to other organs of the body, either in the bloodstream or in the circulating lymph.

5.1.2 Ingestion

Ingestion of plutonium released into the environment may result from eating foods, drinking water, or swallowing particles trapped in the upper

respiratory system as a result of inhalation. In the case of accidental release of plutonium over a relatively short time, the major route of entry into the body during the release is via inhalation. Longer term exposure via food and water may be moderated or eliminated by remedial measures initiated after the event; however, for completeness, ingestion of contaminated foods and water is included in the following considerations.

Probable sources and intake. (a) Particles on leafy vegetables.

Plutonium-239 deposited on growing crops may be ingested by individuals directly by consuming raw or processed vegetables and fruits or indirectly by drinking milk or eating the flesh of animals grazed on contaminated forage crops. In either case, the time of deposition relative to the various stages in the plant growth cycle is a major factor affecting intake by man. Obviously, much less of the deposited material will enter the food chain if the deposition occurs during a period when there is little vegetation available for contamination than if the deposition occurs immediately prior to harvesting the crop. With increasing time between deposition and harvest, the transmission of the deposited materials through the food chain will diminish as a result of dilution by new plant growth and removal by weathering. Dilution and removal of radioactivity following a single deposition on vegetation have been characterized by an effective removal half-time related to a single exponential function. Thus the time-dependent concentration of deposited material on the crops is expressed by

$$C(t) = C_0 \exp\left(-\frac{0.693t}{T_e}\right),$$

where C_0 is initial concentration as deposited ($\mu\text{Ci}/\text{kg}$ on vegetation), $C(t)$ is concentration at time t after deposition, and T_e is effective removal half-time. Most studies of the removal of radioactive particulate materials by weathering processes have been related to weapons tests fallout and grasses or grasslike vegetation. However, some of this work has included other plants, such as cabbage, potatoes, sugar beets, and desert shrubs.⁶²⁻⁶⁴ A fortunate similarity in the half-residence time on various plants has been observed for a variety of radionuclides. Thompson⁶⁵ has suggested that this indicates the common behavior of particulate materials on plants and that for most practical problems a useful approximation of

the effective removal half-time (in days) of any material on plants is given by

$$T_e = \frac{13T_p}{13 + T_p},$$

where T_p is radiological half-life (days). Because of the long radiological half-life of ^{239}Pu , the effective half-life of PuO_2 retained on vegetation might be expected to be about 13 days.

Human intake of plutonium ($\mu\text{Ci}/\text{day}$) from vegetables contaminated in a single event would decrease with time after deposition as

$$I(t) = K C(t) = \frac{KD_0}{Y} e^{-0.0533t},$$

where K is average rate of consumption (kg/day), D_0 is initial aerial deposit ($\mu\text{Ci}/\text{m}^2$), and Y is crop yield (kg/m^2). This relation does not include a sticking factor, which may be nearly 1.0 for micron-size particles, or a target area factor. While the vegetation may not completely cover the land, in general the trajectory of fallout particles is unlikely to be straight down; hence the conservative assumption that the growing plants intercept all particles may not be far wrong.

Crop yields vary with a great variety of local conditions; consequently, it is necessary to refer to average yields for the country as a whole and to realize that locally these figures may be a factor of 2 or so high or low. Leafy vegetables that are commonly eaten raw (e.g., cabbage, lettuce, endive, etc.) yield on the average about 7 tons/acre ($1.6 \text{ kg}/\text{m}^2$).⁶⁶ Those that usually are cooked (e.g., artichokes, broccoli, brussels sprouts, spinach, etc.) yield about half that amount ($\sim 0.8 \text{ kg}/\text{m}^2$). For the same fallout density, curies of plutonium per square meter of crop, the deposition density on the crop (Ci/kg) might be expected to be less on the crop producing the greatest weight yield. Thus, purely on a crop-yield basis, the vegetables eaten cooked would retain about twice as much plutonium as the uncooked varieties; on the other hand, it may be assumed that the additional steps employed in preparing cooked foods are likely to result in some decontamination, perhaps by a factor of about 2. Consequently, as a first approximation, the leafy vegetables that are eaten raw

may be assumed to be representative of both cooked and uncooked varieties (i.e., $Y = 1.6 \text{ kg/m}^2$).

A study of human diet in New York, Chicago, and San Francisco⁶⁷ indicates that the average annual per capita consumption of fresh vegetables, excluding root crops, is about 43 kg. Some of this may be ascribed to low-surface-area vegetables such as beans and peas, so that 36.5 kg/year ($K = 0.1 \text{ kg/day}$) is probably a reasonable, although somewhat conservative, estimate.

Application of the above factors leads to an estimate of average plutonium intake rate ($\mu\text{Ci/day}$) at a given time after deposition:

$$I(t) = \frac{D_0}{16} e^{0.533t} .$$

If vegetable consumption were maintained undiminished for a period of about two and one-half months after an accidental release of plutonium, the total intake (μCi) would be

$$I = \int_0^{\infty} I(t) dt \approx 1.2D_0 .$$

(b) Ionic forms in water and food. Even the soluble forms of plutonium are not readily absorbed by plant roots and translocated to aerial portions of the plant. Jacobson and Overstreet⁶⁸ observed the absorption of PuO_2^{2+} from a culture solution to be only 0.01% and that of Pu^{3+} to be 0.0045% for a 24-hr exposure. Rediske, Cline, and Selders⁶⁹ found the concentration in seedling plants to be 9×10^{-4} that of the soil. A long-term cropping study by Romney⁷⁰ showed that only about $2 \times 10^{-5}\%$ of the total amount of PuO_2 was removed from the soil in 12 crops of ladino clover harvested over a three-year period from Nevada Test Site soil heavily contaminated by plutonium dispersed in nonnuclear high-explosive tests. Thus the uptake of plutonium into food or feed crops grown on contaminated soil is not expected to result in significant transfer of ^{239}Pu into the food chain of man.

Significant amounts of ^{239}Pu can be ingested by animals grazing on contaminated forage crops, but the amount assimilated from the GI tract into the bloodstream of the animals is expected to be extremely small (see below).⁷¹ Furthermore, of any quantity absorbed from the GI tract, only

small fractions are deposited in edible tissues. Transfer from blood to milk, for example, entails a concentration reduction by about a ratio of 40 to 1.

(c) Inhaled particles. With the exception of the minor fraction that is expectorated, most of the particulate material retained in the N-P and the T-B regions is cleared rapidly to the GI tract. In addition, about 40% of the PuO_2 deposited in the pulmonary region is transferred to the GI tract with a relatively short half-time. This pathway of elimination from the respiratory tract represents a source of ingestion. The total amount of ^{239}Pu reaching the GI tract within the first week after a single inhalation exposure is given in Table 5.2.

Transport and retention in GI tract. Poorly soluble particles of PuO_2 may reach the GI tract via clearance from the respiratory system or by ingestion of leafy vegetables. The total dose delivered to the walls

Table 5.2. Inhaled PuO_2 reaching GI tract within the first six days

Particle diameter (μm) ^a		Percentage of inhalation exposure reaching GI tract ^b
$\rho = 1 \text{ g/cm}^3$	$\rho = 10 \text{ g/cm}^3$	
0.6	0.2	10
1	0.3	24
2	0.6	59
3	1	73
4	1.3	82
6	1.9	88
10	3.2	99
20	6	98
30	10	97
60	19	94
	30	89
	40	80
	56	70
	60	63

^aRefers to particles of a single size.

^bExposure = time integral of airborne concentration times the average breathing rate.

of the GI tract depends on the location of the particles during transit through the various segments and on the retention time in each segment. The question of proximity of particles to the gut wall has been treated by Clark, Thompson, and Fish⁷² in connection with studies on nuclear rocket debris. In preliminary studies on mice, particles were found within 500 μ of the intestinal wall about six times more often than would be expected from a random geometrical distribution. The maximum range of ²³⁹Pu alpha particles in a tissue-like medium is about 48 μ , and only those particulates lying within this distance of the wall can affect the tissues lining the GI tract. Estimates of the probability of particles being located within 48 μ m from the wall are given in Table 5.3.

Table 5.3. Fraction of particles estimated to be within 48 μ m of the intestinal wall

Segment	Segment radius ^a (cm)	Fraction within 48 μ m of wall	
		Particles \sim 1 μ m	Particles \sim 100 μ m
Jejunum	1.25 ^b	0.008	0.005
Ileum	0.63 ^b	0.02	0.09
Ascending colon	1.25 ^c	0.008	0.05
Sigmoid colon	3.5 ^c	0.003	0.02

^aThese figures refer to the internal caliber of the segment.

^bEquivalent to 1/2 and 1/4 in. respectively; see Ref. 73.

^cFrom Ref. 74.

Transit time of particles through the GI tract varies widely among individuals.⁷⁵ Studies of transit time for insoluble ceramic spheres 30 to 40 μ m in diameter were conducted at the Argonne Cancer Research Hospital.⁷⁶ Twelve human subjects were observed for periods of time up to ten days following ingestion of ¹³⁴Cs-tagged spheres. DeAgazio⁷⁷ analyzed the

average percentage of particles remaining as a function of time after ingestion, and the indicated retention function was well represented by a single exponential ($T_{1/2} = 27$ hr) over the ten-day span of the study.

Plutonium dioxide particles that may be released in the event of a reactor accident are expected to be on the order of a few microns or smaller. Consequently, it may be estimated that only 0.3 to 2% of the ingested particles will be near enough to the intestinal wall to produce a significant dose. Thus, if the ingested amount, I (μCi), were conservatively assumed to remain in the ileum with a half-time of 27 hr, the effective integrated exposure ($\mu\text{Ci-days}$) would be

$$E = 0.032I .$$

Transfer from GI tract to bloodstream. Uptake of plutonium from the GI tract via partial solution of PuO_2 must be small indeed. Early studies by Scott and his associates⁷⁸ indicated an upper limit of intestinal absorption of 0.007%. More extensive studies by Katz, Kornberg, and Parker⁷⁹ and by Weeks and his associates⁸⁰ show the effect of valence state and chemical form of ingested plutonium on uptake by rats: $\text{Pu}(\text{NO}_3)_4$ administered chronically in pH-2 solutions was absorbed and retained to an average extent of 0.003%. This figure is supported by the observation⁸⁰ that pigs absorb 0.002% from pH-2 solutions of $\text{Pu}(\text{NO}_3)_4$. While much higher absorption fractions have been observed in special cases [e.g., pH-1 solutions of $\text{Pu}(\text{NO}_3)_4$], the figure 0.003% used by ICRP⁵¹ for soluble compounds of plutonium is conservative for PuO_2 . It was concluded by Thompson⁸¹ that the intestinal mucosa presents a very effective barrier to plutonium absorption under the usually anticipated conditions of exposure. An important exception to this general conclusion was the 0.25% uptake of plutonium observed by Ballou⁸² in one-day-old rats.

These conclusions for soluble compounds suggest that the uptake of PuO_2 should be entirely negligible; however, that conclusion may not be completely justified. Frazer and Stewart⁸³ demonstrated the direct uptake of 0.5- μ -diam paraffin particles through the intact gut wall. Saunders and Ashworth⁸⁴ found uptake of 0.1- to 0.2- μ latex particles by the epithelial cells lining the jejunum of mice. The process of pinocytosis is well known in primitive organisms and in suckling mammals (e.g.,

see Clark's work⁸⁵ with colloidal gold administered orally to mice and rats); however, there is evidence demonstrating particulate absorption in the adult animal under certain conditions.^{84, 86} Resin particles as large as 5 μ were taken up by the intestinal epithelium of calves.⁸⁷ The latex particles used by Saunders and Ashworth⁸⁴ were discharged into lymphatic vessels and later were found in many tissues of the body, especially the liver and kidney. These observations offer convincing evidence for the direct uptake of insoluble particles, especially of colloidal size, from the GI tract, but quantitative information is lacking.

5.1.3 Deposition on body surfaces

Plutonium dioxide that is not contaminated with fission products presents essentially no problem with respect to irradiation of the skin. However, if deposition of PuO₂ particles in the eyes or the penetration into a wound should occur, it could lead to radiation exposure of sensitive tissues.

Following the approach of Humphrey,⁸⁸ the human body is represented in this discussion by a series of cylinders approximating the dimensions of a man. In this treatment, only the face and head, together approximated by a 15-cm-diam cylinder, are considered. Theoretically, the Stokes number (discussed above) is the important parameter governing the impaction of particles on cylinders in laminar flow. In turbulent flow, additional factors are involved, and these will be mentioned later. For the approximation based on potential flow about an infinitely long cylinder, numerous authors⁸⁹⁻⁹² have shown that a critical Stokes number exists below which deposition by inertial impaction will not occur. Taylor,⁹⁰ and later Levin,⁹² calculated the critical Stokes number to be 0.125. Thus,

$$\text{critical Stk. No.} = 0.125 = \frac{V_0 d^2 \rho}{18\eta D},$$

where

V_0 (cm/sec) = local mean wind speed = 44.7U (mph),

d = particle diameter (cm),

ρ = particle density (g/cm³),

η = gas viscosity = 184.5×10^{-6} poise (air at 23°C),

D = cylinder diameter = 15 cm.

With the above substitutions,

$$d_c = \text{critical diameter} = \frac{118}{\sqrt{U\rho}} (\mu) .$$

On this basis, a 100-mph wind would be required to deposit 3.7- μ -diam spheres of density 10 (12 μ for $\rho = 1 \text{ g/cm}^3$). A more realistic wind speed of 10 mph would result in no deposition for density-10 particles smaller than 12 μ or unit-density particles smaller than 37 μ . Furthermore, for particle sizes larger than the critical diameter, impaction efficiency increases slowly with Stokes number, approximately following the empirical equation of Landahl and Herrmann,⁹³

$$E = \frac{S^3}{S^3 + 1.54S^2 + 1.76} ,$$

where E is impaction efficiency (fraction) and S is Stokes number. It is unlikely that simple inertial impaction will produce significant deposition of PuO_2 particles on the human body; however, natural levels of turbulence in the atmosphere may result in a small, but finite, deposition rate. While there is no completely satisfactory treatment of the theory of turbulent deposition, the work of Owen⁹⁴ is of some interest. Owen concluded that in the final stage of approach to the surface, a particle is projected across a nonturbulent "free-flight" distance, which is independent of particle size and initial velocity. This approach has been criticized on the basis of the well-known variation of particle stop distance with both size and velocity.⁹⁵⁻⁹⁷ Nevertheless, as shown by the work of Klebanoff⁹⁸ and Hinze,⁹⁹ the contribution to the turbulence energy in the low-wave-number range (large eddies) decreases as the surface is approached, while the contribution in the high-wave-number range is increased. Thus the larger particles, which respond primarily to larger eddies, receive most of their impetus toward the surface while they are relatively farther away than the

smaller particles, which are affected by the smaller-scale eddies. Consequently there may be a tendency to compensate for the longer stop distance of large particles. Chamberlain¹⁰⁰ noted that for submicron particles Owen's results lead to

$$V_g = 4 \times 10^{-3} U_* ,$$

where V_g is deposition velocity and U_* is friction velocity. If the friction velocity for natural flow over the ground is 40 cm/sec, $V_g \approx 0.2$ cm/sec. This form of turbulent deposition tends to be applied rather uniformly on all exposed surfaces, whether on the windward or the leeward side of an obstacle. In addition, as a result of added turbulence in the wake produced on the leeward side, enhanced deposition is observed, especially for particles small enough to become entrained in the wake.¹⁰¹ For purposes of estimating radiation exposures, it is probably safe to assume that the deposition velocity is about 0.5 cm/sec and that the target area (the eyes) is approximately 4 cm²; thus the total intake to the eyes (μCi) would be estimated to be two times the integrated exposure ($\mu\text{Ci-sec/cm}^3$).

5.2 Systemic Distribution and Retention

The distribution and retention of injected plutonium has been studied in mouse,¹⁰² rat,¹⁰³⁻¹¹⁰ dog,¹¹¹⁻¹¹⁴ swine,^{115,116} and man.¹¹⁷ While the results are not entirely consistent, it is possible to draw a few general conclusions concerning the early distribution of injected plutonium compounds. In all cases the primary sites of deposition are the bone and the liver. Conditions favoring the atom-by-atom absorption of plutonium in a monomeric state lead to a higher percentage deposition in the bone, while polymeric forms tend to be deposited more in the liver. Although small amounts of systemic plutonium are deposited in tissues other than bone and liver, the concentrations involved are not considered significant with the possible exception of the gonads (Sect. 5.2.4).

5.2.1 Transport in the bloodstream

Qualitatively, plutonium can display either of three different modes of behavior in the blood: first, a readily diffusible form that may be

ionic or a complex capable of diffusing out of the bloodstream; a second form involves complexes with relatively large proteins that do not diffuse out of the circulatory system; and, finally, even larger colloidal aggregates that may enter the blood directly or be produced in the blood following the absorption of certain ionic forms. Little is known about the forms of plutonium reaching the blood by routes other than intravenous injection. However, information from animal studies and from autopsies of exposed and unexposed humans permits some reasonable guesses. Tissue distribution of plutonium absorbed from the GI tract,¹¹⁸ from intramuscular injection,^{78,119,120} and through the intact skin¹²¹ suggests that it enters the blood in an ionic or a diffusible complex form, resulting in predominantly skeletal deposits. In contrast, in human autopsy studies^{117,121-124} and in some inhalation studies of PuO₂ in dogs,¹²⁵ plutonium has been seen to deposit predominantly in the liver. This observation suggests that plutonium may be absorbed from a PuO₂ lung deposit in the Pu⁴⁺ state or in a particulate form, or both.

5.2.2 Deposition and retention in bone

Studies of the relative concentration of plutonium in different parts of the skeleton have not produced completely consistent results. In general, however, highest concentrations are noted in vertebrae and lowest concentrations in the flat bones of the skull. No comprehensive study has been made of the effect of age on bone deposition or retention; however, limited observations suggest that age has no substantial effect.^{126,127} Total skeletal retention of plutonium has been measured many times in experimental animals. On the basis of a study with seven dogs over a four-year period, Rysina and Erokhin¹¹² estimated the biological half-life of plutonium to be 9 years in the rib and 11 years in the femoral diaphysis. Based on work of Stover, Atherton, and Keller¹¹³ with 25 dogs, it has been estimated that about 15% of skeletal plutonium is lost in 4 years, corresponding to a biological half-life of approximately 17 years. Although direct measurements of plutonium retention in the skeleton of man have not been made, estimates of biological half-life can be related to total excretion rates. From the work of Langham and his associates,^{117,128,129}

it is estimated that about 20% is lost by excretion from the body in the first 50 years, suggesting a biological half-life in excess of 150 years. Consequently, for the purposes of calculating internal dose to bone, little error is involved if skeletal deposits are assumed to be retained permanently. From the literature on intramuscular injection of plutonium in rats,^{78,119,120} it is estimated that about 60% of the absorbed plutonium is deposited in bone, about 4% in the liver, and perhaps 30% is excreted. This proportion may be assumed to be approximately true for absorption from wounds and from the GI tract. Absorption from the lung probably is best described by data of Foreman, Moss, and Langham,¹²¹ thus 56% goes to the liver, 42% to the skeleton, and 2% to other tissues of the body.

5.2.3 Deposition and retention in liver

Early assessments of plutonium distribution in the body assumed that 90% of the systemic burden would be in the skeleton and only 7% in the liver.⁵³ While that partitioning may be true for some routes of entry to the bloodstream, as discussed above, it is clear that it grossly underestimates the fraction going to the liver in some important cases. The division of the total systemic burden between liver and bone depends on the chemical and physical state of the plutonium in the bloodstream. However, because of the difference in relative total mass of the two tissues, the concentration in liver can be expected to be roughly the same or considerably higher than that in the bone. Thus liver, along with bone, is a major site of plutonium deposition.⁸¹ Early studies with mice and rats indicated rapid clearance of plutonium from the liver relative to the rate of loss from bone,^{103,104,119} but the results from studies with larger animals have emphasized the potential hazards of plutonium deposits in the liver. In one study with beagle dogs, only 20% of the deposited plutonium was lost from the liver in four years.¹¹² The very limited data available for plutonium in man discussed above suggest that retention times in liver are not significantly different from those in bone. Data in the literature are somewhat contradictory; however, the conservative assumption of no significant loss of plutonium from the liver is probably not greatly in error.

5.2.4 Deposition and retention in gonads

Human data. One report, published in 1962, shows that fallout plutonium in a composite "gonad" sample from six cadavers was present in a concentration second only to that in the pulmonary lymph nodes.¹³⁰ The spleen and kidney contained an average of 0.6 pCi/kg, while the pulmonary lymph nodes contained 6.3 and the gonads 4.5 times the concentration found in the lungs (0.78 pCi/kg). Age at time of death was in each case greater than 70 years. Nothing is known concerning the elimination rate of plutonium from deposits in human gonads; however, animal data suggest that the biological half-life is at least 450 days in rat testes and may be much longer, perhaps infinite.¹³¹

Animal data. Work done by Taylor¹³¹ at the Institute for Cancer Research in England indicates that 0.06% of a single intravenous injection of plutonium nitrate is deposited in the testes of rats. Stover and her associates¹³² reported that $2 \times 10^{-3}\%$ of an intravenous injection of Pu(IV) citrate was deposited per gram of testes in a single beagle dog; based on the testes weighing approximately 15 g, the total deposited plutonium was about 0.03% of the injected dose. Bustad and his associates¹³³ administered noncitrate plutonium nitrate (pH 2 to 2.5) to miniature swine by intratracheal injection, and the amount found in the testes of two animals sacrificed on the 25th day after exposure was approximately 0.02% of the total amount reaching the bloodstream. More to the case at hand, Morrow and his associates¹³⁴ exposed 22 dogs to single inhalations of PuO₂ particles and found that 0.068% of the absorbed plutonium was deposited per gram of ovaries plus adrenals. If these tissues are assumed to weigh approximately 1.3 g and if the amount in the ovaries is 75% of the combined ovary and adrenal deposit, as in Bustad's study, the result suggests that about 0.066% of the absorbed plutonium was deposited in the ovary. Based on the above animal studies, it seems prudent to assume that approximately 0.1% of the plutonium reaching the bloodstream is deposited in the gonads, either ovary or testes. The observed rate of elimination of plutonium from the testes is slow,^{119,135} and one observer saw no obvious reduction of the plutonium content of rat ovaries over a 40-week period.¹³⁶ Deposits within the ovaries are highly localized to the granulosa layer of certain

follicles.¹³⁵ In view of the smaller average size of the ovary (8 g total) than the testes of standard man (40 g total) and the indication of longer retention, it is probably correct to consider exposure to the ovary as the deciding factor in evaluating genetic dose and to assume that no elimination occurs.

Lindenbaum,¹³⁷ of Argonne National Laboratory, has indicated that recent preliminary data on female mice injection with plutonium showed that the concentration in ovaries was about 20 times that in the skeletal muscle and about 6 times that in the heart; this was true both for monomeric and polymeric plutonium even at one and two years postexposure. In fact, the concentration in the ovaries was comparable with that in the liver when the monomeric form was administered; but for the polymeric form, the liver concentration is enhanced and exceeds the concentration in the ovaries.

5.2.5 Elimination of plutonium from the body

Because of the generally slow rate of loss of plutonium from the major deposition sites in the body, it is suggested that no credit be allowed for biological elimination in estimating internal radiation dose. Two other areas of interest that remain are the detection and estimation of accidental exposures to man and animals and the therapeutic enhancement of excretion rate to reduce the dose commitment of the exposed subject.

Diagnosis of plutonium exposure by excretion analysis. During the first few hours following a release of plutonium, it would be desirable to identify those persons actually having sustained an exposure out of the generally larger group of people potentially exposed. In order to initiate possible remedial measures, it might further be necessary to make rough estimates of body burden as a basis for assigning priorities and for choosing the degree of treatment required. Unfortunately, the amount of plutonium that might be considered significant is extremely low, and, in addition, the fraction excreted per unit time is also small; consequently, rapid detection by excretion analysis is not usually possible. A further complication in the interpretation of urinary excretion data for plutonium exposures has been pointed out by Healy.¹³⁸ His treatment of the expected urinary plutonium levels following single inhalation exposures to plutonium dioxide suggests that the urinary excretion rate may be relatively

low during the period immediately after the exposure and may reach a peak a few days to a few months later, depending on the "solubility half-life" in the lungs. In line with Healy's work and the discussion of solubility of PuO_2 in lung fluids, it appears that a significant fraction of the particle mass would have to lie in the particle size range below about 0.01 μm diameter for the early excretion rates to be an appreciable fraction of the amount deposited in the lungs. While it is not clear what the size distribution of inhaled PuO_2 particles would be, there are some indications that a large fraction of the primary particles comprising the airborne agglomerates probably would be sufficiently small to result in rapid appearance of plutonium in the urine. The point is, however, that even though some of the exposure cases likely could be detected by urinary excretion analysis within perhaps a day after inhalation, still the absence of high levels of plutonium in the urine would not be a reliable indication of a negligible exposure. Variability in particle size and possible variations in individual metabolism can easily result in several orders of magnitude difference in plutonium urinary excretion rate, as observed by Swanberg¹³⁹ for two persons sustaining inhalation exposures of approximately the same quantities of PuO_2 . Thus, while a positive finding would clearly identify an exposed individual, the lack of significant amounts of plutonium in the urine could not give an unambiguous indication of an absence of exposure. On the other hand, urinary plutonium excretion data collected over a period of months can be analyzed by methods discussed by Snyder¹⁴⁰ to yield apparently reasonable estimates of body burden.

Therapeutic enhancement of excretion rate. Numerous efforts have been made to speed up the excretion of plutonium because of its relatively high toxicity and low rate of elimination from the body.¹⁴¹⁻¹⁴⁴ Two approaches may be taken: (1) treatment at the level of the intake portal may be undertaken to prevent or reduce the rate of absorption from the lungs or the GI tract, or treatment, administered via the bloodstream, may be directed toward removal of plutonium from the bone and liver and (2) its interception before bone or liver deposition. Although little work has been done on antiabsorption treatment in the GI tract, some studies by Belyaev¹⁴⁵ in Russia have shown that anion-exchange resins administered

within 5 to 10 min after ingestion of plutonium compounds effectively reduced absorption of Pu(IV) citrate by a factor as high as 10, while the absorption of plutonium nitrate was reduced by a factor of 3 or less. Some limited success has been reported in the removal of lung-deposited plutonium by treatment with chelating agents. Prompt inhalation of EDTA or DTPA aerosols after intratracheal administration of plutonium was observed¹⁴⁶ to reduce lung retention of plutonium in the rat by a factor of 2. Dogs exposed to PuO₂ by inhalation were treated daily for 15 days with an inhaled DTPA aerosol that increased the urinary excretion rate but did not significantly reduce whole-body retention.¹⁴⁷ Treatment with an inhaled aerosol of polypropylene glycoethylen oxide (Pluronic F68, a surface-active agent) reduced PuO₂ retention by about 80%.¹⁴⁷

Norwood^{148,149} has described the treatment of five plutonium inhalation cases with DTPA. In each case treatment was begun several years after exposure. Dosages of 2 g of DTPA or less per day were administered as the trisodium calcium salt by intravenous drip. During initial treatment, urinary excretion of plutonium increased by at least 40-fold, and in one case by a factor of 120. Two of these cases had previously been treated with EDTA, which had effected only a six- to tenfold increase in plutonium excretion. Fecal excretion of plutonium was increased during DTPA treatment by an average factor of 6, which is particularly significant, since these patients (exposed by inhalation) were normally excreting several times as much in the feces as in the urine. Also of significance was the consistent observation that the effect of DTPA was sustained over a period of many days after treatment, differing in this respect from EDTA. One of these cases was treated over a period of two years.¹⁴⁹ With continued intermittent treatment, the effectiveness decreased, after a year, to about 20% of that initially observed. After a period of several months without treatment, resumption of DTPA administration again increased plutonium excretion in both urine and feces to approximately the level attained with initial treatment.

References

1. R. C. Thompson, "Biological Factors," pp. 785-829 in Plutonium Handbook, a Guide to the Technology, ed. by O. J. Wick, vol. II, Gordon and Breach, New York, 1967.
2. R. H. Wilson, "Controlling and Evaluating Plutonium Deposition in Humans," *ibid.*, pp. 831-44.
3. J. M. Nielsen and T. M. Beasley, "Radiochemical Determination of Plutonium for Radiological Purposes," *ibid.*, pp. 921-36.
4. Mieczyzslaw Taube, Plutonium, Pergamon and Macmillan, New York, 1964.
5. B. A. J. Lister, Health Physics Aspects of Plutonium Handling, British Report AERE-L-151 (1964).
6. R. S. Stone, "Health Protection Activities of the Plutonium Project," *Proc. Amer. Phil. Soc.* 90, 11 (1946).
7. K. Williams, Studies of the Toxicology of Plutonium, British Report AERE-R-2970 (June 1959).
8. Committee II of the International Commission on Radiological Protection, "Bibliography for Biological, Mathematical and Physical Data," *Health Phys.* 3, 235 (1960).
9. R. C. Thompson (ed.), "Proceedings of the Hanford Symposium on the Biology of the Transuranic Elements," *Health Phys.* 8, 561 (1962).
10. W. H. Langham, "Physiology and Toxicology of Plutonium-235 and Its Industrial Medical Control," *Health Phys.* 2, 172 (1959).
11. A. V. Lebedinsky and Yu. I. Moscalev (eds.), Plutonium-239 Distribution, Biological Activity and Acceleration of Excretions, State Medical Publishing House, Moscow, 1962.
12. P. E. Morrow et al., "Deposition and Retention Models for Internal Dosimetry of the Human Respiratory Tract, Task Group on Lung Dynamics," *Health Phys.* 12, 173-207 (1966).
13. N. A. Fuchs, The Mechanics of Aerosols, chap. 11, Pergamon, Oxford, 1964.
14. *Ibid.*, p. 139.
15. P. G. Gormley and M. Kennedy, "Diffusion from a Stream Flowing through a Cylindrical Tube," *Proc. Roy. Irish Acad.* 52A, 163-69 (1949).

16. A. Einstein, "Über die von der Molecular-kinetischen Theorie der Wärme geforderte Bewegung von in ruhenden Flüssigkeiten suspendierte Teilchen," *Ann. Physik* 17, 549-60 (1905).
17. B. R. Fish, Oak Ridge National Laboratory, unpublished calculations, 1969.
18. C. N. Davies, "Dust Sampling and Lung Disease," *Brit. J. Ind. Med.* 9, 120 (1952).
19. W. Findeisen, "Über das Absetzen kleiner in der Luft suspendierten Teilchen in der menschlichen Lunge bei der Atmung," *Pflügers Arch. Ges. Physiol.* 236, 367-79 (1935).
20. A. M. Lucas and L. C. Douglas, "Principles underlying ciliary activity in the respiratory tract. II. A comparison of nasal clearance in man, monkey and other mammals," *Arch. Otolaryngol.* 20, 518 (1934).
21. A. C. Hilding, "Ciliary streaming in the bronchial tree and the time element in carcinogenesis," *New Engl. J. Med.* 256, 635 (1957).
22. A. C. Hilding, "Ciliary streaming through the larynx and trachea; relation to direction of ciliary beat and significance in sites of respiratory disease," *J. Thorac. Surg.* 37, 108 (1959).
23. A. C. Hilding, "Experimental sinus surgery; some experiments on ventilation and sinusitis," *Laryngoscope* 58, 1098 (1948).
24. A. E. Barclay, K. J. Franklin, and R. G. MacBeth, "A contribution to the study of ciliary movement," *J. Physiol.* 90, 347 (1937).
25. T. G. Clark et al., Biohazards of Aerospace Nuclear Systems, SC-CR-67-2845 (December 1967).
26. L. Silverman and C. E. Billings, "Pattern of airflow in the respiratory tract," pp. 9-46 in Inhaled Particles and Vapours, ed. by C. N. Davies, Pergamon, Oxford, 1961.
27. T. G. Clark et al., Nuclear Safety Environmental Studies: Biohazards of Aerospace Nuclear Systems - Final Report, SC-CR-69-3291 (December 1969).
28. T. F. Hatch and P. Gross, Pulmonary Deposition and Retention of Inhaled Aerosols, p. 11, Academic, New York, 1964.
29. V. Negus, Comparative Anatomy and Physiology of the Nose and Paranasal Sinuses, p. 337, E and S Livingstone, Ltd., Edinburgh, 1958.
30. A. A. Maximow and W. Bloom, A Textbook of Histology, 7th ed., p. 578, W. B. Saunders, Philadelphia, 1957.

31. H. D. Landahl and S. Black, "Penetration of Air-Borne Particulates Through the Human Nose," J. Ind. Hyg. Toxicol. 29, 269-77 (1947).
32. H. D. Landahl and T. Tracewell, "Penetration of Air-Borne Particulates Through the Human Nose, II," J. Ind. Hyg. Toxicol. 31, 55-59 (1949).
33. N. Rashevsky, Some Medical Aspects of Mathematical Biology, chap. 5, Charles C. Thomas, Springfield, Ill., 1964.
34. A. W. Proetz, Applied Physiology of the Nose, 2d ed., p. 315, Annals Publishing Co., St. Louis, 1953.
35. D. F. Proctor, "Physiology of the Upper Airway," Handbook of Physiology, Section 3: Respiration, vol. 1, chap. 8, ed. by W. O. Fenn and H. Rahn, American Physiological Society, Washington, D.C., 1964.
36. Proetz, op. cit., ref. 34, p. 311.
37. A. Hilding, "Note on Some Changes in the Hydrogen Ion Concentration of Nasal Mucus," Ann. Otol., Rhinol., Laryngol. 43, 47 (March 1934).
38. A. R. Tweedie, "Nasal Flora and Reaction of the Nasal Mucus," J. Laryngol. Otol. 49, 586 (September 1934).
39. T. T. Mercer, "On the Role of Particle Size in the Dissolution of Lung Burdens," Health Phys. 13, 1211-21 (1967).
40. J. M. Yoffey, "The Lymphatic Pathway for Absorption from the Nasopharynx," Lancet, 529 (Apr. 26, 1941).
41. J. M. Yoffey and E. R. Sullivan, "Lymphatic Pathway from the Nose and Pharynx," as cited by Proetz, op. cit., ref. 34, p. 336.
42. J. Tonndorf et al., "Absorption from Nasal Mucous Membrane," Ann. Otol., Rhinol., Laryngol. 62, 630 (1953).
43. A. M. Wijk and H. S. Patterson, J. Ind. Hyg. Toxicol. 22, 31 (1940).
44. B. Altshuler, Inhaled Particles and Vapours, p. 47, Pergamon, Oxford, 1961.
45. L. Dautrebande, H. Beckmann, and W. Walkenhorst, Arch. Ind. Health 16, 179 (1957).
46. H. D. Landahl, T. N. Tracewell, and W. H. Lassen, Arch. Ind. Hyg. Occup. Med. 3, 319 (1951).
47. A. E. Barclay and K. J. Franklin, "The Rate of Excretion of India Ink Injected into the Lungs," J. Physiol. (London) 90, 482-84 (1937).

48. C. N. Davies, Comments on Report of Task Group on Lung Dynamics, unpublished talk presented at the Radiobiology Forum, Medical Research Council, London, Feb. 28, 1967.
49. C. N. Davies, "A Formalized Anatomy of the Human Respiratory Tract," pp. 82-87 in Inhaled Particles and Vapours, ed. by C. N. Davies, Pergamon, Oxford, 1961.
50. A. C. Hilding, "Phagocytosis, Mucus Flow and Ciliary Action," Arch. Environ. Health 6, 61-71 (1963).
51. Recommendations of the International Commission on Radiological Protection, Report of Committee II on Permissible Dose for Internal Radiation, Pergamon, Oxford, 1959.
52. Hatch and Gross, op. cit., ref. 28, pp. 82ff.
53. Morrow et al., op. cit., ref. 12, p. 186.
54. L. J. Casarett, "Some Physical and Physiological Factors Controlling the Fate of Inhaled Substances. II. Retention," Health Phys. 2, 379-86 (1960).
55. C. L. Sanders, "Maintenance of Phagocytic Function Following $^{239}\text{PuO}_2$ Particle Administration," Health Phys. 18, 82-85 (1970).
56. W. J. Bair, "Deposition, Retention, Translocation and Excretion of Radioactive Particles," pp. 192-207 in Inhaled Particles and Vapours, ed. by C. N. Davies, Pergamon, Oxford, 1961.
57. K. G. Scott et al., "Deposition and Fate of Plutonium, Uranium and Their Fission Products Inhaled as Aerosols by Rats and Man, Arch. Pathol. 48, 31 (1949).
58. B. R. Fish, "Inhalation of Uranium Aerosols by Mouse, Rat, Dog and Man," pp. 151-65 in Inhaled Particles and Vapours, ed. by C. N. Davies, Pergamon, Oxford, 1961.
59. R. G. Thomas, "Influence of Aerosol Properties upon Gross Distribution and Excretion," Health Phys. 10, 1013-28 (1964).
60. L. J. Leach et al., "A Five-Year Inhalation Study with Natural Uranium Dioxide (UO_2) Dust. I. Retention and Biologic Effect in the Monkey, Dog and Rat," Health Phys. 18(6), 599-612 (June 1970).
61. P. E. Morrow, personal communication, May 1970.
62. J. Moorby and H. M. Squire, "The Loss of Radioactive Isotopes from the Leaves of Plants in Dry Conditions," Radiation Botany, vol. 4, 1964.

63. W. E. Martin, "Losses of ^{90}Sr , ^{89}Sr and ^{131}I from Fallout-Contaminated Plants," Radiation Botany, vol. 4, 1964.
64. Agricultural Research Council Radiobiological Laboratory, Surveys of Radioactivity in Human Diet and Experimental Studies, ARCRL-5, pp. 51-52 (1961).
65. S. E. Thompson, Effective Half-Life of Fallout Radionuclides on Plants with Special Emphasis on Iodine-131, UCRL-12388 (1965).
66. J. E. Knott, Handbook for Vegetable Growers, Wiley, New York, 1962.
67. Radiological Health Data, U.S. Department of Health, Education, and Welfare, Public Health Service, vol. IV(4) through VI(2), April 1963 to February 1965.
68. L. Jacobson and R. Overstreet, "The Uptake by Plants of Plutonium and Some Products of Nuclear Fission Absorbed on Soil Colloids," Soil Sci. 65, 129-34 (1948).
69. J. H. Rediske, J. F. Cline, and A. A. Selders, The Absorption of Fission Products by Plants, HW-36734 (1955).
70. E. M. Romney, unpublished data referred to by J. H. Olafson and K. H. Larson in Plutonium, Its Biology and Environmental Persistence, UCLA-501 (December 1961).
71. R. O. McClellan, H. W. Casey, and L. K. Bustad, "Transfer of Some Transuranic Elements to Milk," Health Phys. 8, 689 (1962).
72. T. G. Clark, J. L. Thompson, and B. R. Fish, Retention of Small Particles in the Gastrointestinal Tract and Their Proximity to the Wall During Transit, ORNL-3849, pp. 223-26 (July 1965).
73. J. L. Kantor and A. M. Kasich, Handbook of Digestive Diseases, 2d ed., p. 296, C. V. Mosby Co., St. Louis, 1947.
74. C. J. Best and N. B. Taylor, Physiological Basis of Medical Practice, Williams and Wilkins, Baltimore, 1961.
75. Clark, Thompson, and Fish, op. cit., ref. 72, pp. 223-24.
76. G. V. LeRoy, J. H. Rust, and R. J. Hasterlik, The Consequences of Ingestion by Man of Real and Simulated Fallout, ACRH-102, Argonne Cancer Research Hospital.
77. A. W. DeAgazio, Dose Calculation Models for Re-Entering Nuclear Rocket Debris, NUS-229 (Rev.) (October 1965).

78. K. G. Scott et al., "The Metabolism of Plutonium in Rats Following Intramuscular Injection," *J. Biol. Chem.* 176, 283 (1948).
79. J. Katz, H. A. Kornberg, and H. M. Parker, "Absorption of Plutonium Fed Chronically to Rats," *Amer. J. Roentgenol.* 73, 303 (1955).
80. M. H. Weeks et al., "Further Studies on the Gastrointestinal Absorption of Plutonium," *Radiat. Res.* 4, 339 (1956).
81. R. C. Thompson, "Biological Factors," pp. 785-829 in Plutonium Handbook, chap. 23, Gordon and Breach, New York, 1967.
82. J. E. Ballou, "Effects of Age and Mode of Ingestion on Absorption of Plutonium," *Proc. Soc. Exptl. Biol. Med.* 98, 726 (1958).
83. A. C. Frazer and H. C. Stewart, "Emulsification and Absorption of Fats and Paraffins in the Intestine," *Nature (London)* 149, 167-68 (1942).
84. E. Saunders and C. T. Ashworth, "A Study of Particulate Intestinal Absorption and Hepatocellular Uptake. Use of Polystyrene Latex Particles," *Exp. Cell Res.* 22, 137-45 (1961).
85. S. L. Clark, Jr., "The Ingestion of Proteins and Colloidal Materials by Columnar Absorptive Cells of the Small Intestine in Suckling Rats and Mice," *J. Biophys. Biochem. Cytol.* 5, 41-50 (1959).
86. R. J. Barnett, "The Demonstration with the Electron Microscope of the End-Products of Histochemical Reactions in Relation to the Fine Structure of Cells," *Exp. Cell Res.*, suppl. 1, 65-89 (1959).
87. J. M. Payne, B. F. Sansome, and R. J. Garner, "Uptake of Small Resin Particles (1-5 μ diameter) by the Alimentary Canal of the Calf," *Nature (London)* 188, 586-87 (1960).
88. A. E. Humphrey, TASK RATIO: Estimating Impaction of Aerosols on a Man Target (Rev.), Report of Institute for Cooperative Research, University of Pennsylvania, Nov. 1, 1961 (ASTIA catalog No. AD-278245).
89. M. Glauert, Aeronautical Research Committee Report No. 2025, H.M.S.O., London, 1940.
90. G. I. Taylor, Aeronautical Research Committee Report No. 4350, D.W.T. 3, H.M.S.O., London, 1940.
91. I. Langmuir and K. B. Blodgett, Mathematical Investigation of Water Droplet Trajectories, General Electric Research Laboratory Report R.L.-225 (Dec. 1944-June 1945); also in Collected Works of Irving Langmuir, ed. by C. G. Suits, vol. 10, Pergamon, London, 1961.

92. L. M. Levin, Studies in the Physics of Roughly Dispersed Aerosols (originally published in Russian; Akad. Nauk. U.S.S.R., Moscow, 1961). Translated June 11, 1963, by Department of Commerce, OTS, Joint Publications Research Service for U.S. Chemical Corps Biological Laboratories (reference CCBL:FD2-3742..T-38-1., translation No. 815).
93. H. D. Landahl and R. G. Herrmann, "Sampling of Liquid Aerosols by Wires, Cylinders and Slides, and the Efficiency of Impaction of Droplets," *J. Colloid Sci.* 4, 103-36 (1949).
94. P. R. Owen, "Dust Deposition from a Turbulent Airstream," pp. 8-25, in Aerodynamic Capture of Particles, ed. by E. G. Richardson, Pergamon, New York, 1960.
95. C. N. Davies, comments on paper by P. R. Owen, *ibid.*, pp. 50-51.
96. H. L. Green and W. R. Lane, Particulate Clouds, 2d ed., pp. 194-95, Van Nostrand, Princeton, N.J., 1964.
97. Fuchs, *op. cit.*, ref. 13, p. 73.
98. P. S. Klebanoff, National Advisory Committee for Aeronautics, NACA Tech. Notes 3178, 1954.
99. J. O. Hinze, Turbulence, p. 502, McGraw-Hill, New York, 1959.
100. A. C. Chamberlain, "Aspects of the Deposition of Radioactive and Other Gases and Particles," pp. 63-68 in Aerodynamic Capture of Particles, ed. by E. G. Richardson, Pergamon, New York, 1960.
101. G. Asset and T. G. Hutchins, "Leeward Deposition of Particles on Cylinders from Moving Aerosols," *Amer. Ind. Hyg. Assoc. J.* 28, 348-53 (1967).
102. J. Schubert et al., "Tissue Distribution of Monomeric and Polymeric Plutonium as Modified by a Chelating Agent," *Radiat. Res.* 15, 220 (1961).
103. L. Van Middlesworth, Study of Plutonium Metabolism in Bone, MDDC-1022 (1947).
104. J. Carritt et al., "The Distribution and Excretion of Plutonium Administered Intravenously to the Rat," *J. Biol. Chem.* 171, 273 (1947).
105. H. Foreman et al., "Ca EDTA and the Excretion of Plutonium," *Proc. Soc. Exptl. Biol. Med.* 89, 339-42 (1955).
106. J. F. Fried et al., "Superior Chelating Agents for the Treatment of Plutonium Poisoning, *Atompraxis* 5(1), 1 (1959).

107. J. G. Hamilton and K. G. Scott, "Effect of Calcium Salt of Versene upon Metabolism of Plutonium in the Rat," *Proc. Soc. Exptl. Biol. Med.* 83, 301 (1953).
108. M. W. Rosenthal and J. Schubert, "Kinetics of Body Distribution of Plutonium as Influenced by Zirconium," *Radiat. Res.* 6, 349 (1957).
109. J. Schubert et al, "Plutonium and Yttrium Content of the Blood, Liver, and Skeleton of the Rat at Different Times after Intravenous Administration," *J. Biol. Chem.* 182, 635 (1950).
110. D. M. Taylor, "Some Aspect of the Comparative Metabolism of Plutonium and Americium in Rats," *Health Phys.* 8, 673 (1962).
111. M. R. White and J. Schubert, "The Action of Salts of Zirconium and Other Metals on Plutonium and Yttrium Distribution and Excretion," *J. Pharmacol. Exp. Therap.* 104, 317 (1952).
112. T. N. Rysina and R. A. Erokhin, "The Distribution and Elimination of Plutonium in Dogs in the Long-Term Periods after Introduction," pp. 117-26 in Biological Effects of Radiation and Problems of Radioactive Isotope Distribution, AEC-tr-5265; translated from a publication of the State Publishing House of Literature in the Field of Atomic Science and Technology, Moscow, 1961.
113. B. J. Stover, D. R. Atherton, and N. Keller, "Metabolism of Pu²³⁹ in Adult Beagle Dogs," *Radiat. Res.* 10, 130 (1959).
114. W. J. Bair et al., "Retention, Translocation and Excretion of Inhaled Pu²³⁹O₂," *Health Phys.* 8, 639 (1962).
115. L. K. Bustad et al., "Preliminary Observations on Metabolism and Toxicity of Plutonium in Miniature Swine," *Health Phys.* 8, 615 (1962).
116. V. H. Smith et al., "Effectiveness of DTPA in Removing Plutonium from the Pig," *Proc. Soc. Exptl. Biol. Med.* 107, 120 (1961).
117. W. H. Langham et al., "The Los Alamos Scientific Laboratory's Experience with Plutonium in Man," *Health Phys.* 8, 753 (1962).
118. J. Katz, H. A. Kornberg, and H. M. Parker, "Absorption of Plutonium Fed Chronically to Rats," *Amer. J. Roentgenol.* 73, 303 (1955).
119. W. Kisielecki and L. Woodruff, "Studies on the Distribution of Plutonium in the Rat," in Biology Division Quarterly Report August 1947 to November 1947, ANL-4108 (March 1948).
120. D. M. Taylor and F. D. Sowby, "The Removal of Americium and Plutonium from the Rat by Chelating Agents," *Phys. Med. Biol.* 7, 83 (1962).

121. H. Foreman, W. Moss, and W. Langham, "Plutonium Accumulation from Long-Term Occupational Exposure," *Health Phys.* 2, 326 (1960).
122. C. E. Newton, Jr., et al., "Tissue Sampling for Plutonium Through an Autopsy Program," in Proceedings of the 12th Annual Bio-Assay and Analytical Chemistry Meeting Held in Gatlinburg, Tennessee, October 13-14, 1966, CONF-661018, p. 220 (1967); also see BNWL-SA-918 (Sept. 30, 1966).
123. C. R. Lagerquist et al., "Plutonium Content of Several Internal Organs Following Occupational Exposure," in Proceedings of the 13th Annual Bio-Assay and Analytical Chemistry Meeting Held in Berkeley, California, October 12-13, 1967, CONF-671048, p. 103 (1968).
124. P. J. Magno, P. E. Kauffman, and P. R. Groulx, "Plutonium-239 in Human Tissues and Bone," *Radiol. Health Data Rep.* 10, 47-50 (1969).
125. W. J. Bair, J. F. Park, and W. J. Clarke, Long-Term Studies of Inhaled Plutonium in Dogs, AFWL-TR-65-214 (March 1966).
126. E. Painter et al., Clinical Physiology of Dogs Injected with Plutonium, AECD-2042 (June 1946).
127. D. H. Copp, D. J. Axelrod, and J. G. Hamilton, "The Deposition of Radioactive Metals in Bone as a Potential Health Hazard," *Amer. J. Roentgenol., Radium Therapy Nucl. Med.* 58, 10 (1947).
128. W. H. Langham, "Physiology and Toxicology of Plutonium-239 and Its Industrial Medical Control," *Health Phys.* 2, 172 (1959).
129. W. H. Langham, "Determination of Internally Deposited Radioactive Isotopes from Excretion Analysis," *Amer. Ind. Hyg. Assoc. Quart.* 17(3), 305 (1956).
130. P. W. Krey, D. Bogan, and E. French, "Plutonium in Man and His Environment," *Nature (London)* 195, 263 (1962).
131. D. M. Taylor, unpublished data presented to ICRP Committee II, Nov. 11, 1963.
132. B. J. Stover et al., pp. 109-23 in Delayed Effects of Bone-Seeking Radionuclides, ed. by C. W. Mays et al., University of Utah Press, Salt Lake City, 1969.
133. L. K. Bustad et al., "Preliminary Observations on Metabolism and Toxicity of Plutonium in Miniature Swine," *Health Phys.* 8, 615-20 (1962).
134. P. E. Morrow et al., "The Retention and Fate of Inhaled Plutonium Dioxide in Dogs," *Health Phys.* 13, 113-33 (1967).

135. S. Ullberg et al., "Distribution of Plutonium in Mice. An Autoradiographic Study," *Acta Radiol.* 58, 459 (1962).
136. B. Kawin and N. L. Dockum, "Distribution and Retention of Plutonium in Rats," in Hanford Biology Research Annual Report for 1957, HW-53500, pp. 95-101 (January 1958).
137. Arthus Lindenbaum, Argonne National Laboratory, private communication, August 1971.
138. J. W. Healy, "Estimation of Plutonium Lung Burden by Urine Analysis," *Am. Ind. Hyg. Assoc. Quart.* 18, 261 (1957).
139. F. Swanberg, Jr., "Comparison of Urinary Excretion Data from Selected Plutonium Exposure Cases at Hanford," *Health Phys.* 8, 761-65 (1962).
140. W. S. Snyder, "Major Sources of Error in Interpreting Urinalysis Data to Estimate the Body Burden of Pu²³⁹: A Preliminary Study," *Health Phys.* 8, 767 (1962).
141. R. C. Thompson (ed.), "Proceedings of the Hanford Symposium on the Biology of the Transuranic Elements," *Health Phys.* 8, 561 (1962).
142. J. Schubert, "Removal of Radioelements from the Mammalian Body," *Ann. Rev. Nucl. Sci.* 5, 369 (1955).
143. M. W. Rosenthal (ed.), Therapy of Radioelement Poisoning, ANL-5584 (August 1956).
144. M. W. Rosenthal, "Radioisotope Absorption and Methods of Elimination: Factors Influencing Elimination from the Body," pp. 541-63 in Radioisotopes in the Biosphere, ed. by R. S. Caldecott and L. A. Snyder, University of Minnesota, 1960.
145. Yu. A. Belyaev, "Possible Ways of Influencing the Elimination of Plutonium from the Animal Organism," pp. 180-87 in Biological Effects of Radiation and Problems of Radioactive Isotope Distribution, AEC-tr-5265; translated from a publication of the State Publishing House of Literature in the Field of Atomic Science and Technology, Moscow, 1961.
146. V. H. Smith, "The Removal of Internally Deposited Plutonium," in Hanford Biology Research Annual Report for 1958, HW-59500, pp. 63-72 (January 1959).
147. E. G. Tombropoulos, W. J. Bair, and J. F. Park, "Effect of Diethylene-triamine-pentaacetic Acid and Polypropylenoglycolethylene Oxide Polymer on Excretion of Inhaled ²³⁹PuO₂ in Dogs," *Nature* 198, 703 (1962).

148. W. D. Norwood, "DTPA-Effectiveness in Removing Internally Deposited Plutonium from Humans," *J. Occup. Med.* 2, 371 (1960).
149. W. D. Norwood, "Long-term Administration of DTPA for Plutonium Elimination," *J. Occup. Med.* 4, 130 (1962).
150. W. J. Bair, *Toxicology of Inhaled Plutonium - Experimental Animal Studies*, BNWL-SA-3469 (1970).
151. W. J. Bair, *Plutonium Inhalation Studies (A Series of Lectures Given in Japan in 1969 at the Invitation of the Japanese Atomic Energy Commission)*, BNWL-1221 (1970).

6. COMPUTATION OF INTERNAL DOSE

From the foregoing discussions of the metabolism and effects of plutonium, it should be clear that the problem of computing potential doses from plutonium release involves a complex variety of interrelated treatments of plutonium behavior. Evaluation requires the knowledge or assumption of the exposure conditions, including compound, particle size, concentration, and exposure time. Included in this chapter are relatively simple mathematical formulas and parameters used to compute doses from an intake of plutonium. Additionally, a sample calculation is provided that uses these formulas and information from earlier chapters to present the means by which the consequences of a release from a liquid-metal-cooled mixed-oxide-fueled fast reactor may be estimated.

6.1 Physical Dosimetry and Dose Equivalent

At present the dose to the lung from inhaled $^{239}\text{PuO}_2$ particles is calculated by assuming that the energy emitted from all particles in the lung is uniformly distributed throughout the lung tissue. This has been referred to as the "organ/mean-dose" or "smeared-dose" concept. Similarly, the absorbed dose may be calculated for a plutonium deposit uniformly dispersed in the bone or in liver. The unit of absorbed dose is the rad, corresponding to an energy absorption of ionizing radiation of 100 ergs per gram of any medium. For all practical purposes, $^{239}\text{PuO}_2$ particles emit 5.14-MeV alpha particles having a range in tissue of less than 40 μ , recoil atoms having an average energy of about 0.084 MeV, and an assortment of low-energy x and gamma rays contributing less than 0.01 MeV per disintegration. The alpha particles and recoil atoms are assumed to be completely absorbed in the given organ, and a fraction of the x- and gamma-ray energy is absorbed, depending on the size of the organ. In general, an effective energy (E_{eff}) can be computed for a given radioisotope in each organ. Thus it would be possible to calculate the absorbed dose for a uniform deposit of a radioactive material in each of several organs; however, because of variations in the quality of different radiations, relative sensitivity of organs and their importance to bodily

function, and, in some cases, wide divergence from uniform dispersion, it is the practice to compare organ dose on the basis of a dose equivalent. For protection purposes, as opposed to radiobiology in general, the dose equivalent (DE , rems) is defined as the product of the absorbed dose (D , rads), a quality factor (QF), a dose distribution factor (DF), and other necessary modifying factors:¹

$$DE = D (QF) (DF) \dots$$

As a convenience in computation, an effective energy per disintegration is defined, as shown in Table 6.1. The dose equivalent per microcurie-day of exposure is given by

$$\frac{DE}{\mu\text{Ci}\cdot\text{day}} = 51.2 \frac{E_{\text{eff}}}{m},$$

where m is mass of the organ in grams. Factors similar to those included in Table 6.1 were used to establish the effective energies for other components of LMFBR fuel indicated in Chapter 2. The effective energies for each of those elements in lung, bone, liver, and ovary are given in Table 6.2.

Table 6.1. Effective energy for ^{239}Pu internal dose computations

	E , energy (MeV/dis)	QF , quality factor	E_{eff} (MeV)		
			Bone ^a	GI tract ^b	Other organs
Alphas	5.14	10	257	0.51	51.4
Alpha recoils	0.084	20	8.4	0.01	1.68
X and gamma rays	0.0085	1	0.04		
Total			270 ^a	0.52	53

^a $DF = 5$; values rounded off to two significant digits.

^bModifying factor = 0.01.

Table 6.2. Effective energies for various components of LMFBR fuel^a in lung, bone, liver, and ovary

Nuclide	Activity fraction (Ci of nuclide/Ci of mixture)	E_{eff} (MeV)			
		Lung	Bone	Liver	Ovary
^{238}U	7.6×10^{-7}	43	220	43	43
^{237}Np	7.4×10^{-8}	49	250	49	49
^{238}Pu	2.53×10^{-2}	57	284	57	57
^{239}Pu	8.03×10^{-3}	53	270	53	53
^{240}Pu	1.04×10^{-2}	53	270	53	53
^{241}Pu	0.83	0.053	14	1.0	1.6
^{242}Pu	1.3×10^{-5}	51	250	51	51
^{241}Am	1.84×10^{-3}	57	283	57	57
^{243}Am	5.8×10^{-5}	54	272	54	54
^{242}Cm	0.122	64	400	78	78
^{244}Cm	1.68×10^{-3}	60	300	60	60

^aBased on estimated steady-state inventory in 1000-MW(e) LMFBR (see Table 2.1, Chap. 2).

6.2 Dose Calculations for Inhaled Plutonium

The dose to the lung is calculated using the model of the ICRP Task Group on Lung Dynamics.² Based on the calculated particle size distribution (see Table 6.17) and comparison with estimates of the ICRP Task Group on Lung Dynamics,² the initial deposition of inhaled plutonium would differ only slightly with the density of the aggregates. For example, considering a particle of 0.5 μm diameter, nasal deposition is expected to be nearly zero; pulmonary deposition is predicted to be about 25% of the inhaled quantity, independent of density (ρ) in the range 1 to 10 g/cm^3 ; and deposition in the tracheobronchial airways may vary from 1.6% ($\rho = 1 \text{ g}/\text{cm}^3$) to 4.3% ($\rho = 10 \text{ g}/\text{cm}^3$).

Under the assumed exposure conditions, a fraction f_a of the plutonium inhaled is deposited in the pulmonary region of the lungs, where 40% of the initial deposit is cleared with a 1-day half-life and the remaining 60% is cleared with a half-life of 500 days. Thus an intake of 1 μCi would result in an exposure commitment of

$$I = f_{\alpha} \left(\frac{0.4 \times 1}{0.693} + \frac{0.6 \times 500}{0.693} \right) = 432f_{\alpha} \text{ } \mu\text{Ci-days} ,$$

For an adult male (mass of P region = 955 g), this exposure results in a 50-year dose commitment (commitment to age 70) of

$$51.2 \times \frac{E_{\text{eff}}}{m} 432f_{\alpha} = 51.2 \times \frac{53}{955} \times 432f_{\alpha} = 1230f_{\alpha} \text{ rems}/\mu\text{Ci inhaled} .$$

For the case of $f_{\alpha} = 0.25$ (approx. a 1- μm particle), this would be 308 rems/ μCi . Setting $f_{\alpha} = 1.0$ yields the 50-year dose commitment per microcurie deposited in the P region of the lung. In the case of an adult female ($m = 0.8 \times 955 = 764$ g), the 50-year dose commitment is 1540 rems per microcurie deposited.

Calculation of dose commitment to a growing lung is somewhat more complex than the approach used above. The portion of the dose commitment per microcurie inhaled that will be absorbed during the interval t_1 to t_2 is given by

$$D_{1,2} = 51.2 \times 53f_{\alpha} \int_{t_1}^{t_2} \left(\frac{Re^{-\rho t} + Se^{-\sigma t}}{m} \right) dt .$$

For the adult lung, $R = 0.4$, $\rho = (0.693/1)(\text{day}^{-1})$, $S = 0.6$, and $\sigma = (0.693/500)(\text{day}^{-1})$. If the same parameters are assumed to hold for all ages from newborn to adult, then

$$D_{1,2} = 1088f_{\alpha} \int_{t_1}^{t_2} \left(\frac{1}{m} \right) e^{-0.693t} dt + 1632f_{\alpha} \int_{t_1}^{t_2} \left(\frac{1}{m} \right) e^{-(0.693/500)t} dt .$$

The lung weight increases nonlinearly with time; consequently $(1/m)$ decreases with time. The functional relationship between $(1/m)$ and time can be approximated by various forms; however, it is convenient to interpolate between the end-point values (t_1, m_1) and (t_2, m_2) using single exponential functions. Thus we assume for the first integral

$$\left(\frac{1}{m} \right) e^{-0.693t} = Ae^{-\alpha t} e^{-0.693t} = Ae^{-\alpha t} ,$$

and

$$\int_{t_1}^{t_2} Ae^{-\alpha t} dt = \frac{1}{\alpha} (Ae^{-\alpha t_1} - Ae^{-\alpha t_2}) = \frac{1}{\alpha} \left(\frac{e^{-0.693t_1}}{m_1} - \frac{e^{-0.693t_2}}{m_2} \right),$$

where $\alpha = 0.693 + \frac{\ln m_2 - \ln m_1}{t_2 - t_1}$. The second integral can be evaluated in the same way.

Data on weights of human organs are being compiled from various literature sources for use in internal dose calculations.³ Preliminary values for organ weights are used in Tables 6.3 to 6.5.

When the differences in breathing rate are taken into consideration, it can be seen from Tables 6.3 to 6.5 that the 10-year-old child would sustain a slightly greater dose to the lungs, but the 20-year-old female would receive the highest dose commitment to the other organs considered.

Under the conditions outlined in Section 6.1, all the plutonium initially deposited in the P region of the lung is assumed to be rapidly transported to the bloodstream. It is further assumed that of the plutonium reaching the blood, 42% is deposited in the bone and 56% in the liver, and that there is no biological elimination from bone or liver.

Calculation of dose commitment to the bones and liver of children follows essentially the same approach as for the growing lung. Because

Table 6.3. Lung dose commitment to age 70 as a function of age at exposure^a

Age at exposure (years)	Assumed mass of lungs (g)	Average breathing rate (m ³ /hr)	Dose commitment (rems/ μ Ci deposited)
Newborn	66	0.033	8210
1	170	0.16	5510
10	450	0.62	2340
20 (♀)	764	0.88	1540
20 (♂)	955	0.95	1230

^aNote that the order of precision does not warrant more than one significant digit; however, more digits are retained only to facilitate cross comparison.

of the assumption of no biological elimination, the form of the dose integral is considerably simplified. Thus

$$D_{1,2} = K \left[\frac{t_2 - t_1}{\ln m_2 - \ln m_1} \left(\frac{1}{m_1} - \frac{1}{m_2} \right) \right] \text{ rems}/\mu\text{Ci deposited in the P region ,}$$

where $K = 5.30 \times 10^5$ for bone and 1.39×10^5 for liver when t is in years and m in grams.

Results of dose calculations are presented in Tables 6.4 and 6.5.

Table 6.4. Bone dose commitment to age 70 as a function of age at exposure

Age at exposure (years)	Assumed mass of bone (g)	Dose commitment (rems/ μ Ci deposited)
Newborn	500	25,500
1	2,000	24,800
10	5,900	18,900
20 (♀)	6,800	15,600
20 (♂)	10,000	10,600

Table 6.5. Liver dose commitment to age 70 as a function of age at exposure

Age at exposure (years)	Assumed mass of liver (g)	Dose commitment (rems/ μ Ci deposited)
Newborn	100	39,400
1	250	35,800
10	844	24,200
20 (♀)	1450	19,100
20 (♂)	1810	15,300

6.3 Consideration of Other Plutonium Isotopes

As indicated in Table 2.1 of Chapter 2, a number of plutonium isotopes in addition to ^{239}Pu are expected to be present in LMFBR fuel. The relative proportions of the various components will depend upon the operating history of the fuel; however, the particular isotopic mixture of Table 2.1 is taken as an example. Assuming, for the time being, that the plutonium acts separately from all other radionuclides, dose commitments are calculated using the data given in Table 6.6.

Table 6.6. Assumed mixture of plutonium isotopes

Nuclide	Activity fraction ^a ($\mu\text{Ci}/\mu\text{Ci}$ mixture)	Radiological half-life (days)	Exposure in 50 years per unit deposit in bone, liver, or ovary ($\mu\text{Ci-days}/\mu\text{Ci}$ deposited)
^{238}Pu	0.029	3.3×10^4	15,170
^{239}Pu	0.0092	8.9×10^6	18,260
^{240}Pu	0.012	2.4×10^6	18,260
^{241}Pu	0.95	4.8×10^3	6,429
^{242}Pu	0.000015	1.4×10^8	18,260

^aSpecific activity = 4.625 Ci per gram of Pu isotope mixture.

An example calculation for the ^{238}Pu contribution to lung dose commitment (LDC) will serve to illustrate the steps followed to arrive at the various dose estimates given in Tables 6.7 to 6.10.

RF = P-region retention function

$$= f_a \left[0.4e^{-0.693t} + 0.6e^{-(0.693t/500)} \right] e^{-(0.693t/T_r)}$$

$$\text{Expo} = \text{exposure per unit deposit in P region} = \int_0^t RF dt$$

Table 6.7. Lung dose commitment to age 70 for females 20 years old at time of exposure^a

Nuclide	Effective half-life (days)	Dose (rems/ μ Ci-day)	Exposure per unit intake (μ Ci-days/ μ Ci mix inhaled)	Lung dose commitment (rems/ μ Ci mix deposited)
²³⁸ Pu	493	3.82	12.38	47.3
²³⁹ Pu	500	3.55	3.98	14.1
²⁴⁰ Pu	500	3.55	5.16	18.3
²⁴¹ Pu	453	0.00355	3.73	1.3
²⁴² Pu	500	3.42	0.00644	0.02
Total				81.0 ^b

^a Assumed mass of P region = 764 g.

^b Total commitment = 81.0 rems/ μ Ci mix \times 4.625 μ Ci/ μ g = 375 rems/ μ g mix deposited.

Table 6.8. Bone dose commitment to age 70 for females 20 years old at time of exposure^a

Nuclide	Effective energy (MeV)	Dose (rems/ μ Ci-day)	Bone dose commitment (rems/ μ Ci mix deposited in P region)
²³⁸ Pu	284	2.14	394.6
²³⁹ Pu	270	2.03	143.2
²⁴⁰ Pu	270	2.03	185.2
²⁴¹ Pu	14	0.105	270.4
²⁴² Pu	250	1.88	0.2
Total			993.6 ^b

^a Assumed mass of bone = 6800 g, fraction of inhaled plutonium reaching bone = 0.105, and effective half-life = radiological half-life.

^b Total commitment = 993.6 rems/ μ Ci mix \times 4.625 μ Ci/ μ g = 4595 rems/ μ g mix deposited in the P region.

Table 6.9. Liver dose commitment to age 70 for females 20 years old at time of exposure^a

Nuclide	Effective energy (MeV)	Dose (rems/ μ Ci-day)	Liver dose commitment (rems/ μ Ci mix deposited in P region)
²³⁸ Pu	57	2.01	495.16
²³⁹ Pu	53	1.87	175.72
²⁴⁰ Pu	53	1.87	227.36
²⁴¹ Pu	1.0	0.0353	120.76
²⁴² Pu	51	1.80	0.28
Total			1019.3 ^b

^a Assumed mass of liver = 1450 g, fraction of inhaled plutonium reaching liver = 0.14, and effective half-life = radiological half-life.

^b Total commitment = 1019.3 rems/ μ Ci mix \times 4.625 μ Ci/ μ g = 4714 rems/ μ g mix deposited in the P region.

Table 6.10. Ovary dose commitment to age 70 for females 20 years old at time of exposure^a

Nuclide	Effective energy (MeV)	Dose (rems/ μ Ci-day)	Ovary dose commitment (rems/ μ Ci mix deposited in P region)
²³⁸ Pu	57	365	160.28
²³⁹ Pu	53	339	56.88
²⁴⁰ Pu	53	339	73.60
²⁴¹ Pu	1.6 ^b	10.2	62.52
²⁴² Pu	51	326	0.08
Total			353.36 ^c

^a Assumed mass of ovaries (2) = 8 g, fraction of inhaled plutonium reaching ovary = 0.00025, and effective half-life = radiological half-life.

^b This value computed by B. R. Fish (1971); all others from ICRP Publication 2.

^c Total commitment = 353.36 rems/ μ Ci mix \times 4.625 μ Ci/ μ g = 1634 rems/ μ g mix deposited in the P region.

$$I = \frac{1}{0.693} \left\{ 0.4 \frac{T_r}{T_r + 1} \left[1 - e^{-0.693t} \left(\frac{T_r + 1}{T_r} \right) \right] \right. \\ \left. + 0.6 \frac{500T_r}{T_r + 500} \left[1 - e^{-0.693t} \left(\frac{T_r + 500}{500T_r} \right) \right] \right\}$$

for $t = 50 \times 365.25 = 18,260$ days and $T_r = 3.3 \times 10^4$ days (for ^{238}Pu).

$$I = 1.433 [0.4 + 0.6 \times 493] = 426.9 \text{ } \mu\text{Ci-days}/\mu\text{Ci } ^{238}\text{Pu deposited.}$$

However, only the fraction 0.029 of the total plutonium activity is ^{238}Pu ; consequently, the ^{238}Pu contribution to the exposure is:

$$I = 0.029 \times 426.9 = 12.38 \text{ } \mu\text{Ci-days } ^{238}\text{Pu}/\mu\text{Ci mix deposited.}$$

$$\text{LDC}/\mu\text{Ci-day } ^{238}\text{Pu} = 51.2 \times \frac{E}{m} = 51.2 \times \frac{57}{764} = 3.82 .$$

Finally, the ^{238}Pu portion of the LDC = $12.38 \times 3.82 = 47.3$ rems/ μCi mix deposited in the pulmonary region of the lung.

6.4 Consideration of Other Transuranics

Depending on the operating history of the reactor the fuel may have a composition similar to that indicated in Table 2.1 of Chapter 2. In the following dose calculations, Tables 6.11 to 6.15, it is assumed that any released fuel particles that are inhaled will have the isotopic composition given in Table 2.1. The fraction of each isotope reaching the reference organ via inhalation (f_α) is taken from ICRP Publication 2 (Ref. 4) except for the plutonium isotopes (same as in the previous section). The fraction of ^{238}U reaching the liver is assumed to be the same as for ^{237}Np , and the same fraction is assumed to reach the ovaries as assumed for the plutonium isotopes.

Table 6.11. Assumed mixture of transuranium isotopes
in aerosols released from an LMFBR accident

Nuclide	Activity fraction ^a ($\mu\text{Ci}/\mu\text{Ci}$ mixture)	Radiological half-life (days)	Exposure in 50 years per unit deposit in bone, liver, or ovary ($\mu\text{Ci-days}/\mu\text{Ci}$ deposited)
^{238}U	7.6×10^{-7}	1.6×10^{12}	18,260
^{237}Np	7.4×10^{-8}	8.0×10^8	18,260
^{238}Pu	0.025	3.3×10^4	15,170
^{239}Pu	0.0080	8.9×10^6	18,260
^{240}Pu	0.010	2.4×10^6	18,260
^{241}Pu	0.83	4.8×10^3	6,429
^{242}Pu	1.3×10^{-5}	1.4×10^8	18,260
^{241}Am	0.0018	1.7×10^5	17,590
^{243}Am	5.8×10^{-5}	2.9×10^6	18,260
^{242}Cm	0.122	160	234.4
^{244}Cm	0.0017	6.7×10^3	8,205

^aSpecific activity = 5.291 Ci/g of plutonium isotopic mixture.

Table 6.12. Lung dose commitment to age 70 for
females 20 years old at time of exposure

Nuclide	Effective energy (MeV)	Effective half-life (days)	Exposure per unit intake ($\mu\text{Ci-days}/\mu\text{Ci}$ mix inhaled)	Dose (rems/ $\mu\text{Ci-day}$)	Lung dose commitment (rems/ μCi mix inhaled)
^{238}U	43	120	1.99×10^{-5}	2.88	0.00006
^{237}Np	49	(300) ^a	4.78×10^{-6}	3.28	0.00002
^{238}Pu	57	493	2.70	3.82	10.31
^{239}Pu	53	500	0.870	3.55	3.09
^{240}Pu	53	500	1.13	3.55	4.00
^{241}Pu	0.053	453	81.5	0.00355	0.289
^{242}Pu	51	500	0.00141	3.42	0.00481
^{241}Am	57	(500)	0.199	3.82	0.762
^{243}Am	54	(500)	0.00633	3.62	0.0229
^{242}Cm	64	(123)	3.26	4.29	13.96
^{244}Cm	60	(465)	0.169	4.02	0.681
Total					33.13 ^b

^aIn the absence of data, parameters in parentheses are estimated.

^bTotal commitment = $33.13 \times 5.291 \mu\text{Ci}/\mu\text{g Pu} = 175.3 \text{ rems}/\mu\text{g Pu}$
inhaled.

Table 6.13. Bone dose commitment to age 70 for females 20 years old at time of exposure

Nuclide	Effective energy (MeV)	Fraction reaching bone of amount inhaled, f_{α}	Dose (rems/ μ Ci-day)	Bone dose commitment (rems/ μ Ci inhaled)
^{238}U	220	0.083	1.66	0.0019
^{237}Np	250	0.11	1.88	0.0003
^{238}Pu	284	0.105	2.14	86.17
^{239}Pu	270	0.105	2.03	31.30
^{240}Pu	270	0.105	2.03	40.54
^{241}Pu	14	0.105	0.105	59.06
^{242}Pu	250	0.105	1.88	0.047
^{241}Am	283	0.063	2.13	4.34
^{243}Am	272	0.063	2.05	0.138
^{242}Cm	400	0.075	3.01	6.46
^{244}Cm	300	0.075	2.26	2.34
Total				230.41 ^a

^aTotal commitment = $230.41 \times 5.291 \mu\text{Ci}/\mu\text{g Pu} = 1219 \text{ rems}/\mu\text{g Pu}$ mix inhaled.

Table 6.14. Liver dose commitment to age 70 for females 20 years old at time of exposure

Nuclide	Effective energy (MeV)	Fraction reaching liver of amount inhaled, f_{α}	Dose (rems/ μ Ci-day)	Liver dose commitment (rems/ μ Ci inhaled)
^{238}U	43	(0.013) ^a	1.52	0.0003
^{237}Np	49	0.013	1.73	0.00003
^{238}Pu	57	0.14	2.01	108.15
^{239}Pu	53	0.14	1.87	38.42
^{240}Pu	53	0.14	1.87	49.76
^{241}Pu	1.0	0.14	0.0353	26.38
^{242}Pu	51	0.14	1.80	0.060
^{241}Am	57	0.088	2.01	5.732
^{243}Am	54	0.088	1.91	0.179
^{242}Cm	78	0.1	2.75	7.876
^{244}Cm	60	0.1	2.12	2.920
Total				239.48 ^b

^aAssumed to be the same as for ^{237}Np .

^bTotal commitment = $239.48 \times 5.291 \mu\text{Ci}/\mu\text{g Pu} + 1267 \text{ rems}/\mu\text{g Pu}$ mix inhaled.

Table 6.15. Ovary dose commitment to age 70 for females 20 years old at time of exposure^a

Nuclide	Effective energy (MeV)	Dose (rems/ μ Ci-day)	Ovary dose commitment (rems/ μ Ci inhaled)
²³⁸ U	43	275	0.00096
²³⁷ Np	49	314	0.00011
²³⁸ Pu	57	365	35.00
²³⁹ Pu	53	339	12.43
²⁴⁰ Pu	53	339	16.11
²⁴¹ Pu	1.6	10.2	13.66
²⁴² Pu	51	326	0.019
²⁴¹ Am	57	365	2.95
²⁴³ Am	54	346	0.092
²⁴² Cm	78	499	3.57
²⁴⁴ Cm	60	384	1.32
Total			85.16 ^b

^aFraction of inhaled isotope reaching ovary is assumed to be 0.00025 for all nuclides in this table.

^bTotal commitment = $85.16 \times 5.291 \mu\text{Ci}/\mu\text{g Pu} = 450.6$ rems/ $\mu\text{g Pu}$ mix inhaled

6.5 Gastrointestinal Tract Intake During Release

It is estimated that all the PuO₂ deposited in the tracheobronchial airways (4% of intake) and 40% of the plutonium deposited in the pulmonary region (10% of intake) will be transferred rapidly to the gastrointestinal (GI) tract. In addition, a further intake, amounting to approximately 10% of these quantities, may result from direct deposition in the eyes, nares, and mouth. From the discussion of transfer of plutonium from the GI tract to the bloodstream (Sect. 5.1.2), it may be estimated that absorption into the blood is not more than about 0.25%, probably more like 0.003%, of the PuO₂ reaching the GI tract. Comparison of the calculated amounts reaching the bloodstream via the GI tract with the amounts estimated to reach the blood by way of dissolution in the lungs suggests that the lung route is far more significant, a factor of 300 or more.

6.6 Ingestion of Plutonium in Food and Water

As discussed in Section 5.1.2, the uptake of plutonium into food or feed crops grown on PuO_2 -contaminated soil is not expected to result in significant transfer of plutonium into the food chain of man. Direct deposition of plutonium onto leafy vegetables, however, may result in some degree of intake if the contaminated crops are not identified and withheld from consumption. According to the approximations outlined in Section 5.1.2, it may be estimated that the total intake of plutonium from the consumption of contaminated vegetables might amount to 1.2 times the quantity initially deposited per square meter. Nevertheless, the inhalation route remains the controlling factor by at least one order of magnitude because of the small uptake of plutonium from the GI tract compared with the lung.

6.7 Summary Calculations

6.7.1 Source term evaluations

As initial conditions, it is arbitrarily assumed that 100 g of PuO_2 is released along with 10,000 lb of sodium into an inerted structure surrounding the reactor vessel. Approximately 50 kg of sodium oxide is formed when this hot sodium reacts with the 1% oxygen content in the vessel cavity and constitutes the available aerosol source term. The remaining sodium will fall to the floor of the cavity. The plutonium is intimately mixed with and constitutes a part of the aerosol source term. For purposes of this report, it is assumed that the characteristic leak rate from the cavity to the outer containment barrier is 400%/day and that the leak rate from the outer containment is constant at 0.3%/day.

The Atomics International HAA-3 code has been used to compute the subsequent aerosol source term with time (depicted in Fig. 6.1)⁵ and important input assumptions are listed in Table 6.16.

As can be seen from Fig. 6.1, fallout removal processes are very effective. To carry the calculation of potential doses to completion requires use of the meteorological dispersion factors and dose models discussed earlier.

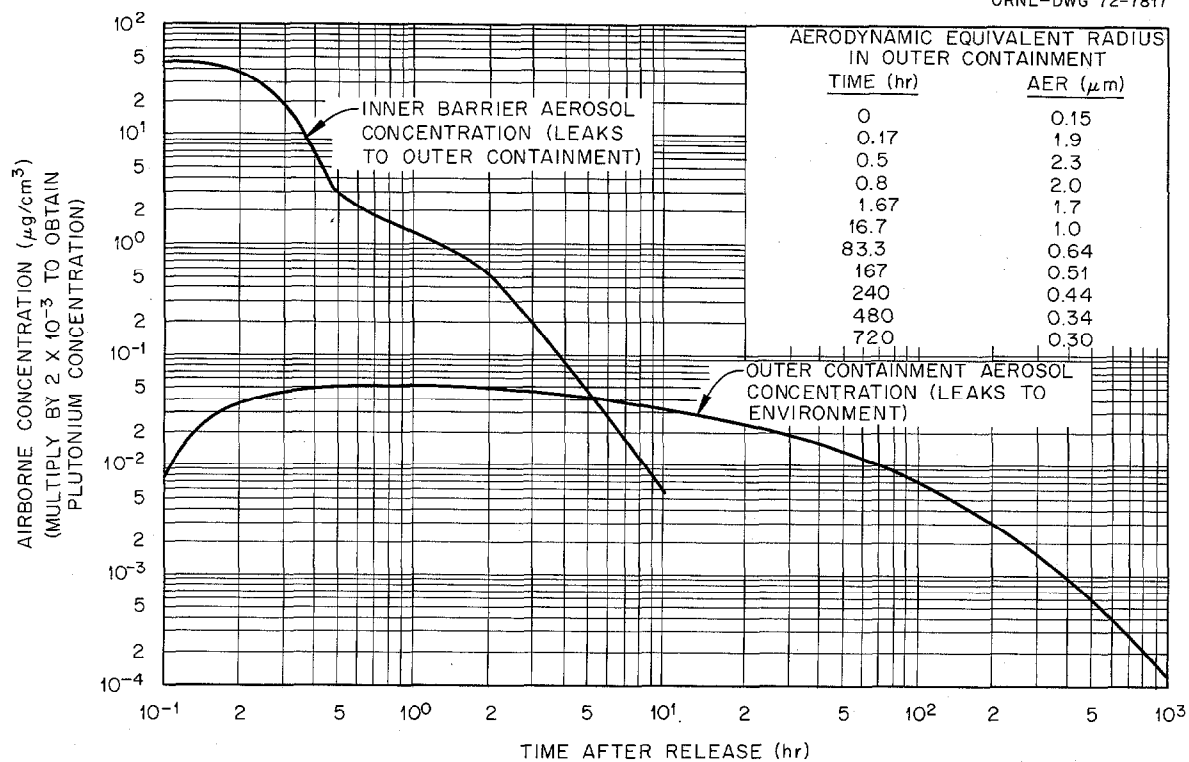


Fig. 6.1. Aerosol behavior following assumed release.

Table 6.16. Aerosol behavior input assumptions used by Atomics International⁵

Primary barrier volume, cm^3	1×10^9
Outer containment volume, cm^3	4.35×10^{10}
Primary barrier leak rate, ^a %/day	400
Outer containment leak rate, ^a %/day	0.3
Initial size of airborne particles, μm	0.5
Initial size distribution	Log-normal $\sigma = 2$
Theoretical particle density, ^b g/cm^3	2.27
Particle density modification factor	0.5
Gravitational collision efficiency factor	0.5

^a Assumed constant.

^b Based on 50 kg of Na_2O at $2.27 \text{ g}/\text{cm}^3$; 100 g of PuO_2 does not significantly affect this number.

6.7.2 Leakage and dispersion

For the given illustration, the dispersion factors employed are 0.1 of those presented in Fig. (A) of Regulatory Safety Guide 4,* and 1000 m is used as the distance of interest. Table 6.17 lists the released masses together with diffusion factors for various times of interest.

Table 6.17. Leakage and dispersion (from 100 g initial release)

Time	Cumulative Pu leaked (g)	Leaked Pu over time period (g)	X/Q at 1000 m (sec/m ³)	TIC ^a (g-sec/m ³)	MMD particle size over time period
0-8 hr	3.8×10^{-3}	3.8×10^{-3}	6.5×10^{-5}	2.5×10^{-7}	0.4
8-24 hr	8.7×10^{-3}	4.9×10^{-3}	1.5×10^{-5}	7.4×10^{-8}	0.5
1-4 days	1.9×10^{-2}	1.0×10^{-2}	5.3×10^{-6}	5.3×10^{-8}	0.4
4-30 days	2.8×10^{-2}	0.9×10^{-2}	1.2×10^{-6}	1.1×10^{-8}	0.4
				4×10^{-7}	

^aTime-integrated concentration.

6.7.3 Calculation of dose

The required input for computation of biological uptake and dose is the isotopic mixture of the plutonium, the time-integrated concentration, and the effective particle size of the inhaled material (since the latter determines the fraction deposited of any inhaled material). Using the deposited fractions (f_{α}) from Fig. 5.7 the dose factors in Table 6.18 were computed, for the case of the adult female.

In summary, using the HAA-3 code to estimate the aerosol behavior following the assumed release, the standard dispersion conditions employed in contemporary safety evaluations, and the retention and dose models presented, a 100-g release of plutonium from the reactor is expected to lead ultimately to a release of about 30 mg to the atmosphere. This in turn is calculated to result in a potential dose commitment of the order of 90 mrem at a distance of 1000 m.

*This value was suggested as a suitable tool of convenience in performing calculations of accident situations in environmental statements (Federal Register Docket 71-17569 Filed 11-30-71).

Table 6.18. Dose factors for sample case (adult female)

Time period	Aerodynamic equivalent diameter (μm)	f_a	L , Lung deposition during period ^a (picograms)	Dose commitment to age 70 from exposure during time period (mrem)			
				Liver (4.71) ^b	Bone (4.60) ^b	Ovary (1.63) ^b	Lung (0.375) ^b
0-8 hr	2.3	0.19	12	54	53	19	4.3
8-24 hr	1.9	0.21	3.8	18	17	6.2	1.4
1-4 days	1.6	0.22	2.9	13	13	4.7	1.1
4-30 days	0.8	0.28	0.74	3.5	3.4	1.2	0.28
Total			19	89	86	31	7.1

^a L = breathing rate ($2.44 \times 10^{-4} \text{ m}^3/\text{sec}$) \times TIC (Table 6.17) $\times f_a \times 10^{12}$ (picograms/gram).

^bDose factors (mrem/picogram deposited) from Tables 6.7 to 6.10.

Beyond this simple numerical exercise, however, an important point is that the computation of dose, employing the considerations in this and prior chapters, involves consideration of the interrelation and influence of each step in affecting the others. The tools offered in this report do permit a consistent and reasonable treatment of these interrelationships. As additional data are obtained through the ongoing experimental and analytical studies, such as those by Bair,⁶ further refinements to the models and parameters summarized in this section should be considered.

References

1. M. F. Fair, "Radiation Quantities and Units," chap. 3, p. 119 in Principles of Radiation Protection, ed. by K. Z. Morgan and J. E. Turner, Wiley, New York, 1967.
2. Task Group on Lung Dynamics (P. E. Morrow et al.), "Deposition and Retention Models for Internal Dosimetry of the Human Respiratory Tract," Health Phys. 12, 173-207 (1966).
3. Mary Jane Cook, Oak Ridge National Laboratory, private communication, August 1971.
4. Report of Committee II on Permissible Dose for Internal Radiation, 1959; ICRP Publication 2, Pergamon, Oxford, 1959.
5. R. S. Hubner et al., Heterogeneous Aerosol Agglomeration Code (HAA-3) User Report, AI-AEC-13038.
6. W. J. Bair, Toxicology of Inhaled Plutonium: Experimental Animal Studies, BNWL-SA-3649 (1970); also CONF-700930-2, from Seminar on Radiation Protection Problems Relating to Transuranium Elements, Karlsruhe, Germany, Sept. 21, 1970.

7. SUMMARY

The magnitude of the internal exposure hazard that might exist in the vicinity of an LMFBR after a hypothetical reactor accident is calculated in the following manner.

1. Select or determine a quantitative source term that includes the total mass and the changes in particle size distribution with time.

2. Trace the changes in total mass (kilograms) and aerosol concentration (grams per cubic centimeter) from the primary to the secondary containment system.

3. Trace the changes in the aerosol released from the reactor containment and the effects of meteorological dispersion (where desirable, changes in aerosol characteristics during dispersion and transport may be considered). If the concentration and particle size distribution can be determined at the selected distances of interest, then we have the information necessary to determine the amount of PuO_2 in aerosol form that could be inhaled and retained within the human body.

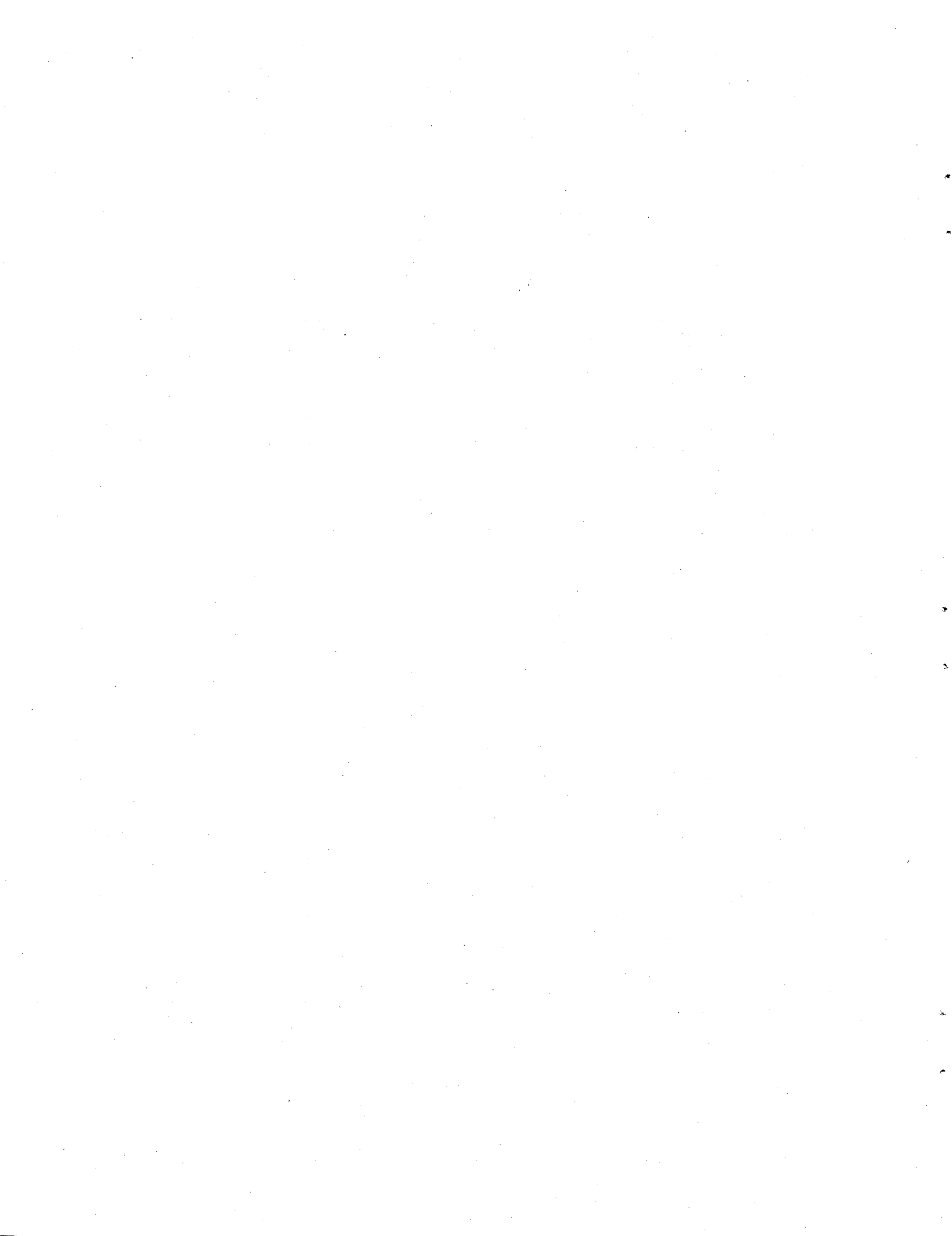
4. The critical organ is determined by the choice of pathway for the transfer of plutonium through a biological system.

5. In the final step, dose calculations are made that are related to the radiation effects on the critical organ, that is, bone or liver.

Aerosol models have been used to predict the decay of airborne mass concentration with time and to determine the changes in particle size distribution. Models for agglomeration and settling included a thorough evaluation of all parameters that could be considered in a postulated accident. Such studies include the conditions of release, changes in particle size distribution over extensive time periods, effect of secondary evolution of airborne sodium not initially mixed with fuel aerosols, effects of electrical charges (and the effects of radioactivity on charges), and the extent to which diffusiophoresis, thermophoresis, and other mechanisms would affect plate-out in a full-sized containment vessel under accident conditions.

In this report an arbitrary initial plutonium aerosol release and size distribution were selected as source terms to be used in subsequent calculations. Initially it may be assumed that 100 g of plutonium dioxide

aerosol was released within the containment system. After selecting the source term for accidental release, in-containment aerosol behavior and standard meteorological dispersion, calculations have been used to describe the possible dispersion of plutonium-bearing aerosols. This information in turn has been used to compute, through use of available dosimetric models, potential doses from the arbitrarily assumed release. In this fashion we have attempted to illustrate how a logically consistent evaluation of the potential consequences of a release from a liquid-metal-cooled mixed-oxide-fueled fast reactor can be accomplished.



NUCLEAR SAFETY

A BIMONTHLY REVIEW JOURNAL PREPARED BY NSIC

Nuclear Safety covers significant developments in the field of nuclear safety.

The scope is limited to topics relevant to the analysis and control of hazards associated with nuclear reactors, operations involving fissionable materials, and the products of nuclear fission.

Primary emphasis is on safety in reactor design, construction, and operation; however, safety considerations in reactor fuel fabrication, spent-fuel processing, nuclear waste disposal, handling of radioisotopes, and related operations are also treated.

Qualified authors are invited to submit interpretive articles, which will be reviewed for technical accuracy and pertinency. Authors will be advised as soon as possible of acceptance or suggested changes. Send inquiries or 3 copies of manuscripts (with the draftsman's original line drawings plus 2 copies, and with continuous-tone glossy prints of photographs plus 2 copies) to J. P. Blakely, Oak Ridge National Laboratory, P. O. Box Y, Oak Ridge, Tennessee 37830.

Nuclear Safety is prepared by the Nuclear Safety Information Center at Oak Ridge National Laboratory for the U.S. Atomic Energy Commission, Division of Technical Information. For subscriptions, address Superintendent of Documents, U.S. Government Printing Office, Washington, D. C. 20402. The subscription rate is \$3.50 per year. Below is an order blank for your convenience.

U. S. GOVERNMENT PRINTING OFFICE
DIVISION OF PUBLIC DOCUMENTS
WASHINGTON, D. C. 20402

POSTAGE AND FEES PAID
U. S. GOVERNMENT PRINTING OFFICE

OFFICIAL BUSINESS
RETURN AFTER 5 DAYS

Name _____
Street _____
City _____ State _____ ZIP _____

To Ensure Prompt, Accurate Shipment, Please Print or Type Address on Mailing Label Above

MAIL ORDER FORM TO:

Superintendent of Documents, U. S. Government Printing Office, Washington, D. C., 20402

Enclosed find \$ _____ (check, money order, or Superintendent of Documents coupons).

Please send me _____ subscriptions to *Nuclear Safety* at \$3.50 per subscription. (Single issues are sold at \$0.60 per issue.)

Please charge this order to my Deposit Account No. _____
Name _____
Street _____
City _____ State _____ ZIP _____

FOR USE OF SUPT. DOCS.	
Enclosed	_____
To be mailed later	_____
Subscription	_____
Refund	_____
Coupon refund	_____
Postage	_____

POSTAGE AND REMITTANCE: Postpaid within the United States, Canada, Mexico, and all Central and South American countries except Argentina, Brazil, Guyana, French Guiana, Surinam, and British Honduras. For these and all other countries, add \$1.00 for each annual subscription; for a single issue, add one-fourth of the single-issue price. Payment should be by check, money order, or document coupons, and MUST accompany order. Remittances from foreign countries should be made by international money order or draft on an American bank payable to the Superintendent of Documents or by UNESCO book coupons.

